1-1-2014

Epigenetic Regulation of Progenitor Cell Commitment by Hdac3

Mudit Gupta
University of Pennsylvania, guptam@mail.med.upenn.edu

Epigenetic Regulation of Progenitor Cell Commitment by Hdac3

Abstract
Tissue-specific progenitor cells emerge during development to expand and differentiate into the multiple cell lineages that populate the embryo. Appropriate differentiation of these precursor cells requires coordinated expression of numerous lineage-specific genes and repression of alternative fate programs. Epigenetic regulators are enzymes capable of activating or silencing large genomic domains by altering histone modifications, DNA methylation status and chromatin organization. Although differentiating progenitor cells undergo epigenetic changes and epigenetic factors are required for appropriate cell behavior, the precise mechanism of how these proteins influence cell fate remains unclear. In this dissertation, I examine the role of histone deacetylase 3 in control of neural crest and cardiac progenitor cell commitment. Using Cre-mediated genetic deletion, I generated tissue-specific mouse models to study the function of Hdac3 in both neural crest and cardiac cells. These studies revealed a critical role for Hdac3 in maintaining neural crest proliferation and cell survival through regulation of a core network of factors required for craniofacial development. In cardiac progenitors, Hdac3 maintains appropriate differentiation into the cardiomyocyte, smooth muscle and endothelial cell lineages that make up the developed heart. Hdac3 represses a cardiomyocyte-specific gene program and prevents precocious differentiation of progenitors into the myocyte lineage. Surprisingly, this protein does not require deacetylase activity to repress myocyte commitment, and instead serves as a tether to retain myocyte-specific genomic loci at the nuclear periphery. This novel mechanism of gene repression and lineage specification highlights the role that nuclear architecture plays in controlling transcriptional activity and progenitor cell behavior.

Degree Type
Dissertation

Degree Name
Doctor of Philosophy (PhD)

Graduate Group
Cell & Molecular Biology

First Advisor
Jonathan A. Epstein

Second Advisor
Nancy A. Speck

Keywords
Cardiac Development, Histone Deacetylase 3, Lamina Associated Domains, Progenitor Commitment

Subject Categories
Cell Biology | Developmental Biology | Molecular Biology

EPIGENETIC REGULATION OF PROGENITOR CELL COMMITMENT BY HDAC3

Mudit Gupta

A DISSERTATION

in

Cell and Molecular Biology

Presented to the Faculties of the University of Pennsylvania

in

Partial Fulfillment of the Requirements for the

Degree of Doctor of Philosophy

2014

Supervisor of Dissertation

_____

Jonathan A. Epstein, MD
Professor, Cell and Developmental Biology

Graduate Group Chairperson

_____

Daniel S. Kessler, PhD
Associate Professor, Cell and Developmental Biology

Dissertation Committee

Nancy A. Speck, PhD, Professor, Cell and Developmental Biology
Edward E. Morrisey, PhD, Professor, Department of Medicine
Christopher J. Lengner, PhD, Assistant Professor, Department of Animal Biology, School of Veterinary Medicine
Paul J. Gadue, PhD, Assistant Professor, Pathology and Laboratory Medicine
Mitchell J. Weiss, MD, PhD, Professor, Department of Hematology, St. Jude Children's Research Hospital

Acknowledgements

First, I would like to thank Jon for his incredible mentorship and for building a lab that is the perfect learning environment for a graduate student. He has taught me much more in four years than I thought I could possibly learn. I would also like to thank the current and former members of the Epstein lab who have put up with me all this time and to our MCRC colleagues for their wonderful work. Many thanks to members of the Gearhart and Berger labs for patiently introducing me to the techniques and expertise that made this work possible. I would like to thank Mitch, Nancy, Ed, Chris and Paul for serving on my thesis committee and for their input throughout this process. I would also like to thank the combined degree office including Skip, Maggie and Maureen for navigating the way through this training road. Finally, I would like to thank my family both in Michigan and in Philly for all their patience and support. Many people have contributed in many ways to this thesis.

ABSTRACT

EPIGENETIC REGULATION OF PROGENITOR CELL COMMITMENT BY HDAC3

Mudit Gupta

Jonathan A. Epstein

Tissue-specific progenitor cells emerge during development to expand and differentiate into the multiple cell lineages that populate the embryo. Appropriate differentiation of these precursor cells requires coordinated expression of numerous lineage-specific genes and repression of alternative fate programs. Epigenetic regulators are enzymes capable of activating or silencing large genomic domains by altering histone modifications, DNA methylation status and chromatin organization. Although differentiating progenitor cells undergo epigenetic changes and epigenetic factors are required for appropriate cell behavior, the precise mechanism of how these proteins influence cell fate remains unclear. In this dissertation, I examine the role of histone deacetylase 3 in control of neural crest and cardiac progenitor cell commitment. Using Cre-mediated genetic deletion, I generated tissue-specific mouse models to study the function of Hdac3 in both neural crest and cardiac cells. These studies revealed a critical role for Hdac3 in maintaining neural crest proliferation and cell survival through regulation of a core network of factors required for craniofacial development. In cardiac progenitors, Hdac3 maintains appropriate differentiation into the cardiomyocyte, smooth muscle and endothelial cell lineages that make up the developed heart. Hdac3 represses a cardiomyocyte-specific gene program and prevents precocious differentiation of progenitors into the myocyte lineage. Surprisingly, this protein does not

require deacetylase activity to repress myocyte commitment, and instead serves as a tether to retain myocyte-specific genomic loci at the nuclear periphery. This novel mechanism of gene repression and lineage specification highlights the role that nuclear architecture plays in controlling transcriptional activity and progenitor cell behavior.

Table of Contents

List of Tables

List of Figures

Chapter 1. Introduction

Summary

The cells that make up a developing organism are called upon to proliferate, apoptose, differentiate or remain uncommitted in a precise and coordinated fashion. To undergo such dramatic changes, cells must be able to activate and silence broad sets of genes in a synchronized manner. Epigenetics has emerged as a powerful system of regulation that enables control of gene expression without changing the DNA itself. In this chapter, I will summarize how these precursor cells were first defined and studied, review known regulators of cell behavior and introduce nuclear architecture as a novel mechanism of epigenetic regulation during development. A portion of this introduction has been adapted from a chapter written by Jonathan Epstein, Rajan Jain and me for a textbook on congenital heart disease, "*Cardiac Malformation*" by Rickert-Sperling, Kelly and Driscoll which is, as yet, unpublished. The portions included here were primarily written by me.

Progenitor cell biology

Patterning of a multicellular organism from a single, totipotent cell requires a series of commitment steps as the original cell expands and differentiates into the numerous tissues that make up the body. In mammalian development, development begins with fertilization of the egg, formation of the zygote and a series of cleavage events generating the blastocyst. Each blastocyst is a multi-layered structure made up of an inner cell mass surrounded by the trophoblast layer. The trophoblast eventually forms extraembryonic structures including the placenta. The inner cell mass, however, is made up of cells that will give rise to the entirety of the embryo (Hogan et al., 1986). The cells of the inner cell mass can be isolated and grown in culture, yielding embryonic stem cells (ESCs). A stem cell is defined as a clonal precursor with ability to both self-renew and differentiate into more committed progeny. For example, pluripotent ESCs are able to self-renew, forming more embryonic stem cells, and differentiate into every cell type found in the embryo.

In contrast to stem cells, the term progenitor has entered common use to refer to a more differentiated precursor cell. A progenitor cell is defined as a clonal precursor with a limited set of progeny and no capacity for self-renewal. As development progresses from the blastocyst stage to specification of the three germ layers endoderm, ectoderm and mesoderm to organogenesis, multipotent somatic stem cells are retrieved to expand and differentiate into tissue-specific progenitor cells that give rise to more limited sets of progeny that comprise various tissues. These fate decisions

require precise regulation at each step to ensure cell expansion and differentiation occurs normally. Proper understanding of the regulatory mechanisms behind progenitor cell behavior is essential for both identifying the causes of congenital defects and harnessing stem and progenitor cells for treatment of disease. A hallmark of progenitor cell differentiation is altered expression of a wide program of lineage-specific genes. For example, differentiation of a hematopoietic stem cell into a common myeloid progenitor requires upregulation of dozens of myeloid-specific genes and silencing of a lymphoid-specific gene program, repressing the alternative fate (Weissman et al., 2001). This simultaneous gene activation and gene silencing requires precise coordination. In this thesis, I focus on an epigenetic modifier, Hdac3, which functions as a regulator of progenitor cell fate by synchronizing expression of broad gene programs in both neural crest and cardiac progenitors.

Hematopoietic progenitors

The best-studied precursor cell is the hematopoietic stem cell (HSC). Through classical studies in mice, Till and McCulloch injected single precursor cells derived from bone marrow into lethally irradiated mice and observed colony formation in the spleen proportional to the number of injected cells (Till and McCulloch, 1961). This seemingly simple observation was the first direct evidence for the existence of a stem cell with the capacity to self-renew, repopulate a depleted animal and differentiate into clones of progeny. From this early observation, our understanding of hematopoietic development grew as new techniques for identification of specific cell populations with antibodies to

surface markers, isolation of marked cells with high-speed cell sorting and assays to promote derivation of every hematopoietic lineage (reviewed by Weissman et al., 2001). Utilizing these technologies to characterize the hematopoietic stem cell, the Weissman group identified a population of multipotent progenitors (MPPs) downstream of HSCs without the capacity for self-renewal and with a more limited variety of progeny (Morrison et al., 1997). From the appearance of this first progenitor downstream of HSCs, the hematopoietic hierarchy branches into myeloid and lymphoid lineages with the common myeloid progenitor and common lymphocyte progenitor cells. These two cell types give rise to even more restricted sets of progeny, express different gene programs and can be isolated individually based on different surface markers. From this point in the hierarchy, subsequent progenitor cells become even more restricted to differentiating into a limited number of cell types and still without the capacity to self-renew (Weissman et al., 2001). Taken together, several decades of classical lineage tracing and clonal analysis studies have defined a hematopoietic hierarchy that serves as the template for progenitor cell maturation pathways in a variety of embryonic tissues (Figure 1.1).

Neural crest

Another cell type that exemplifies progenitor cell behavior is the neural crest. The neural crest is often described as the “fourth germ layer,” giving rise to a wide variety of lineages and forming a significant portion of the vertebrate embryo. First identified by Wilhelm His in 1868, the neural crest was originally termed *Zwischenstrang*, the intermediate cord, for its physical proximity to the developing neural tube and epidermal

ectoderm (reviewed by Achilleos and Trainor, 2012; Crane and Trainor, 2006). Arthur Milnes Marshall later named this structure the “neural crest,” as it forms upon the fusion of the two neural ridges dorsal to the “neural canal.”

This remarkable collection of multipotent cells has the ability to differentiate into a broad range of lineages including neurons of the peripheral nervous system, secretory cells of the adrenal medulla, smooth muscle, bone and melanocytes (reviewed by Dupin and Sommer, 2012). Once neural crest cells were identified and isolated in the late nineteenth and early twentieth centuries, classical fate mapping studies were required to determine the capacity of these cells. In an early form of lineage tracing, Le Douarin and colleagues capitalized on the morphological differences between chick and quail cells to analyze both neural crest differentiation and sensitivity to environmental cues (Le Douarin et al., 1975). Utilizing a chick-quail chimera system, the authors began by ablating a portion of the trunk neural tube in chick embryos early in development, before the onset of neural crest migration. Next, a different segment of neural tube from a stage-matched quail embryo was grafted onto the chick host and cells were allowed to migrate from the quail donor into the host tissue. Histological analysis revealed that neural crest cells from the heterotopic quail graft were able to migrate into the chick embryo, appropriately differentiate into cholinergic neurons and engraft.

This breakthrough study revealed that quail neural crest cells from a domain that normally becomes adrenergic neurons have the capacity to differentiate into cholinergic neurons if placed in the appropriate environment. *In vitro* studies of cultured chick neural

crest cells revealed that this population gives rise to both melanocytes and adrenergic cells (Bronner-Fraser et al., 1980). Further studies of isolated, single neural crest cells confirmed that a single progenitor cell has the potential to give rise to both neuronal and melanocyte cells (Bronner-Fraser et al., 1980). With the advent of vital cell dyes, *in vivo* lineage tracing studies of single cells became possible. Labeling of single premigratory or migrating neural crest cells revealed that at both stages, individual neural crest cells have the potential to become both neuronal and non-neural cell types (Bronner-Fraser and Fraser, 1989, 1988). The majority of cranial neural crest cells, for example, give rise to neuronal, glia and melanocyte lineages. This varied, yet limited differentiation capacity is consistent with neural crest cells behaving primarily as progenitors, more restricted than pluripotent stem cell populations.

As noted in the earliest observations of neural crest cells by His and Marshall, the neural crest forms at the interface between surface ectoderm and the dorsal neural plate. Once the two halves of the neural plate curl and fuse at the midline to form the neural tube, this neural plate border comes in direct contact with the surface ectoderm, initiating a series of cell-cell signaling events that promote induction of the neural crest. One of the critical signaling cues of this process is establishment of a BMP gradient (Achilleos and Trainor, 2012). BMP inhibitors secreted by the underlying mesoderm help form zones of low, medium and high BMP signaling that promote induction of the neural plate, neural crest and surface ectoderm, respectively (Marchant et al., 1998).

After induction and specification at the dorsal neural tube, neural crest cells undergo an epithelial-to-mesenchymal transition (EMT) to delaminate and begin migration throughout the embryo. The EMT process involves reorganization of the cell cytoskeleton, dissolution of cell junctions, remodeling of extracellular matrix components and activation of several signaling pathways and transcription factors (Achilleos and Trainor, 2012; Crane and Trainor, 2006). For example, *Snail* genes are expressed during EMT and serve as markers of neural crest cells undergoing delamination. This gene family functions as transcriptional repressors and Snail expression during EMT downregulates *Cadherin* genes, depleting cell junctions and allowing delamination and migration to occur (Taneyhill et al., 2007). Once the cranial, cardiac, vagal and trunk neural crest cells begin to migrate, they follow well-mapped routes to various destinations at each axial level to differentiate into the appropriate tissue types. To navigate these migration routes, neural crest cells express a series of factors to remodel the extracellular matrix, maintain appropriate cell cycling and respond to guidance cues (Achilleos and Trainor, 2012; Sauka-Spengler and Bronner-Fraser, 2008). Matrix metalloproteases including MMP2 permit matrix breakdown, *cyclin D1* and *D2* are upregulated during delamination to promote proliferation of migrating neural crest and expression of Ephrin receptors ensures appropriate guidance of cardiac crest to the aortic arch arteries.

At each stage of neural crest induction, migration and differentiation, a series of transcriptional programs are activated or repressed to ensure proper cell function. Molecular studies in several vertebrate models have identified components of these gene regulatory networks. Despite outlining the transcription factors and target genes

within these networks, our understanding of the upstream activators of the transcriptional programs and the mechanisms for maintaining their coordinated expression remains incomplete. Given the number of developmental defects related to neural crest-derived structures including craniofacial abnormalities and congenital heart diseases, elucidating the mechanisms controlling neural crest behavior is of critical importance.

Cardiac progenitors

A subtype of neural crest cells, the cardiac neural crest, arises from the otic placode through the third somite to give rise to elements of the cardiac outflow tract. Classical work by Kirby revealed that avian cardiac neural crest cells migrate to the developing aortic arch arteries to differentiate into smooth muscle and also contribute to the aorticopulmonary septum (Creazzo et al., 1998; Kirby et al., 1983). Aside from the outflow tract, the majority of the working myocardium arises from several pools of cardiac progenitor cells (CPC). The heart is the first organ to form in the embryo, with a detectable heartbeat present in mice by embryonic day 9. Early characterization of cardiac progenitor cells was performed in chick embryos employing several techniques also used to investigate the neural crest. In the late 1930s, Mary Rawles cultured explants from several regions of early chick embryos to map embryonic regions with the potential to form beating tissue *ex vivo* (reviewed by Eisenberg et al., 2004). Later, transplant experiments by Stalsberg and DeHaan utilized radiolabeled tissue fragments from chick donors to trace migration and engraftment of labeled cells in recipient embryos (Stalsberg and DeHaan, 1969). More recently, linage tracing with vital cell dyes

has enabled tracking of individual CPCs and monitoring of differentiation into the various tissue types found in the heart (Redkar et al., 2001).

These studies used very different methodologies to generate nearly identical fate maps of cardiac progenitor cells. To summarize the findings of these groups and others, committed cardiac precursor cells arise from the primitive streak mesoderm. These mesodermal cells initially express pan-mesoderm marker *Brachyury* which is replaced by cardiac-specific *Mesp1* expression as the mesoderm begins to commit to the cardiac lineage (reviewed by Wu et al., 2008). These *Mesp1*$^{+}$ precursor cells migrate away from the primitive streak, expanding and condensing into the anterior and lateral plate mesoderm on either side of the midline. Once these pockets of CPCs expand medially and fuse, they are known as the cardiac crescent and begin to express cardiac-specific transcription factor *Nkx2.5*. This population of cardiac progenitor cells is known as the first heart field (FHF), expresses markers *Tbx5*, *Mlc2a* and *Hcn4* and goes on to populate the left ventricle and both atria (Liang et al., 2013; Später et al., 2013). Following specification of the FHF, a second wave of progenitors known as the second heart field (SHF) emerges posterior to the cardiac crescent, expresses markers *Isl1* and *Mef2c-AHF* and contributes to the right ventricle, atria and outflow tract (Cai et al., 2003; Verzi et al., 2005).

The cardiac progenitors of both the FHF and SHF are thought to be multipotent, with the ability to differentiate into cardiomyocytes, smooth muscle and endothelial cells. *In vitro* studies with both embryonic stem cell-derived and explanted tissue have

demonstrated that these CPCs contribute to the three cardiac lineages at both the population and single cell level (Kattman et al., 2006, 2011; Moretti et al., 2006, 2010; Wu et al., 2006). ESC-derived cardiac progenitor cells express surface markers Flk1 and PDGFRα, growth factor receptors, enabling their isolation and clonal analysis. Single cell culture of $Flk1^{+}PDGFR\alpha^{+}$ cells revealed that each individual progenitor cell has the capacity to form cardiomyocytes, smooth muscle and endothelial cells (Kattman et al., 2006). Similar findings were seen with isolated $Isl1^{+}$ and $Nkx2.5^{+}$ cells (Moretti et al., 2006; Wu et al., 2006).

In vivo studies of CPC potential and behavior began with early clonal analysis of individual fate mapped precursor cells. Pioneering work by Buckingham established the presence of multiple heart fields and subpopulations within the cardiac progenitor pool with differing developmental commitments (Meilhac et al., 2004a, 2004b). Subsequent studies utilizing progenitor-specific *Cre* alleles confirmed that at the population level, FHF and SHF cardiac progenitors have the capacity to differentiate into cardiomyocyte, smooth muscle and endothelial lineages *in vivo* (Liang et al., 2013; Moretti et al., 2006; Später et al., 2013; Wu et al., 2006). More recently, inducible, progenitor-specific alleles have permitted clonal analysis of individual CPCs. These studies suggest that *in vivo*, single cardiac progenitor cells have a similar ability to differentiate into multiple lineages as previously demonstrated in culture (Lescroart et al., 2014; Peng et al., 2013).

Despite significant evidence that cardiac progenitor cells are multipotent and play a critical role in populating the embryonic heart, the regulatory mechanisms governing

CPC differentiation and lineage commitment remain unclear. *In vitro* culture of ES-derived CPCs has enabled identification of individual signaling molecules and transcription factors required for appropriate progenitor differentiation (Kattman et al., 2006, 2011), however the broader control mechanisms of CPC behavior remain to be determined. Culture studies have demonstrated that both BMP signaling and Wnt inhibition are essential for appropriate commitment to the cardiomyocyte lineage. A broad array of cytoskeletal and sarcomeric factors must be expressed while alternative fate genes must be silenced for myocyte specification to proceed. Coordinated expression of these lineage-specific gene programs is essential to CPC commitment, and epigenetic regulatory factors have emerged as potential mediators of this genetic synchronization.

Epigenetics

Introduction

Epigenetics is the study of heritable changes to the genome and gene expression patterns that are not caused by direct changes to the DNA sequence. Examples of these changes include post-translational modifications to DNA-bound histone proteins, DNA methylation and remodeling of chromatin architecture. Collectively, epigenetic changes are an additional layer of regulation that affects transcriptional activity of genes while leaving the DNA sequences unaltered (reviewed by

Chang and Bruneau, 2012; Lee and Young, 2013; Li and Reinberg, 2011). Sequence variants or mutations affecting enzymes responsible for modifying or sensing epigenetic marks have been identified in patients with congenital heart disease (CHD) and small molecule inhibitors of epigenetic complexes have shown promise as therapies for adult heart diseases (Anand et al., 2013; Zaidi et al., 2013). Additionally, transgenic mice harboring mutations or deletions of genes encoding epigenetic enzymes recapitulate aspects of human disease (Haberland et al., 2009a; Hurd et al., 2010; Trivedi et al., 2007). Taken together, these findings suggest that the evolving field of epigenetics will inform our understanding of human disease and offer new therapeutic opportunities.

Coordinated expression of genes coded by the DNA sequence of the genome requires precise temporal and spatial interactions between protein factors in the nucleus and the DNA. Work over the last half century has revealed that these interactions are highly influenced by the manner in which DNA is packaged and organized as chromatin (reviewed by Zhou et al., 2011). The basic unit of chromatin is the nucleosome, a complex of 147 bases of DNA wound around an octameric core of histone proteins. The spacing and number of nucleosomes determines chromatin density, with the DNA within highly dense heterochromatin being less accessible to nuclear factors than sequences within relaxed, less dense euchromatin. As a result, genes within heterochromatic regions tend to be silenced while euchromatic loci are typically active. Clusters of nucleosomes are further condensed so that the genome can be efficiently packaged into the nucleus.

The first epigenetic modification to be identified was methylation of the DNA itself. Methylation of cytosine residues is typically associated with transcriptional silencing, and a number of enzymes are responsible for adding and removing these methyl groups (Smith and Meissner, 2013). Another type of epigenetic modification involves post-translational modifications of histone proteins, including methylation and acetylation of lysine residues. These modifications modulate the recruitment of additional protein complexes that regulate chromatin density and conformation. A host of "writer" and "eraser" enzymes exists to add and remove specific modifications from histone tails, and the description of these growing families of enzymes is rapidly evolving. Histone methyltransferases and deacetylases are among the most studied of these "writer" and "eraser" enzymes, respectively, in the context of cardiac development and disease. Covalent modifications of histone proteins are sensed by "reader" proteins that affect downstream changes in chromatin in response to changes in epigenetic marks. Included in this class of proteins are chromodomain-containing proteins such as CHD7, a member of a larger family of ATP-dependent chromatin remodeling complexes. Mutations in the gene encoding CHD7 have recently been identified in patients with congenital heart disease (Hurd et al., 2010).

Epigenetic changes during cardiac development

The explosion of next generation sequencing technologies coupled with the improved efficiency of directed differentiation of embryonic stem cells into cardiac lineages has enabled mapping of the landscape of histone modifications over the course

of cardiac differentiation. Most prominently, work by the Bruneau and Boyer laboratories and the Murry group has shed significant light on the dynamics of gene activation and repression during cardiac specification (Paige et al., 2012; Wamstad et al., 2012). By taking snapshots at a series of well-defined time points in mouse and human ESC differentiation, these groups defined the presence of various histone modifications across the genome during cardiogenesis using chromatin-immunoprecipitation coupled with massively paralleled sequencing (ChIP-Seq). Specifically they observed unique histone modifications marking transcription start sites (H3K4me3), enhancers (H3K4me1 and H3K27ac) and inactive chromatin (H3K27me3), thus providing an initial “map” of the dynamic epigenetic landscape during cardiac development. A theme that emerges from these surveys is that genes specific to non-cardiac lineages such as endoderm and ectoderm derivatives are rapidly marked by repressive histone modifications, resulting in active repression of these lineages. These findings support the hypothesis that cell differentiation requires active silencing of alternative lineages. These studies also suggest that cardiac-specific enhancers are marked by monomethylation of lysine 4 (H3K4me1), and further insights will result from integration of the publically available databases resulting from this work with ongoing studies.

Histone modifications

Epigenetic studies have focused on understanding how histone proteins undergo post-translational modifications, which amino acid residues are subject to these modifications and how various combinations of modifications affect gene expression

(Chang and Bruneau, 2012; Ohtani and Dimmeler, 2011). Methylation and acetylation are two of the most common and well-studied histone modifications. Histones can be methylated on a variety of residues and Jumonji domain-containing proteins act as demethylases. Histone acetyltransferases (HATs) acetylate lysine residues primarily on histone tails and histone deacetylase enzymes (Hdacs) reverse this process. Additional forms of histone modification have been described and continue to be discovered, though application to development and disease awaits further study.

Histone deacetylase enzymes

Histone deacetylases (Hdacs) remove acetyl groups from lysine residues, typically resulting in compaction of chromatin and repression of gene expression. There are five classes of Hdac proteins: I, IIa, IIb, III and IV (reviewed by Thiagalingam et al., 2003). Class I includes Hdacs 1, 2, 3 and 8 and these enzymes are expressed in most tissues. Hdacs 1 and 2 are members of several repressive complexes including Sin3, CoREST, NuRD and PRC2. Hdacs 4, 5, 7 and 9 comprise the class IIa subfamily of Hdacs. Class IIa Hdacs exhibit minimal deacetylase activity *in vivo* and *in vitro* due to evolutionary divergence of a critical tyrosine residue within the catalytic pocket. These Hdacs are characterized by a highly conserved Mef2-binding domain. In addition, class IIa Hdacs act as signal integrators through interactions with 14-3-3 chaperone proteins to facilitate shuttling in and out of the nucleus. Class III sirtuins require NAD^+ for deacetylation activity and have been studied in the context of cardiac hypertrophy. Hdac11 is the sole member of class IV Hdacs and is expressed in the heart, however its

function remains poorly described. Of particular to our work, Hdac3 regulates cell fate in both neural crest and cardiac development (Lewandowski et al., 2014; Singh et al., 2011a).

Hdac3

Hdac3 is expressed in both the premigratory neural crest and cardiac progenitor cells during development. Germline deletion leads to lethality during gastrulation, before the neural crest is induced or the heart is formed (Bhaskara et al., 2008). Tissue-specific knockouts have provided insight into Hdac3 function in hematopoietic progenitors, neural crest and CPCs (Lewandowski et al., 2014; Singh et al., 2011a; Summers et al., 2013). Loss of *Hdac3* in premigratory neural crest results in embryonic lethality and abnormal contribution to the developing outflow tract (Singh et al., 2011a). Neural crest cells migrate to developing aortic arch arteries and differentiate into smooth muscle cells, ensuring appropriate patterning of the outflow tract. Previous work from the Epstein lab demonstrated that loss of *Hdac3* results in deficient vascular smooth muscle and congenital outflow tract defects including double outlet right ventricle and aortic coarctation, due in part to decreased Notch signaling.

CPC-specific deletion of *Hdac3* results in embryonic lethality late in gestation and ventricular hypoplasia (Lewandowski et al., 2014). Hdac3 acts as a repressor of Tbx5, a known driver of cardiogenesis which also plays critical roles in development of the

cardiac conduction system and atrial septation (Li et al., 1997; Wamstad et al., 2012). Through deacetylation of Tbx5, Hdac3 prevents expression of cardiomyocyte-specific genes, promoting a thin myocardial phenotype. Cardiomyocyte-specific deletion of *Hdac3* during mid-late gestation with the alpha-myosin heavy chain Cre (*aMHC-Cre*) permits survival until 3-4 months of age, when mice succumb to severe cardiac hypertrophy and fibrosis (Montgomery et al., 2008). Interestingly, work from the Epstein and Lazar labs demonstrated that deleting *Hdac3* in postnatal myocardium and skeletal muscle with myosin creatine kinase Cre (*MCK-Cre*) results in a very mild phenotype and no lethality unless the mice are stressed by a high fat diet (Sun et al., 2011). Switching the mice from normal chow to a high fat diet results in severe hypertrophic cardiomyopathy and fibrosis followed by lethality of all animals within several weeks. Myocardial *Hdac3* inactivation causes extensive metabolic dysregulation of lipid and glucose processing. Consistent with these findings, Hdac3 is unique among Hdacs for its interaction with the NCoR-SMRT co-repressor complex that has been previously implicated in metabolic regulation (Codina et al., 2005; Guenther et al., 2001; Sun et al., 2012).

Hdac3 is also a potent regulator of cell proliferation and directly regulates p21. Previous work in cancer cells and hematopoiesis linked Hdac3 to cell cycle progression and DNA replication (Summers et al., 2013; Zeng et al., 2006). Transgenic overexpression of *Hdac3* in cardiomyocytes causes increased proliferation and ventricular hyperplasia (Trivedi et al., 2008). Expression analysis indicated that Hdac3 represses several cyclin-dependent kinase inhibitors, reducing levels of these cell cycle checkpoints and promoting rapid proliferation of cardiomyocytes.

Recent work from the Lazar group has raised the intriguing possibility that Hdac3 functions as a transcriptional repressor in a deacetylase-independent manner. While liver-specific deletion of *Hdac3* results in severe hepatosteatosis, re-introduction of a mutant form of Hdac3 lacking deacetylase activity is able to rescue most of the functional and transcriptional deficiency (Sun et al., 2012, 2013). Furthermore, global loss of detectable Hdac3 enzymatic activity does not result in any overt developmental phenotype (You et al., 2013). This surprising finding stands in stark contrast to the early embryonic lethality associated with germline knockout of *Hdac3* (Bhaskara et al., 2008). Given the previous studies connecting Hdac3 to cardiac development and emerging evidence for a non-deacetylase function of Hdac3, it is possible that Hdac3 serves as a regulator of progenitor cell commitment in a deacetylase-independent manner.

Chromatin architecture

An emerging level of epigenetic regulation is the spatial orientation and three-dimensional structure of chromatin (reviewed by Van Bortle and Corces, 2013; Li and Reinberg, 2011; Meister et al., 2011). Dense, heterochromatic regions are associated with repressed gene activity and euchromatic regions with a more open conformation permit increased access by transcription factors to the DNA and are associated with increased gene transcription. Regulating higher order chromatin structure in this way

allows for simultaneous control of large genomic regions and coordination of gene expression–a requirement for large-scale processes such as cell differentiation and stress response. For example, epigenetic mapping has demonstrated that as cells exit pluripotency during development and become more lineage-restricted, levels of heterochromatin increase and the genome becomes more compact while cell fates stabilize (Paige et al., 2012).

Genome-nuclear lamina interactions

New insight into chromatin organization within the interphase nucleus has made it clear that the localization of genes within the nucleus can affect gene expression. Several recent studies have revealed, for example, that the conformation of chromatin at the nuclear periphery versus in the nucleoplasm is very different (Bickmore and van Steensel, 2013; Pickersgill et al., 2006). The inner surface of the nuclear membrane is coated by a thin layer of intermediate filament proteins called lamins. Chromatin found at the nuclear lamina, lamina associated domains (LADs), tends to be transcriptionally silent and forced tethering of reporter genes to the nuclear periphery results in repression (Reddy et al., 2008). Genome-wide mapping studies have revealed that the organization of chromatin at the nuclear lamina versus the interior of the nucleus is dynamic and varies over the course of cell differentiation (Peric-Hupkes et al., 2010). The significance of these changes during development is still a matter of intense study; however, it is clear that several diseases with cardiac manifestations are caused by mutations in nuclear lamina-associated proteins. These laminopathies include

Hutchinson-Gilford progeria syndrome and Emery-Dreifuss muscular dystrophy and are due to mutations in genes encoding Lamin A and its interacting protein Emerin, respectively (Ho et al., 2013; Shin et al., 2013). While these diseases are caused by disruptions of the nuclear lamina, further study is required to establish whether changes in chromatin organization are responsible for the observed phenotypes.

Hdacs and LADs

Regions of chromatin in lamina associated domains are typically decorated with repressive histone marks and contain genes that are transcriptionally silent (Bickmore and van Steensel, 2013; Guelen et al., 2008). Additionally, epigenetic complexes including NuRD and NCoR-SMRT are found at the nuclear periphery, suggesting that these complexes may function to repress lamina-bound chromatin (Berk et al., 2014; Demmerle et al., 2012; Pegoraro et al., 2009). To determine whether the Hdacs within these complexes are responsible for silencing genes within LADs, Nurminsky and colleagues analyzed the effect of *Hdac1* or *Hdac3* knockdown on chromatin attachment to the lamina and subsequent gene expression (Milon et al., 2012). Analysis in *Drosophila* S2 cells demonstrated that Hdac1 is responsible for deacetylation and gene repression of genes within LADs, while Hdac3 primarily acts as a tether, retaining chromatin at the lamina. This finding is supported by work from Reddy and Singh, demonstrating that in a complex with a BTB domain-containing transcription factor and a lamina-bound anchor protein, Hdac3 facilitates the tethering of LADs to the nuclear periphery in mammalian cells (Zullo et al., 2012). When combined with mapping studies

showing dynamic movement of LADs during ESC differentiation, it is possible that Hdacs regulate LADs to help modulate lineage-critical gene expression and influence progenitor cell commitment (Figure 1.3 and Peric-Hupkes et al., 2010).

Conclusions

Understanding the control mechanisms underlying progenitor cell fate decisions is important for identifying the factors critical for normal development and mapping the systems disrupted in disease. In the neural crest and cardiac progenitor populations, epigenetic regulators offer the ability to coordinate expression of dozens of target genes at critical time points, ensuring appropriate expansion and differentiation. Hdac3 has a canonical repressive function as a modifier of histone proteins; however, recent work suggests a deacetylase-independent activity. Emerging clues from the literature suggest that Hdac3 may regulate gene positioning and nuclear architecture, however the role of this non-canonical function in progenitor cell biology remains unclear.

Figure 1.1: Hierarchy of hematopoietic precursor commitment

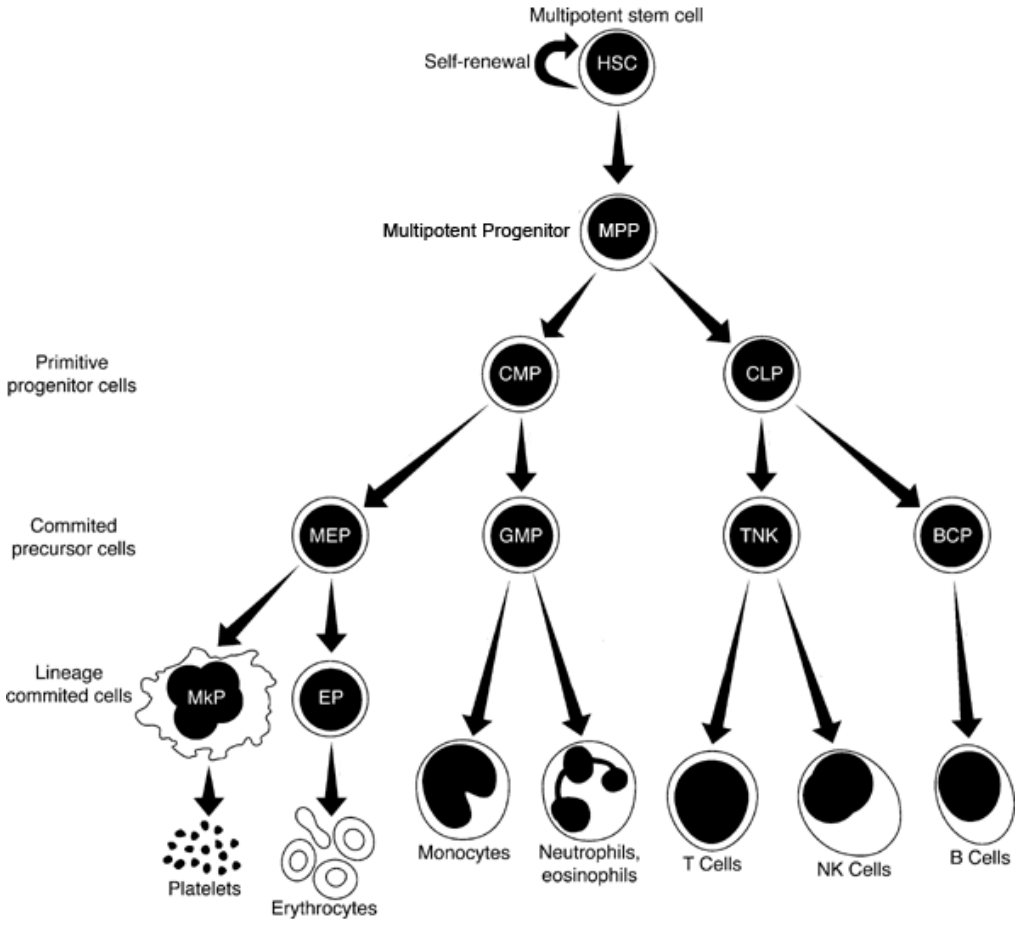

Figure 1.1: Hierarchy of hematopoietic precursor commitment

Schematic of hematopoietic precursor cell commitment from self-renewing, multipotent hematopoietic stem cells (HSC) to multipotent progenitors (MPP) to common lymphoid progenitors (CLP) and common myeloid progenitors (CMP). These cells commit to specific lineages as granulocyte–macrophage progenitors (GMP), megakaryocyte erythroid progenitors (MEP), megakaryocyte progenitors (MkP) and T-cell natural killer cell progenitors (TNK). This hierarchy serves as a model for progenitor cell commitment in several other tissues including neural crest and cardiac progenitors. Adapted from Robb, 2007.

Figure 1.2: Hierarchy of cardiac precursor commitment

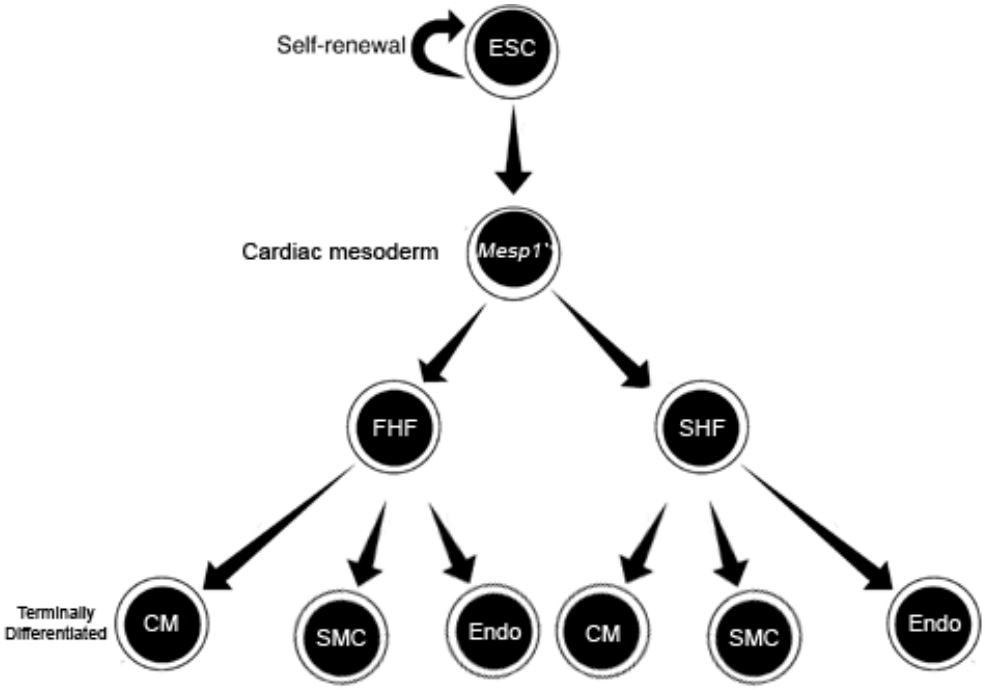

Figure 1.2: Hierarchy of cardiac precursor commitment

Schematic of *in vitro* cardiac precursor cell commitment from self-renewing, pluripotent embryonic stem cells (ESC) to cardiac mesoderm marked by Mesp1 expression to first heart field (FHF) and second heart field progenitors (SHF). These cells commit to specific lineages as cardiomyocytes (CM), smooth muscle cells (SMC) and endothelial cells (Endo). Adapted from Robb, 2007.

Figure 1.3: Hdac3 complexes with cKrox and Lap2β to mediate transcriptional silencing of Lamina-associated domains (LADs)

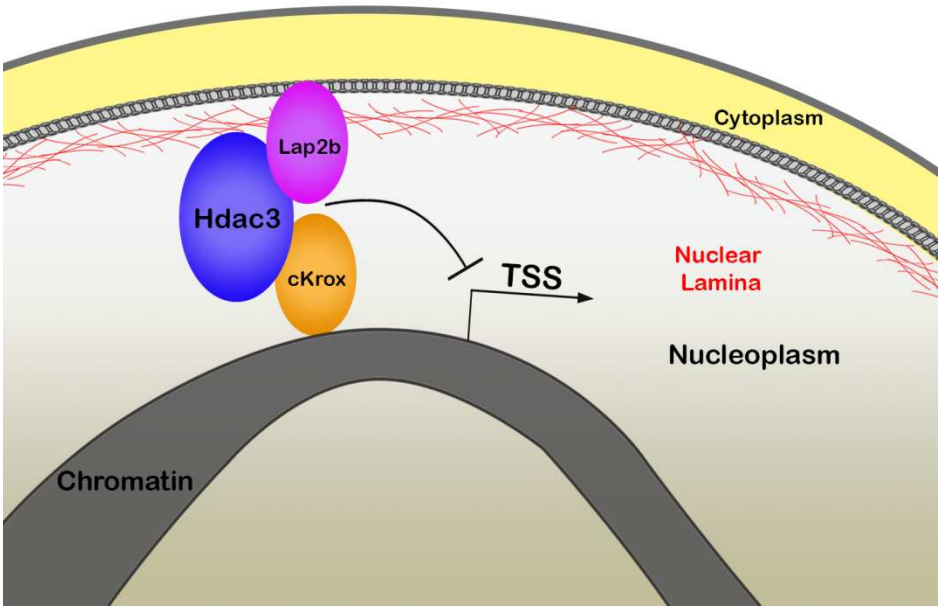

Figure 1.3: Hdac3 complexes with cKrox and Lap2β to mediate transcriptional silencing of Lamina-associated domains (LADs)

Accumulation of HDACs and other transcriptional repressors at the nuclear lamina creates a “silencing environment” responsible for low expression levels of genomic loci positioned at the nuclear periphery. Hdac3 complexes with transcription factor cKrox and lamina-associated protein Lap2β to maintain certain lamina-associated domains (LADs) at the nuclear periphery and repressing genes contained within these regions as schematized by a transcriptional start site (TSS). Adapted from Zullo et al., 2012.

Chapter 2: Murine craniofacial development requires Hdac3-mediated repression of *Msx* gene expression

The work described in this chapter was published in *Developmental Biology* in conjunction with Nikhil Singh (Singh et al., 2013).

Summary

In Chapter 1, I introduced the neural crest as a progenitor cell population emerging from the dorsal neural tube that gives rise to smooth muscle, melanocyte, bone, cartilage and neuronal derivatives throughout the body. Hdac3 is an epigenetic modifier that typically functions as a repressor to silence transcriptional activity. Previous work has described the role of Hdac3 in cardiac neural crest differentiation into aortic arch artery smooth muscle, however the role of Hdac3 in other neural crest subpopulations remains unclear (Singh et al., 2011a). In this chapter I describe the role of Hdac3 in neural crest patterning of craniofacial structures. Mice in which *Hdac3* has been conditionally deleted in premigratory neural crest demonstrate fully penetrant craniofacial abnormalities, including microcephaly, cleft secondary palate and dental hypoplasia. Consistent with these abnormalities, I show dysregulation of cell cycle genes and increased apoptosis in neural crest structures in mutant embryos. Known regulators of cell cycle progression and apoptosis in neural crest, including Msx1, Msx2 and Bmp4, are upregulated in *Hdac3*-deficient cranial mesenchyme. These results suggest that Hdac3 serves as a critical regulator of craniofacial morphogenesis, in part by repressing core apoptotic pathways in cranial neural crest cells.

Introduction

As I introduced in Chapter 1, vertebrates are unique among metazoans in their reliance on neural crest cells to form a wide array of head structures. These neural crest-derived craniofacial components are analogous to mesodermally- and ectodermally-derived structures in invertebrates (Gans and Northcutt, 1983). In midgestation in the mouse, neural crest cells populate the pharyngeal arches – a series of paired outpouchings that flank the developing pharynx, as well as the frontonasal prominence, an area that eventually gives rise to the nose and forehead. The first pharyngeal arch, which is the largest and most rostral of the arches, contains the neural crest cells that will form structures in the face and neck (Alappat et al., 2003). Driven by the proliferation and continued influx of migrating neural crest cells, two distinct outgrowths arising from the first arch, known as the maxillary and mandibular prominences, grow ventrally and flank the developing oropharynx, eventually fusing at the ventral midline in what becomes the face. Failure of neural crest cells to migrate or proliferate appropriately can result in hypoplasia of these structures and the absence of fusion, which can manifest as abnormal facies and clefting (Ito et al., 2003; Vallejo-Illarramendi et al., 2009).

In addition to appropriate proliferation and migration, neural crest patterning depends upon carefully controlled apoptosis of premigratory crest cells. In the developing hindbrain, a premigratory neural crest population arises in each of eight rhombomeres. However, the majority of neural crest cells in rhombomeres 3 and 5 undergo apoptosis, and the few surviving cells make small contributions to the discrete

streams of migrating neural crest that populate and pattern the developing pharyngeal arches (Graham et al., 1993; Sechrist et al., 1993; Birgbauer et al., 1995; Köntges et al., 1996; Ellies et al., 2002). Loss of this selective apoptosis through ablation of rhombomere 4 causes increased survival and migration of crest cells from rhombomeres 3 and 5, resulting in ectopic muscle attachment sites on the developing mandible (Ellies et al., 2002). A signal for selective apoptosis of neural crest cells specifically in these two rhombomeres is induced by increased expression of *Msx2* (Graham et al., 1994). A related member of this muscle segment homeobox family of genes, *Msx1*, is also a proapoptotic factor in neural crest cells and controls programmed cell death by regulating several caspases in the apoptotic pathway (Tríbulo et al., 2004).

Several human syndromes have implicated *MSX* genes in craniofacial development. Some patients with autosomal-dominant Boston-type craniosynostosis harbor a missense mutation in *MSX2* and present with a variety of malformations including abnormal skull shape and cleft palate (Warman et al., 1993; Jabs et al., 1993). Additionally, deletion of the *MSX1* gene in patients with Wolf-Hirschhorn syndrome manifests with a spectrum of ear, tooth, and skull defects (Ivens et al., 1990). These disorders highlight the critical role that Msx factors play in regulating how the neural crest contributes to the derivative structures that make up the calvaria and face.

Murine genetics have also proven invaluable in deciphering the genetic programs that coordinate the proliferation, migration and apoptosis of cranial neural crest cells. For instance, models of conditional deletion and overexpression of Msx1 and Msx2 have

further delineated roles for these molecules in various aspects of craniofacial development. Msx1 has been studied extensively in the developing tooth and is highly expressed in neural crest-derived dental mesenchyme, where it is required for proper condensation and development of the molar tooth germ beyond the bud stage (Satokata et al., 1994; Chen et al., 1996). Deletion of the *Msx1* gene in mice results in reduced *Bmp4* expression in the dental mesenchyme, supporting the well-studied interaction of *Msx* genes and *Bmp4* (Graham et al., 1994; Chen et al., 1996; Bei et al., 2000). In addition to its role in neural crest patterning and apoptosis in the developing hindbrain (Graham et al., 1993, 1994), Msx2 also regulates osteogenesis and functions with Msx1 to control cranial neural crest differentiation into bones of the calvaria (Han et al., 2007; Roybal et al., 2010). Interestingly, both overexpression and inactivation of *Msx2* causes defects in calvaria and tooth development (Dodig et al., 1999; Satokata et al., 2000), suggesting that the Msx1/Msx2 apoptotic pathway must be exquisitely regulated during craniofacial development.

While neural crest proliferation and localized apoptosis are critical for normal craniofacial morphogenesis, little is known about how the pathways controlling these processes are regulated at the epigenetic level. In this chapter, I demonstrate that the class I histone deacetylase Hdac3 regulates genetic programs involved in murine craniofacial development. Global deletion of *Hdac3* results in lethality prior to E9.5 (Bhaskara et al., 2008). Conditional genetic deletion of *Hdac3* in neural crest results in cleft palate, hypoplastic teeth and a variety of defects in calvarial structures of neural crest origin. Loss of *Hdac3* leads to upregulation of established mediators of neural crest

apoptosis, including *Msx1*, *Msx2* and *Bmp4*. These results suggest that Hdac3-mediated repression of Msx signaling plays a critical role in craniofacial development.

Results

Hdac3 is widely expressed during craniofacial development and is efficiently deleted in neural crest derivatives by Wnt1-Cre

In order to explore the epigenomic regulation of craniofacial development, we deleted the class I histone deacetylase *Hdac3* in premigratory neural crest cells using the *Wnt1-Cre* transgene and a floxed *Hdac3* allele (*Hdac3*^{f}) (Jiang et al., 2000; Mullican et al., 2011). Using the Z/EG reporter allele (Novak et al., 2000), we observed that both *Wnt1-Cre; Hdac3*$^{f/f}$ (which we have termed *Hdac3*^{Wnt1NCKO}*); Z/EG* and *Wnt1-Cre; Z/EG* control embryos demonstrate intact migration of neural crest cells into the developing face and pharyngeal arch region at E9.5 (Figure 2.1A, Figure 2.2). Immunohistochemistry of staged embryos demonstrates that Hdac3 is widely expressed in the developing head at E9.5 and E10.5, including in neural crest, ectoderm and endoderm (Figure 2.1B and data not shown). Expression of *PlexinA2*, a neural crest marker (Brown et al., 2001), appears unaltered in *Hdac3* mutant embryos at E9.5 (Figure 2.2), further indicating that neural crest migration is normal at this stage. In *Hdac3*^{Wnt1NCKO} embryos, Hdac3 protein expression is lost in neural crest-derived craniofacial mesenchyme, while expression is retained in ectoderm and endoderm (Figure 2.1B). In the absence of neural crest expression of Hdac3, the maxillary and mandibular prominences of the first pharyngeal arch demonstrate mild hypoplasia as early as E10.5 (Figure 2.1B,C). This is in contrast to the caudal pharyngeal arches,

which demonstrate no hypoplasia at E10.5 in the absence of Hdac3 expression (Singh et al., 2011).

Hdac3^{Wnt1NCKO} embryos exhibit severe craniofacial abnormalities in late gestation, resulting in perinatal lethality

Embryos in which Hdac3 is deleted in neural crest cells are found at expected Mendelian ratios in late gestation and are viable until birth, but uniformly succumb at P0 (Singh et al., 2011). *Hdac3^{Wnt1NCKO}* mice are born with microcephaly, micrognathia, a shortened snout and eyelid closure defects, with preservation of body morphology (Figure 2.3A). Optical projection tomography and histology of *Hdac3^{Wnt1NCKO}* P0 heads reveals cleft palate, which is also apparent in late gestation embryos (Figure 2.3B,C). The palate defect is characterized by a large posterior cleft, without additional facial clefting (Figure 2.3B). Cleft palate is fatal in perinatal mice; afflicted pups are unable to generate suction and nurse, and subsequently die at P0 from dehydration and accumulation of air in the digestive tract (Condie et al., 1997; Qiu et al., 1995). Consistent with these reports, *Hdac3^{Wnt1NCKO}* pups are unable to feed, as evidenced by the lack of a milk spot (Figure 2.3A). The gross craniofacial defects observed in *Hdac3^{Wnt1NCKO}* mice are fully penetrant and are summarized in Table 2.1. We observed similar craniofacial abnormalities using a second neural crest driver, *Pax3^{Cre}* (Engleka et al., 2005); these abnormalities are also fully penetrant both at P0 and in late gestation (Figure 2.4 and data not shown).

Loss of Hdac3 in neural crest leads to bone defects in the calvaria and viscerocranium

In the adult vertebrate, osteoblasts are among the most abundant cell types generated by cranial neural crest. These neural crest-derived osteoblasts contribute to the bones of the face, the skull base and the entirety of the calvaria, with the exception of the parietal bone (Santagati and Rijli, 2003). Hdac3 has previously been implicated in multiple stages of osteoblast differentiation and maturation. In committed, undifferentiated osteoblasts that express the *Osx-Cre* transgene, deletion of Hdac3 leads to subtle abnormalities in calvarial osteoblast differentiation, and progressive abnormalities in trabecular bones that lead to perinatal runting and death early in adulthood (Razidlo et al., 2010).

Consistent with a pro-osteogenic role for Hdac3 at the earliest stages of bone development in neural crest, *Hdac3*^{Wnt1NCKO} mice - in which Hdac3 is deleted prior to osteoblast specification (before the onset of *Osx-Cre* expression) - exhibit severe bone defects in the calvaria and viscerocranium (Figure 2.5). Alcian blue/alizarin red staining of the late embryonic and perinatal mice reveals decreased ossification of the calvaria, particularly in the region of the frontal bone, where ossified bone is nearly undetectable by alizarin red staining (Figure 2.5A). The open frontal fontanel leads to hemorrhage in some newborn pups following parturition (Figure 2.5B). The parietal bone develops normally in *Hdac3*^{Wnt1NCKO} mutants, consistent with its mesodermal origin (Figure 2.5A).

In mutant embryos, ossification abnormalities of the viscerocranium were also identified in the mandible, skull base, and tympanic ring (Figure 2.5A).

Additional bone abnormalities in E17.5 mutant embryos are detectable by Goldner's trichrome staining. Neural crest-derived calvarial bones, including the frontal bone, are thin and show minimal mineralization (Figure 2.5B). Additionally, at variable penetrance, absence of ossification in the sphenoid bone plate results in encephalocoele, in which the brain herniates into the nasal sinuses (Figure 2.5B). The bone defects observed in *Hdac3*^{Wnt1NCKO} mice are summarized in Table 2.1.

To establish whether loss of *Hdac3* in the developing calvaria affects migration and survival of neural crest, or differentiation of osteogenic precursors, we fate mapped cranial crest cells to the E12.5 calvaria using the Z/EG reporter, measured apoptosis with TUNEL staining and evaluated pre-osteoblast differentiation by Runx2 immunohistochemistry (Figure 2.6). We observed that mutant cranial crest exhibit normal migration to the calvaria and normal expression of the critical ossification regulator Runx2 at the frontal bone primordium (Ishii et al., 2003), but demonstrate increased apoptosis compared to controls. These observations suggest that the bone abnormalities in the *Hdac3*^{Wnt1NCKO} mice are associated with decreased survival of neural crest cells, and are unlikely to be due to a primary abnormality in differentiation or migration.

Hdac3 is required for normal odontogenesis

Seminal work in amphibians and avian models established that the cranial neural crest makes up a significant portion of the developing tooth, specifically the dental mesenchyme (LeDouarin, 1982; reviewed by Maas and Bei, 1997). Further studies in mouse demonstrate that patterning of the developing molar tooth germ is influenced by the interaction of the epithelium and mesenchyme. Recombination experiments with neural crest and epithelium revealed that early (E9.5-12.0) oral epithelium can signal to non-dental mesenchyme to form teeth; however, later in development, the dental mesenchyme possesses odontogenic potential to induce non-oral epithelium to become enamel (Kollar et al., 1969; Mina et al., 1987; Lumsden 1988).

In murine tooth development, signals from the epithelium initiate condensation of neighboring mesenchyme composed of neural crest cells at E11.5 (Chen et al., 2000). As epithelial cells invaginate, they envelop neural crest cells, which will eventually form the pulp of the tooth (Figure 2.7A). In *Hdac3*^{Wnt1NCKO} embryos, the early stages of odontogenesis proceed normally, with tooth bud morphology at E15.5 appearing similar to littermate controls through the bud and cap stages (Figure 2.7A-D). However, expansion of the neural crest-derived mesenchyme does not occur between E15.5-E17.5, resulting in hypoplastic teeth with the absence of normal pitting (Figure 2.3C and Figure 2.7E,F). The tooth bud hypoplasia in mutant embryos parallels the hypoplasia observed in other neural crest-derived structures in late gestation (Figure 2.3).

Aberrant cell cycle regulation in Hdac3-deficient cranial mesenchyme leads to a failure of neural crest cell expansion, dental hypoplasia and cleft palate

In order to further delineate the mechanism by which deletion of *Hdac3* results in hypoplasia of neural crest structures, we performed a histological analysis of staged control versus *Hdac3*^{Wnt1NCKO} embryos. In normal palatogenesis, the anterior palate is formed by fusion of the maxillary prominence with the frontonasal prominence. *Hdac3*^{Wnt1NCKO} embryos exhibit posterior cleft palate, suggesting that secondary palatogenesis is disrupted (Figure 2.3B). The posterior aspects of the hard palate (referred to as the secondary palate) are formed from two outgrowths of neural crest-derived mesenchyme that lie on either side of the stomodeum. These outgrowths - the palatal shelves - are detectable at E11.5 in the mouse at both anterior and posterior levels (Figure 2.8A,A'). Between E11.5 and E13.5, the palatal shelves, driven by neural crest cell proliferation, expand towards the mandible (Figure 2.8A,A',B,B'). Between E13.5 and E14.5 the palatal shelves elevate relative to the tongue and fuse in the midline with the nasal septum (Figure 2.8C,C'). This newly formed structure subsequently ossifies, giving rise to the mature secondary palate (Figure 2.8D,D').

Disruption of any of the stages of secondary palatogenesis - palatal shelf formation, expansion, elevation, fusion or ossification – can lead to cleft palate in mice, and similar mechanisms are believed to contribute to secondary cleft palate in humans (He et al., 2011; Ito et al., 2003; Richarte et al., 2007; Vallejo-Illarramendi et al., 2009; Wu et al., 2008). Histological analysis of *Hdac3*^{Wnt1NCKO} embryos reveals that the palatal

shelves form appropriately but are hypoplastic at E12.5 (Figure 2.8E,E',F,F'). Despite appropriate elevation of the medial aspect of the palatal shelves by E14.5, the palatal shelves do not meet at the midline (Figure 2.8G,G'). These results suggest that cleft palate in *Hdac3*^{Wnt1NCKO} embryos is due to a failure of palatal shelf expansion.

Expansion of the palatal shelves is dependent upon proliferation and survival of the neural crest cells that make up the palatal shelf mesenchyme (Ito et al., 2003). In E12.5 mutant versus control palatal shelves that were matched for surrounding anatomical landmarks, we detected a significant increase in apoptosis and a trend towards decreased proliferation, as determined by TUNEL and phospho-histone H3 staining, respectively (Figure 2.8I). Increased TUNEL staining is also visible throughout additional cranial neural crest-derived structures outside of the palatal shelf region including the tooth bud and calvaria, suggesting that hypoplasia of these structures is also mediated by increased apoptosis (Figure 2.6, Figure 2.8I, Figure 2.9E).

To discern the nature of the cell cycle dysregulation in *Hdac3*^{Wnt1NCKO} cranial mesenchyme, we performed expression profiling by quantitative RT-PCR of microdissected anterior cranial tissue of E12.5 mutant embryos and littermate controls (Figure 2.9A). While *Hdac3* expression in mutant tissue is significantly downregulated, expression of the other class I Hdacs is unchanged (Figure 2.9B). Strikingly, the expression of multiple cell cycle regulators is altered in *Hdac3*^{Wnt1NCKO} cranial mesenchyme. *Cdkn1a* (*p21*), *Trp53* (*p53*), *Cdkn1c* (*p57*), *Ccnd1* (*Cyclin D1*), *Ccnd3* (*Cyclin D3*), *CcnG1* (*Cyclin G1*) and *Cdk2* are significantly upregulated in the absence of

Hdac3, while *Cdkn2c* (*p18*) expression is downregulated (Figure 2.9C). This pattern of gene dysregulation is consistent with G1/S arrest of neural crest cells.

Hdac3 has previously been shown to directly repress the cell cycle inhibitor gene *Cdkn1a* (p21) in multiple tissues (Trivedi et al., 2008; Wilson et al., 2008). In order to determine whether the substantial upregulation of *Cdkn1a* observed in *Hdac3*^{Wnt1NCKO} cranial mesenchyme is sufficient to account for cleft palate and microcephaly in these embryos, we deleted *Hdac3* in neural crest on a *Cdkn1a* null background (Deng et al., 1995). Homozygous *Cdkn1a*$^{-/-}$ mice develop normally and are viable and fertile (Deng et al., 1995). We found that loss of *p21* does not rescue the cleft palate and microcephaly observed in *Hdac3*^{Wnt1NCKO} embryos, suggesting that dysregulation of additional cell cycle modulators contributes to altered regulation of neural crest expansion in *Hdac3*-deficient cranial neural crest cells, and ultimately to cleft palate and craniofacial hypoplasia (Figure 2.10).

The loss of Hdac3 results in dysregulation of core networks that regulate craniofacial development

In multiple aspects of embryogenesis, including neural crest development and limb development, the homeobox transcription factors Msx1 and Msx2 and the signaling molecule Bmp4 function to initiate apoptosis (Barlow and Francis-West, 1997; Graham et al., 1994; Lallemand et al., 2005; Marazzi et al., 1997). Msx1 is expressed in the palatal shelves and dental mesenchyme, and regulates development of these neural crest-derived structures (Satokata et al., 1994; Chen et al., 1996; Maas and Bei, 1997;

Bei et al., 2000; Alappat et al., 2003). Msx2 is expressed in the early dental mesenchyme and is also crucial for normal tooth development (Maas and Bei, 1997; Winograd et al., 1997). Bmp4 is primarily expressed by epithelial structures in the developing face, which signal to neural crest-derived mesenchyme to mediate processes such as palatogenesis and odontogenesis, and its expression can be induced by Msx genes in neural crest derivatives (Zhang et al., 2002, Mitsiadis et al., 2010).

We measured the expression of important regulatory genes involved in craniofacial development using a candidate approach, and detected significant upregulation of *Msx1*, *Msx2* and the target gene *Bmp4* in the anterior cranial mesenchyme of E12.5 *Hdac3*^{Wnt1NCKO} embryos, but found no significant differences in the expression of palate-specific markers *Osr2* and *Shox2* (Figure 2.9D, Figure 2.11) (Lan et al., 2004; Yu et al., 2005). *In situ* hybridization reveals substantially more expression of *Msx1* transcripts in the dental mesenchyme of mutant embryos than in littermate controls (Figure 2.9E). We also observe increased expression of *Msx1* in the developing palatal shelves of *Hdac3*-deficient embryos compared to littermate controls (Figure 2.9F). Similar to *Msx1*, *in situ* hybridization for *Msx2* shows elevated expression specifically in the dental mesenchyme of E12.5 *Hdac3*^{Wnt1NCKO} embryos (Figure 2.9E).

Interestingly, transgenic overexpression of *Msx2* leads to cleft secondary palate, skull malformations, micrognathia, tooth hypoplasia and eyelid dysplasia, which phenocopies many aspects of the *Hdac3*^{Wnt1NCKO} abnormalities (Winograd et al., 1997). Gain of BMP signaling also results in craniofacial abnormalities that partially phenocopy

the abnormalities identified in *Hdac3*^{Wnt1NCKO} embryos (He et al., 2010). These observations suggest that the hypoplasia of neural crest-derived structures observed in *Hdac3*^{Wnt1NCKO} embryos may be in part mediated by derepression of *Msx1* and *Msx2* leading to increased apoptosis (Graham et al., 1994; Tríbulo et al., 2004; Park et al., 2005). Consistent with this hypothesis, we observed increased apoptosis in *Hdac3* mutants in dental mesenchyme and palatal shelves, coincident with increased *Msx* expression (Figure 2.9E,F).

To determine whether *Msx* gene upregulation has a functional role in mediating the observed cell cycle dysregulation and failure of neural crest structures to expand during development, we performed siRNA-mediated knockdown of *Msx1* or *Msx2,* individually or in combination, in cultured neural crest mesenchyme from control and *Hdac3*^{Wnt1NCKO} embryos. We observed a partial restoration of wild-type levels of neural crest proliferation following knockdown of either *Msx1* or *Msx2* (Figure 2.12). Taken as a whole, these results suggest that derepression of *Msx1* and *Msx2* in the absence of Hdac3 causes decreased proliferation and increased apoptosis in cranial neural crest cells, manifesting as abnormal facies, cleft palate, dental hypoplasia and bone deficiencies.

In addition to the *Msx* gene products, the T-box transcription factors Tbx2 and Tbx3 have been shown to play significant roles in palate expansion and neural crest development (Zirzow et al., 2009; Mesbah et al., 2012). Tbx2 and Tbx3, like Msx1 and Msx2, are normally expressed in neural crest-derived cranial mesenchyme and are

important in cell cycle regulation during palatogenesis (Zirzow et al., 2009). Loss of *Tbx2* or *Tbx3* in craniofacial development leads to cleft palate due to excessive proliferation, and both proteins have been identified as inhibitors of the cell cycle in palatogenesis (Zirzow et al., 2009). We observe significant upregulation of these members of the T-box transcription factor family in *Hdac3*-deficient craniofacial mesenchyme, consistent with the observed cell cycle dysregulation in neural crest-derived tissue (Figure 2.9D). Overall, the pattern of upregulation of these Msx, T-box transcription factors, cell cycle regulators and the signaling molecule Bmp4 – all known inhibitors of neural crest survival - is consistent with a model in which Hdac3 represses core inhibitors of the neural crest cell cycle in order to drive craniofacial development.

Discussion

At multiple stages of neural crest development, the growth and survival of neural crest cells comes under positive and negative regulation from surrounding cell types, but is also subject to cell autonomous regulation (Sauka-Spengler and Bronner-Fraser, 2008). The homeodomain transcription factors Msx1 and Msx2 are important mediators of neural crest apoptosis in both early and late stages of craniofacial morphogenesis, but the temporal and spatial regulation of their expression is poorly understood. Interestingly, both increased and decreased *Msx* gene levels in developing neural crest lead to severe craniofacial abnormalities (Bei and Maas, 1998; He et al., 2010). That craniofacial morphogenesis is so exquisitely sensitive to *Msx* expression speaks to the importance of fine regulation of the timing and patterning of *Msx1* and *Msx2* transcription during neural crest development.

In this chapter, I demonstrate that loss of *Hdac3* in neural crest results in severe craniofacial malformations including microcephaly, cleft palate, impaired bone formation in the skull and hypoplasia of the teeth. Inactivation of *Hdac3* by *Wnt1-Cre* results in cell cycle dysregulation in neural crest-derived structures, including increased expression of *p21, p53, p57, Cyclin D1, Cyclin D3, Cyclin G1 and Cdk2*. *Hdac3*^{Wnt1NCKO} embryos exhibit elevated expression of *Msx1* and *Msx2* in the anterior cranial mesenchyme, and knockdown of *Msx1* and *Msx2* in mutant tissue partially normalizes neural crest proliferation. Incomplete rescue in this assay may have been due to incomplete knockdown of *Msx1* and *Msx2* using siRNA approaches, but may also suggest that

factors other than *Msx1* and *Msx2* are functionally altered in *Hdac3* mutants and contribute to the cell cycle dysregulation that we observe. Indeed we observe upregulation of *Tbx2* and *Tbx3* in *Hdac3*-deficient cranial mesenchyme, and abnormal T-box factor expression is also likely to contribute to the abnormal phenotype in *Hdac3*^{Wnt1NCKO} mice. Dysregulation of Tbx factors and other regulators of neural crest development is also likely to explain the strong – but not complete – overlap between the phenotype of *Hdac3*^{Wnt1NCKO} mice and *Msx2* transgenic overexpressing mice (Winograd et al., 1997).

Previous work investigating the regulation of *Msx1* transcription in cell lines identified several regulatory elements in the *Msx1* upstream genomic region (Takahashi et al., 1997). *LacZ* reporters of a "minimal" *Msx1* promoter containing these regulatory regions were strongly expressed in the neural crest-derived anterior cranial mesenchyme of E12.5 embryos (Takahashi et al., 1997). Similar work with the *Msx2* promoter region has also identified highly conserved enhancers that contribute to *Msx2* expression in the craniofacial mesenchyme when fused to *lacZ* reporters (Liu et al., 1994). In light of the canonical role of Hdac3 as a transcriptional repressor, it is reasonable to hypothesize that Hdac3 may directly repress *Msx1* and *Msx2* expression in neural crest by deacetylating histones at these promoters/enhancers, either at known or novel regulatory regions. However, my *in vivo* chromatin immunoprecipitation experiments have not demonstrated Hdac3 occupancy of previously described enhancer regions (Brugger et al., 2004; Hussein et al., 2003). As a global modulator of gene expression, Hdac3 is likely to affect the expression of multiple pathways involved in craniofacial development. Additional work is needed to determine whether Hdac3-

mediated repression of *Msx1* and *Msx2* occurs via histone deacetylation at uncharacterized enhancer regions at these loci, through derepression of additional intermediate genes or via direct deacetylation of non-histone targets. Interestingly, recent results suggest that critical functions of Hdac3 in the embryo are independent of its interactions with NCOR1 and SMRT, co-repressors that are necessary for Hdac3 catalytic activity (You et al., 2013). Thus, Hdac3 may mediate important developmental processes through a non-canonical function unrelated to deacetylation of histone targets.

My finding of decreased bone formation in Hdac3 conditional mutants is consistent with the pro-ossification role that Hdac3 is known to play in osteoblast precursors; however, by deleting *Hdac3* prior to the specification and expansion of osteoblast precursors, we observe drastic deficiencies in bone formation not seen after deletion of *Hdac3* in committed *Osx*-expressing cells (Razidlo et al., 2010). My results demonstrate increased apoptosis of neural crest-derived mesenchyme in the developing calvaria, despite intact neural crest migration and normal expression of the osteoblast regulatory molecule Runx2. Paradoxically, deletion of *Msx1* and *Msx2* in neural crest leads to heterotopic bone formation, particularly in the frontal bone region, while *Msx2* transgenic overexpression also results in ectopic bone formation, with decreased mineralization in the interparietal bone (Liu et al., 1995; Roybal et al., 2010; Winograd et al., 1997). While some of the bone abnormalities in *Hdac3*^{Wnt1NCKO} embryos could be attributed to derepression of *Msx* gene expression, it is likely that additional targets of Hdac3 underlie the skeletal abnormalities in these mice. An interesting future area of research will involve determining additional targets of Hdac3 that regulate the early

stages of bone development in neural crest progenitor cells and additional populations of osteoblast precursors.

Materials and Methods

Mice

Wnt1-Cre, *Pax3^{Cre}*, *Hdac3^{flox}*, *Z/EG* and p21 null mice were maintained on mixed CD1/B6/129 genetic backgrounds separated by 4-8 generations of interbreeding from pure parental strains (Engleka et al., 2005; Jiang et al., 2000; Mullican et al., 2011; Novak et al., 2000). Mice were genotyped using previously described Cre-specific PCR primers (5'-TGC CAC GAC CAA GTG ACA GC-3', 5'-CCA GGT TAC GGA TAT AGT TCA TG-3') (Heidt and Black, 2005), and primers designed to distinguish between the control and floxed *Hdac3* allele (5'-GCA GTG GTG GTG AAT GGC TT-3', 5'-CCT GTG TAA CGG GAG CAG AAC TC-3'). Genotyping for the Z/EG transgene was performed by X-Gal staining tail samples. Littermate embryos were analyzed in all experiments unless otherwise noted. The University of Pennsylvania Institutional Animal Care and Use Committee approved all animal protocols.

Histology, immunohistochemistry and in situ hybridization

These techniques were performed on paraformaldehyde-fixed, paraffin embedded slides as previously described (High et al., 2008). Embryos were dissected in cold PBS, fixed overnight in 2% paraformaldehyde, dehydrated into 100% ethanol, embedded in paraffin and sectioned. H&E and Goldner's trichrome staining were performed using standard procedures. Primary antibodies used for

immunohistochemistry were anti-GFP goat polyclonal (Abcam AB6673, 1:100), anti-GFP rabbit polyclonal (Invitrogen A-11122, 1:200), anti-Runx2 rabbit polyclonal (Santa Cruz sc-10758 1:20), anti-phospho histone H3 rabbit polyclonal (Cell Signaling #9701 1:50) and anti-Hdac3 rabbit polyclonal (Santa Cruz sc-11417x, 1:10). Radioactive *in situ* hybridization for *Msx1,Msx2* and *PlexinA2* was performed as previously described (Engleka et al., 2005). *Msx1* probe corresponds to RefSeq #NM_010835 (bp 862-1741), *Msx2* to #NM_013601 (bp 159-1143) and *PlexinA2* as previously described (Brown et al., 2001). TUNEL staining was performed as previously described (Jain et al., 2011). All control and mutant histological and immunohistochemical images shown for comparison were taken at the same exposure and contrast settings, using NIS Elements software. Pharyngeal arch size was quantified using ImageJ software by counting number of pixels in at least three serial sections from control and mutant frontal sections. All quantification was done in a blinded manner.

Cell number, proliferation and apoptosis were quantified by manually counting nuclei, phospho histone H3-, or TUNEL-positive cells, respectively, in adjacent sections of the anatomically-defined palatal shelf region in a blinded manner.

Optical projection tomography

Samples were dehydrated into 100% methanol, embedded in 1% low-melt agarose, cleared overnight in 1:2 (v/v) benzyl alcohol and benzyl benzoate, and scanned

using the Bioptonics OPT scanner (3001M) (Sharpe et al., 2002). Image stacks were reconstructed using OsiriX software. Image contrast was optimized to show anatomic detail.

siRNA transfection

E12.5 anterior craniofacial mesenchyme was microdissected and dissociated to single cell suspension with 0.25% Trypsin-EDTA. Cells were incubated at 37 □C in 5% CO_2 for 16 hours before transfection with 50nM control (Santa Cruz sc-37007), Msx1 (Dharmacon #M-044089-01) or Msx2 siRNA (Dharmacon #M-047845-01) using Lipofectamine RNAiMax (Invitrogen #13778030). 24 hours after transfection, cells were fixed with 4% paraformaldehyde (10 min, room temperature) and permeabilized with 0.2% Triton X-100. Immunocytochemistry was performed with anti-phospho histone H3 rabbit polyclonal (Cell Signaling #9701 1;100). Cell number and proliferation were quantified by manually counting nuclei and phospho histone H3-positive cells in a blinded manner.

Alcian blue/alizarin red staining

Neonatal mice were eviscerated and skinned after being soaked in room temperature water for 3 hours followed by a 1 minute heat shock at 65^{o}C to loosen the

skin. The samples were then fixed for 3 days in 100% ethanol at room temperature. Samples were stained for 2 days at room temperature with Alcian blue solution (0.3mg/ml Alcian Blue, 80% ethanol, 20% acetic acid) to visualize cartilage, and then rinsed and postfixed in 100% ethanol at room temperature, overnight. Samples were then incubated for 24 hours with Alizarin Red solution (0.065mg/ml Alizarin Red S in 0.5% KOH) to visualize bone, followed by incubation in 0.5% KOH until soft tissues were mostly digested. The 0.5% KOH solution was replaced with 25% glycerol in water (added very slowly to sample) and incubated at room temperature until tissues cleared.

RNA isolation, complementary DNA synthesis and quantitative RT-PCR

For E12.5 cranial mesenchyme expression profiling, *Wnt1-Cre; Hdac3*$^{f/f}$ and littermate Cre-negative control embryos were microdissected with tungsten needles in cold PBS. RNA was obtained using the Qiagen RNeasy spin column, with on-column DNAse I digestion. Complementary DNA (cDNA) was synthesized according to kit instructions with the Superscript III system (Invitrogen). Quantitative RT-PCR was performed in triplicate using Sybr Green (Applied Biosystems). *Gapdh* was used as a reference control gene. Quantitative RT-PCR primers (Table 2.2) were designed using IDT software.

Statistics

The student's two-tailed t test was used to ascertain differences between groups. A p-value of less than 0.05 was considered significant.

Table 2.1: Late gestation and perinatal craniofacial abnormalities in *Hdac3*^{Wnt1NCKO} mice

E16.5-P0	***Wnt1-Cre***	***Wnt1-Cre; Hdac3***$^{f/f}$
Microcephaly	0% (0/20)	100% (27/27)
Cleft palate	0% (0/20)	100% (27/27)
Eyelid dysplasia	0% (0/20)	100% (27/27)
Anteriorally displaced foramen magnum	0% (0/20)	100% (27/27)
Absence of:		
Hyoid bone	0% (0/7)	75% (6/8)
Sphenoid bone	0% (0/7)	88% (7/8)
Tympanic ring	0% (0/7)	88% (7/8)
Hypoplasia and incomplete mineralization of:		
Frontal bone	0% (0/7)	100% (8/8)
Mandible	0% (0/7)	100% (8/8)
Maxilla	0% (0/7)	100% (8/8)
Nasal bone	0% (0/7)	100% (8/8)
Orbit	0% (0/7)	100% (8/8)
Temporal bone	0% (0/7)	100% (8/8)
Zygomatic arch	0% (0/7)	100% (8/8)
Interparietal bone	0% (0/7)	100% (8/8)

Table 2.2: Quantitative RT-PCR primer sequence information

Gene name	Protein	Sequence (5’ – 3’)	Product size	Genomic size
Bmp4	Bmp4	GAGCAGAGCCAGGGAAC GAAGAGGAAACGAAAAGCAGAG	138	1140
Ccnd1	Cyclin D1	GCCCTCCGTATCTTACTTCAAG GCGGTCCAGGTAGTTCATG	145	1538
Ccnd3	Cyclin D3	GCGTGCAAAAGGAGATCAAG GATCCAGGTAGTTCATAGCCAG	120	1001
Ccng1	Cyclin G1	CAGTTCTTTGGCTTTGACACG TTCCTCTTCAGTCGCTTTCAC	147	1597
Cdk2	Cdk2	GCATTCCTCTTCCCCTCATC GGACCCCTCTGCATTGATAAG	128	1251
Cdk4	Cdk4	TACATACGCAACACCCGTGGACAT AGTCGTCTTCTGGAGGCAATCCAA	155	931
Cdkn1a	p21	CTTGCACTCTGGTGTCTGAG GCACTTCAGGGTTTTCTCTTG	145	651
Cdkn1b	p27	TGGACCAAATGCCTGACTC GGGAACCGTCTGAAACATTTTC	144	705
Cdkn1c	p57	CAGGACGAGAATCAAGAGCAG CGACGCCTTGTTCTCCTG	150	694

Cdkn2a	p16 Ink4a (Trivedi et al., 2008)	ATCTGGAGCAGCATGGAGTC CGAATCTGCACCGTAGTTGA	198	5198
Cdkn2c	p18	AAACGTCAACGCTCAAAATGG GACAGCAAAACCAGTTCCATC	133	3524
Cdkn2d	p19 Ink4d	CTTCATCGGGAGCTGGTG AGGCATCTTGGACATTGGG	138	1140
Gapdh	Gapdh	CGTCCCGTAGACAAAATGGT GAATTTGCCGTGAGTGGAGT	177	2011
Hdac1	Hdac1	GAGATGACCAAGTACCACAGTG AAACAAGCCATCAAACACCG	135	4741
Hdac2	Hdac2	AGAAGGAGACAGAGGACAAGA CGAGGTTCCTAAAGTTGGAGAG	144	3045
Hdac3	Hdac3	CCATTCTGAGGACTACATCGAC TGTGTAACGGGAGCAGAAC	142	6837
Hdac8	Hdac8	ACCGAATCCAGCAAATCCTC CAGTCACAAATTCCACAAACCG	149	22619
Msx1	Msx1	AAGATGCTCTGGTGAAGGC TGGTCTTGTGCTTGCGTAG	132	2296
Msx2	Msx2	CTCGGTCAAGTCGGAAAATTC GTTGGTCTTGTGTTTCCTCAG	121	3859

Msx3	Msx3	AGTCGCGCACTCTTGTC TATTGCTTCTGGTGAAACTTGC	141	786
Osr2	Osr2	TTGCTCATTCACGAGAGGAC TCCCACACTCCTGACATTTG	145	1101
Shox2	Shox2	CCCACTATCCAGACGCTTTC ACCTTTGTGAAGTTGATTTTCCTG	131	2726
Tbx2	Tbx2	CACAAACTGAAGCTGACCAAC GAAGACATAGGTGCGGAAGG	147	1054
Tbx3	Tbx3	AGCCAACGATATCCTGAAACTG GTGTCTCGAAAACCCTTTGC	150	1946
Trp53	p53	AGTTCATTGGGACCATCCTG GCTGATATCCGACTGTGACTC	149	6524

Figure 2.1: Deletion of Hdac3 in neural crest results in cranial hypoplasia at E10.5

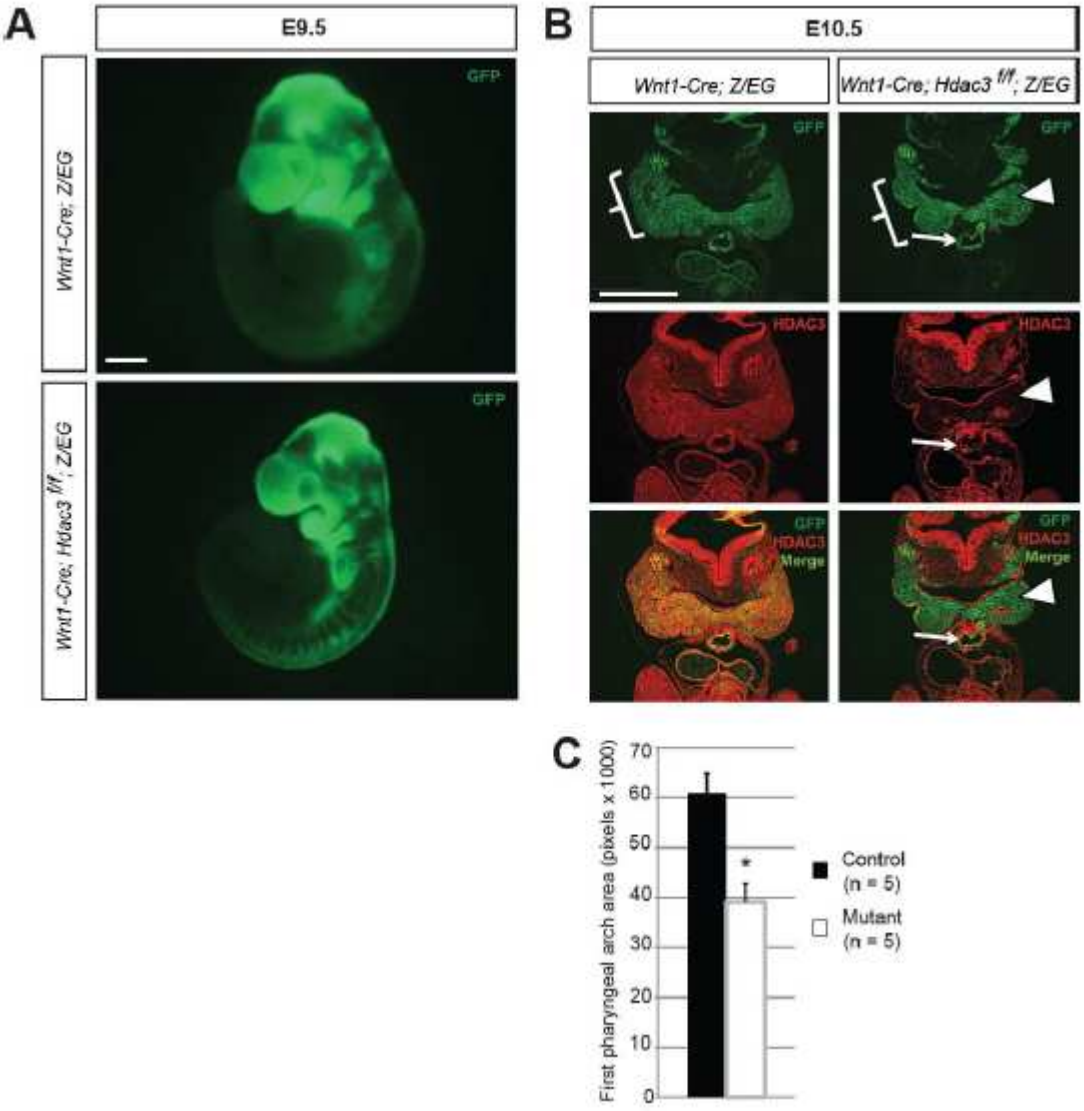

Figure 2.1: Deletion of Hdac3 in neural crest results in cranial hypoplasia at E10.5

(A) Gross images of E9.5 embryos visualized with direct fluorescence. Migration of neural crest cells into the developing face and pharyngeal arch region is grossly intact in the absence of neural crest expression of Hdac3. (B) Immunohistochemistry for GFP and Hdac3 in frontal sections of the facial mesenchyme of E10.5 embryos. *Hdac3* is efficiently deleted in neural crest-derived cranial mesenchyme (arrowhead), as well as the conotruncal cushions of the developing cardiac outflow tract (arrow). Note that cranial crest-derived (GFP+) structures in the mutant are hypoplastic (open bracket). (C) Quantification of the size of the first pharyngeal arch from serial sections of E10.5 control and mutant embryos. Scale bars: (A): 300μm. (B): 400μm.

Figure 2.2: Neural crest migration in *Hdac3*^{Wnt1NCKO} embryos is intact at E9.5

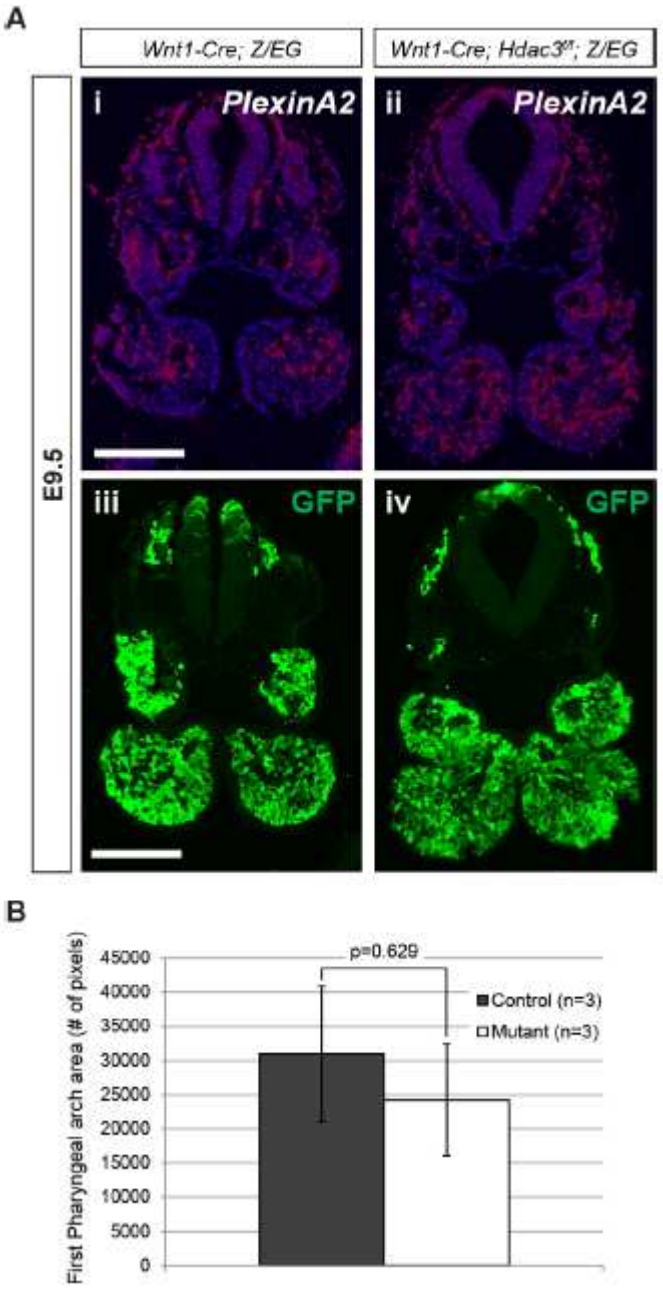

Figure 2.2: Neural crest migration in *Hdac3*^{Wnt1NCKO} embryos is intact at E9.5

(A) Neural crest migration evaluated by *PlexinA2* expression and fate mapping. (Inset i,ii) E9.5 mutant and littermate controls demonstrate similar expression of *PlexinA2*, a marker of neural crest. (Inset iii,iv) Neural crest-derived cells fate mapped by *Wnt1-Cre* and the Z/EG reporter populate the first pharyngeal arch similarly in mutant and control embryos. (B) Quantification of the area occupied by cranial crest-derived GFP+ cells in the first pharyngeal arches of mutant and control embryos reveals no significant difference. Scale bar: (A): 200µm.

Figure 2.3: Craniofacial abnormalities in *Hdac3*^{Wnt1NCKO} mice

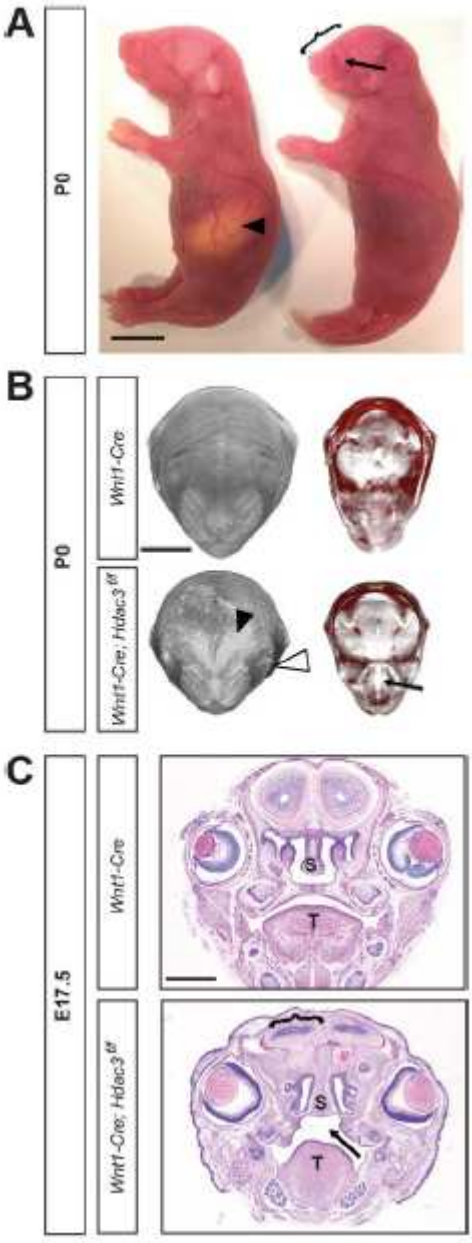

Figure 2.3: Craniofacial abnormalities in *Hdac3*^{Wnt1NCKO} mice

(A) Gross image of a control (left) and mutant P0 pup. Mutants have severe cranial hypoplasia, characterized by a shortened snout (bracket) and micrognathia, and are unable to feed, as indicated by the absence of a milk spot, present in littermate controls (arrowhead). Mutants also exhibit eyelid dysplasia (arrow). (B) Optical projection tomography renderings of P0 heads. (Left panels) Viewed *en face*, an area of hemorrhage (black arrowhead) and eyelid closure defects (white arrowhead) are visible in the mutant. (Right panels) Virtual transverse sections cut through the level of the eyes demonstrate a cleft palate (arrow) in the mutant. (C) H&E stained coronal sections of E17.5 heads. Cleft palate is indicated by the arrow. S: Nasal septum. T: Tongue. Scale bars: (A): 500μm. (B): 2mm. (C): 1.4mm.

Figure 2.4: Deletion of Hdac3 with *Pax3^{Cre}* recapitulates the craniofacial abnormalities observed using *Wnt1-Cre*

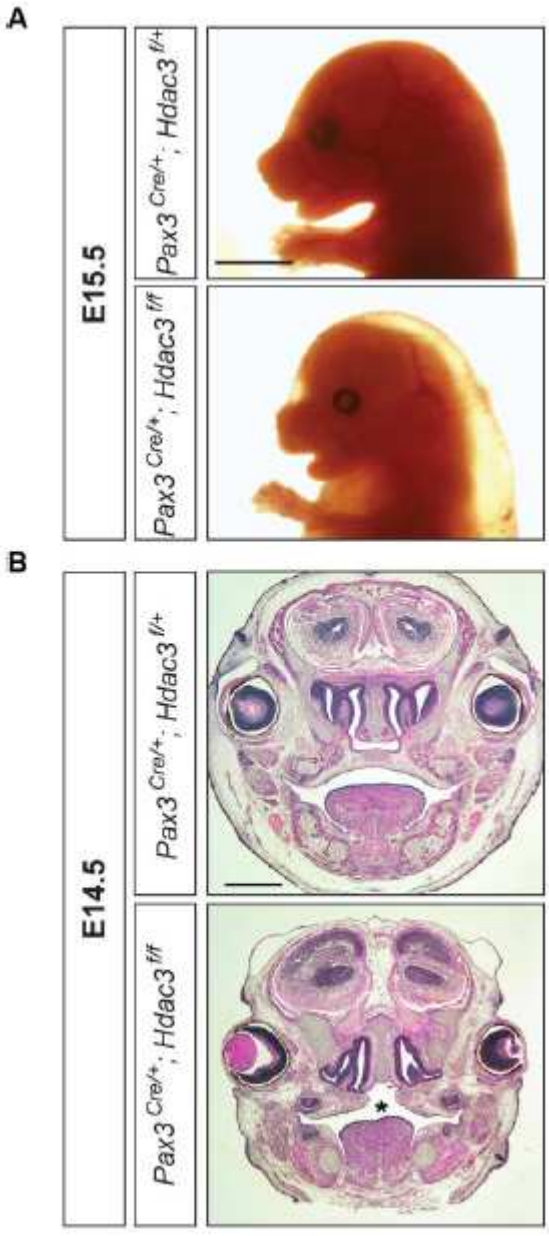

Figure 2.4: Deletion of Hdac3 with *Pax3^{Cre}* recapitulates the craniofacial abnormalities observed using *Wnt1-Cre*

(A) Gross images of E15.5 embryos. Mutant embryos exhibit fully penetrant microcephaly, with micrognathia and a shortened snout. (B) H&E stained frontal sections of E14.5 embryos. Neural crest deletion of Hdac3 with *Pax3^{Cre}* results in cleft palate (*). Scale bars: (A,B): 800μm.

Figure 2.5: *Hdac3*^{Wnt1NCKO} embryos exhibit defects in craniofacial bone formation

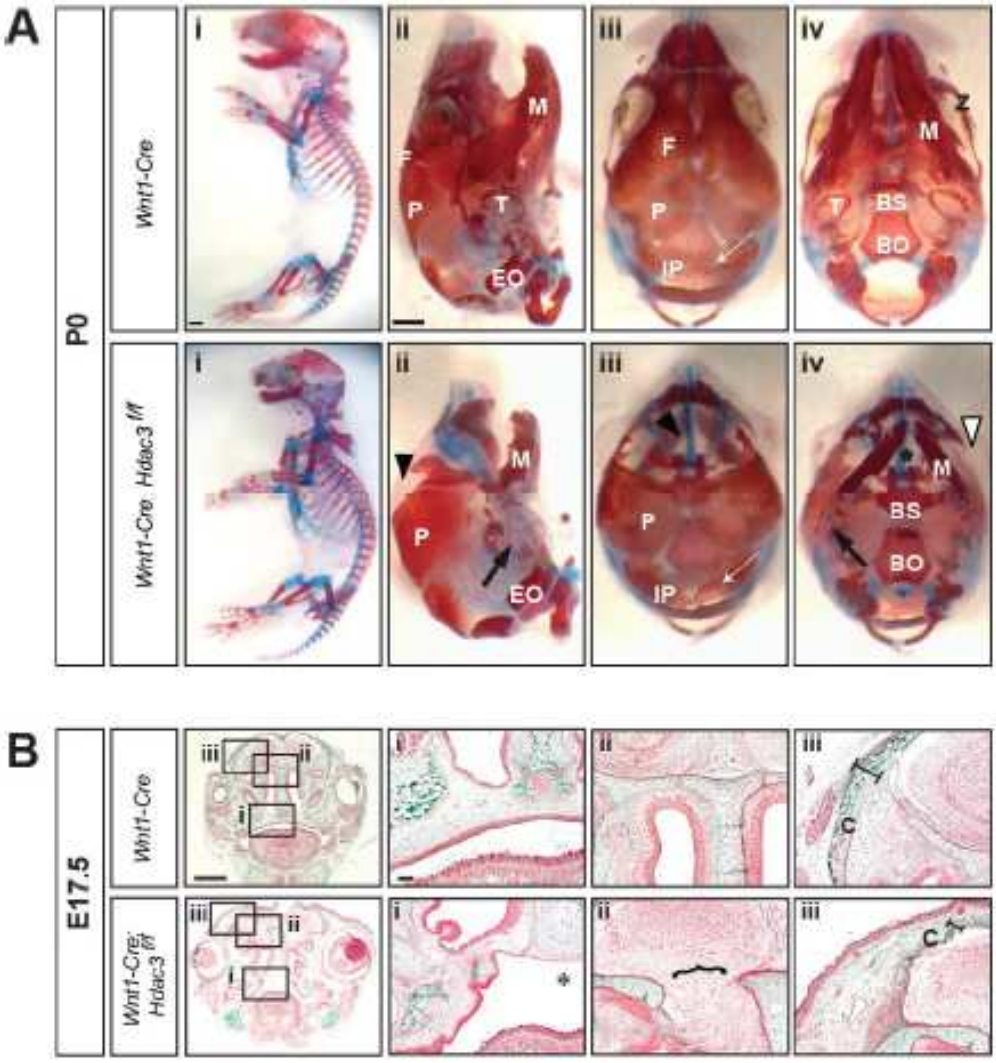

Figure 2.5: *Hdac3*^{Wnt1NCKO} embryos exhibit defects in craniofacial bone formation

(A) Alcian blue and alizarin red staining of P0 heads. Red staining indicates ossified bone, blue staining indicates cartilage. (Inset i) Lateral view of the full skeleton. (Inset ii) Lateral view of the calvaria. (Inset iii) Caudal view of the calvaria. (Inset iv) Rostral view of the skull base. Mutants demonstrate absence of the tympanic ring (T) (black arrow), diminished ossification of the frontal bone (F) (black arrowhead), absence of the ossified secondary palate (SP) (asterisk), and decreased mineralization along the midline of the interparietal bone (IP) (white arrow). Mutants also exhibit hypoplasia and decreased ossification of neural crest-derived viscerocranial structures, including the zygomatic arch (Z) (white arrowhead). Ossification of the mesodermally-derived parietal bone (P) remains intact. (B) Goldner's trichrome staining of E17.5 heads. Green staining represents bone, red staining represents connective tissues. (Inset i) Asterisk indicates cleft palate in the mutant. (Inset ii) Open bracket indicates an area of brain herniating through the base of the skull in the mutant. (Inset iii) Decreased ossification of the calvaria (C) in the mutant, as indicated by a black bar. BO: Basioccipital. BS: Basisphenoid. EO: Exoccipital. IP: Intraparietal. M. Mandible. N. Nasal. Scale bars: (A): 1mm. (B): 1.4mm.

Figure 2.6: *Hdac3*^{Wnt1NCKO} embryos exhibit intact neural crest migration and differentiation of osteogenic precursors, but increased apoptosis in the developing calvaria

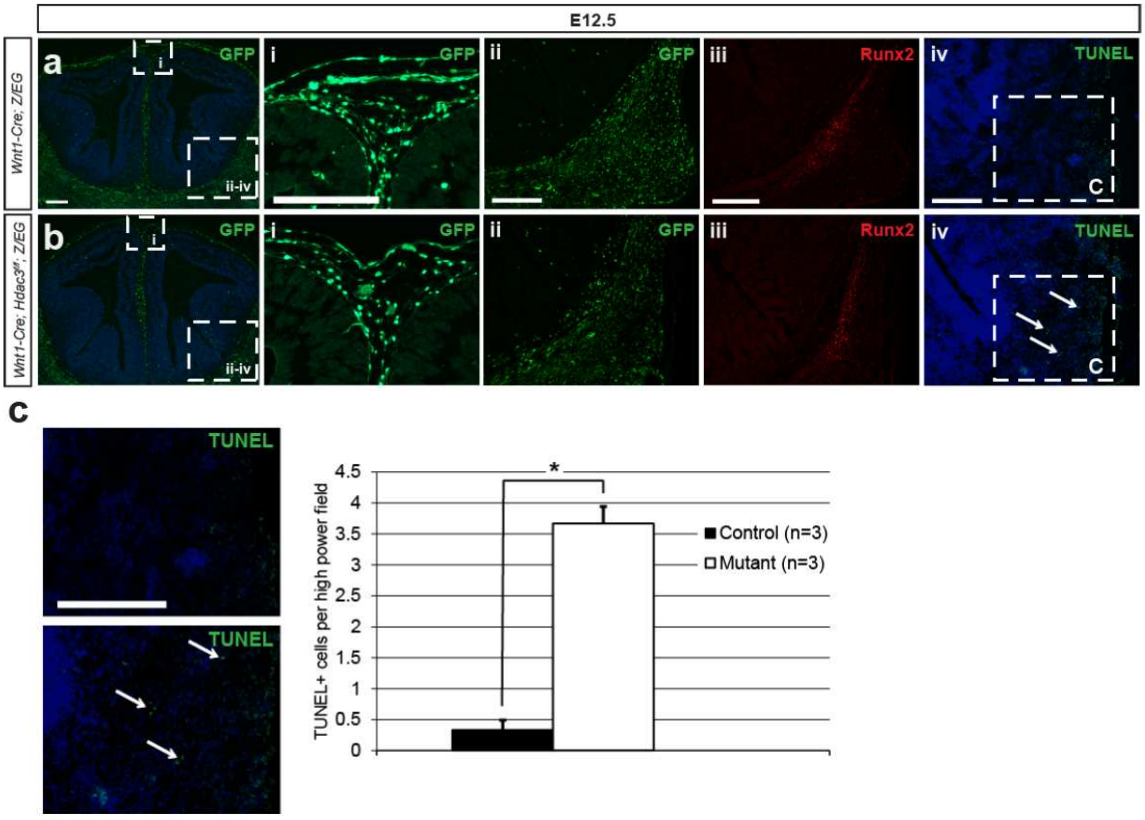

Figure 2.6: *Hdac3*^{Wnt1NCKO} embryos exhibit intact neural crest migration and differentiation of osteogenic precursors, but increased apoptosis in the developing calvaria

(A,B) GFP, Runx2, and TUNEL staining of E12.5 heads. (Insets i,ii) Neural crest cells properly migrate to the outer layers of the developing calvaria and frontal bone primordium, shown here by fate mapping with the Z/EG reporter. (Inset iii) Mutant calvaria exhibit a normal pattern of Runx2 staining by immunohistochemistry, suggesting that differentiation of osteogenic precursors is maintained at this developmental stage. (Inset iv,C) TUNEL staining of adjacent sections reveals that neural crest cells exhibit significantly decreased survival in the frontal bone primordium of *Hdac3*^{Wnt1NCKO} embryos. (*) denotes $p < 0.05$. Scale bars: (A-C): 200μm.

Figure 2.7: The loss of Hdac3 causes hypoplasia of neural crest-derived dental mesenchyme

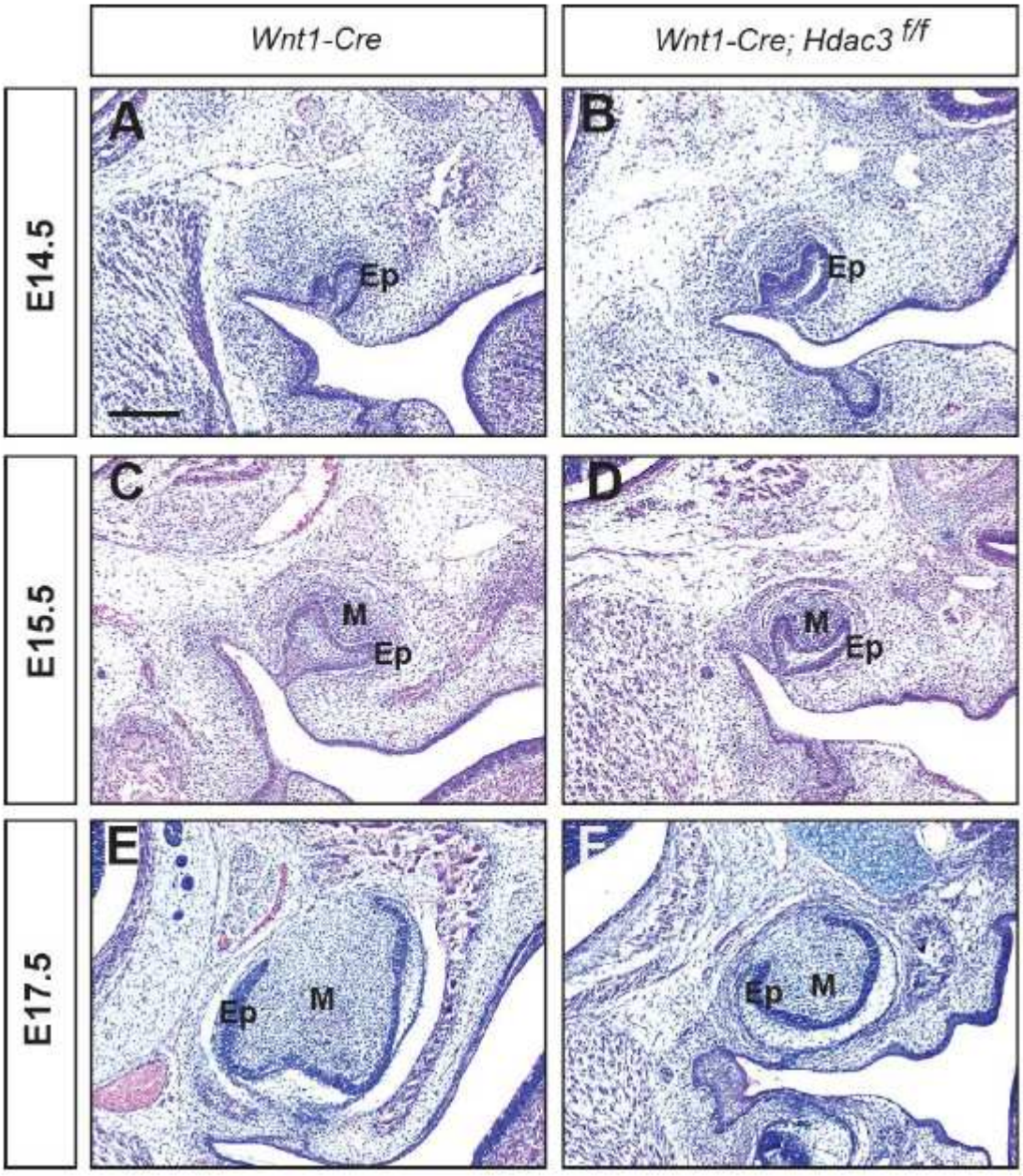

Figure 2.7: The loss of *Hdac3* causes hypoplasia of neural crest-derived dental mesenchyme

(A-F) H & E stained frontal sections of control and mutant heads at E17.5. Early stages of tooth morphogenesis, including epithelial invagination (A,B) and mesenchymal specification (C,D) occur normally in the absence of *Hdac3*. (E,F) However, at E17.5, the dental pulp shows decreased bulk in mutants. Ep: Epithelium. M: mesenchyme. Scale bar: 200μm.

Figure 2.8: Cleft palate in *Hdac3*^{Wnt1NCKO} mice results from increased apoptosis in the neural crest-derived palatal shelves

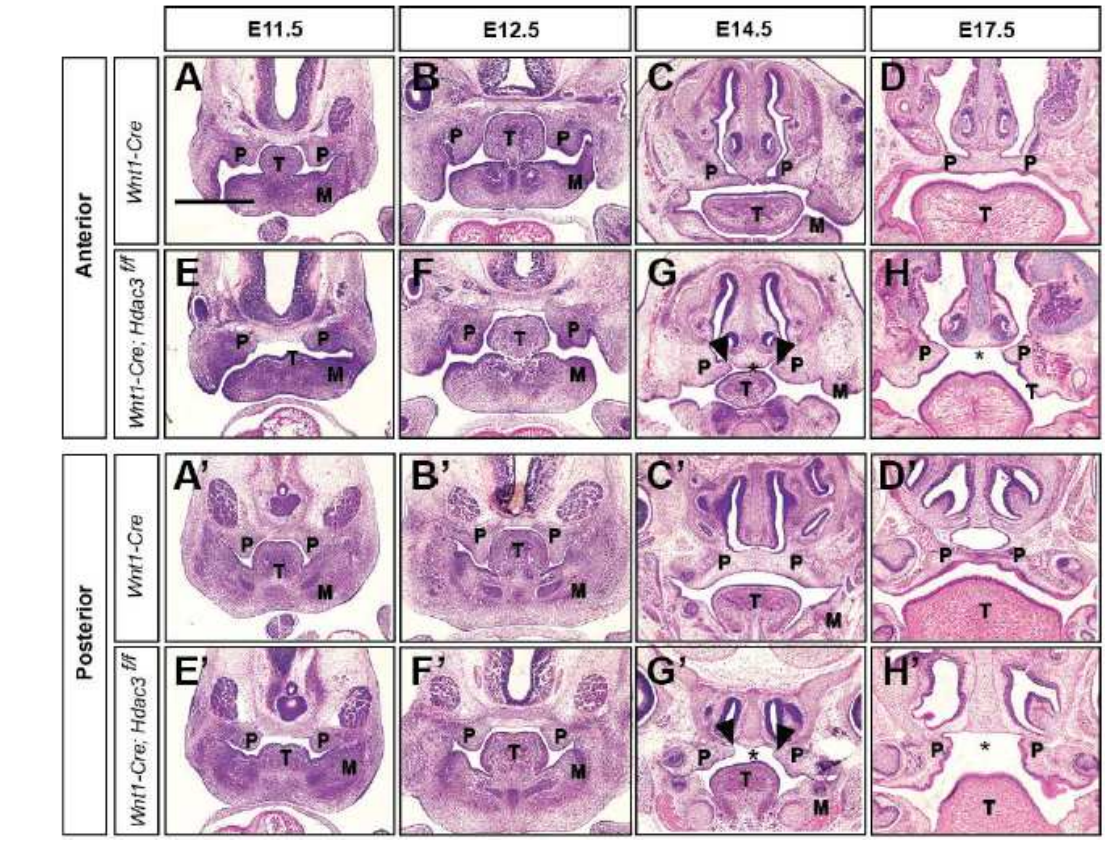

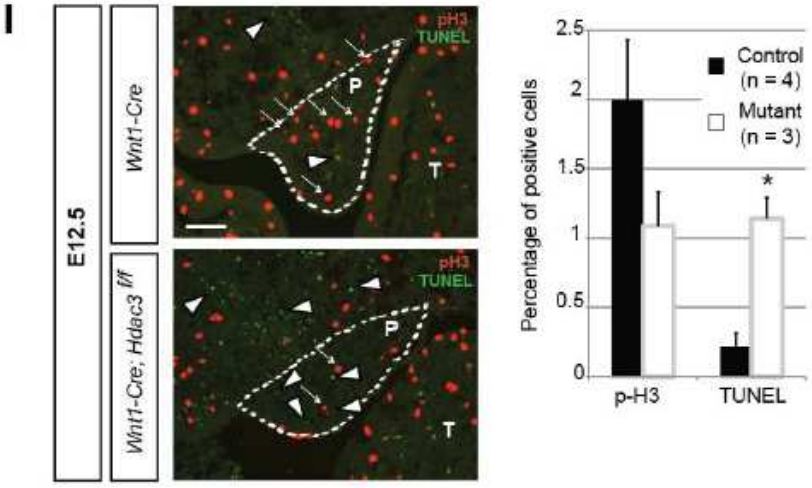

Figure 2.8: Cleft palate in *Hdac3*^{Wnt1NCKO} mice results from increased apoptosis in the neural crest-derived palatal shelves

(A-H,A'-H') H&E stained frontal sections of control and mutant embryos at the level of the anterior and posterior palatal shelves. (A-D,A'-D') In control embryos, the palatal shelves (P) expand towards the mandible (M) before elevating above the tongue (T), meeting in the midline at E14.5 and ossifying by E17.5. (E-H,E'-H') In mutant embryos, the palatal shelves are hypoplastic at E12.5 and do not meet in the midline at E14.5 (*), although the medial aspects of the palatal shelves do elevate above the tongue (arrowheads). (I) Images show the areas defined as palatal shelves in control and mutant embryos at E12.5. Phospho-histone H3 (pH3)- (arrows) and TUNEL- (arrowheads) positive nuclei were counted relative to total nuclei in serial sections of the pharyngeal arch mesenchyme. Asterisk denotes $p < 0.05$. Scale bars: (A-H,A'-H'): 400μm. (I): 50μm.

Figure 2.9: Dysregulation of cell cycle genes and the Msx-Bmp4 apoptotic pathway in *Hdac3*^{Wnt1NCKO} cranial mesenchyme

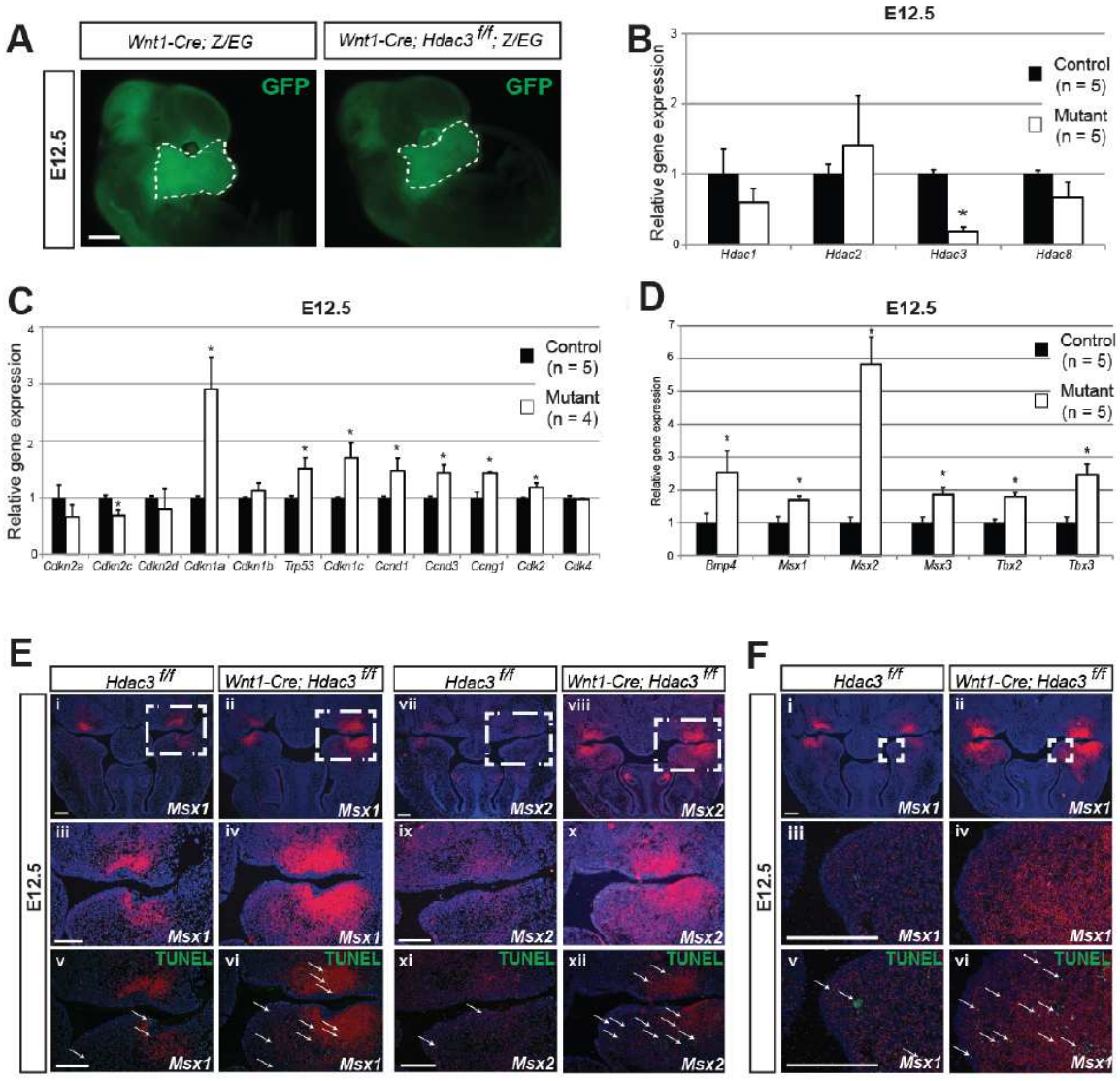

Figure 2.9: Dysregulation of cell cycle genes and the Msx-Bmp4 apoptotic pathway in *Hdac3*^{Wnt1NCKO} cranial mesenchyme

(A) Representative fluorescent images showing the area of cranial mesenchyme microdissected for E12.5 expression profiling. (B-D) Quantitative RT-PCR results. (B) Expression of *Hdac3*, but not other class I Hdacs, is decreased in mutant tissue. (C) Mutant cranial mesenchyme exhibit significant dysregulation of cell cycle regulatory genes. (D) Among important regulatory genes involved in craniofacial development, *Bmp4, Msx* and *Tbx* expression are significantly altered. (E,F) *In situ* hybridization of *Msx1*and *Msx2* in transverse sections of E12.5 heads and TUNEL staining. (E) Expression of *Msx1* transcripts is increased in mutant dental mesenchyme (Insets ii,iv) compared to littermate control (Insets i,iii). Expression of *Msx2* transcripts is increased in mutant dental mesenchyme (Insets viii,x) compared to littermate control (Insets vii,ix). TUNEL staining (Insets v,vi,xi,xii) of adjacent sections merged with images of *Msx* expression reveals increased apoptosis in mutant versus control embryos in the areas of higher *Msx* expression (arrows). (F) Expression of *Msx1* transcripts is increased in mutant palatal shelves (Insets ii,iv) compared to littermate control (Insets i,iii), as well as apoptosis labeled by TUNEL staining of adjacent sections (Insets v,vi) (arrows). (*) denotes $p < 0.05$. Scale bars: (A): 150µm. (E,F): 200µm.

Figure 2.10: Loss of *p21* does not rescue craniofacial abnormalities in *Hdac3*^{Wnt1NCKO} mutants

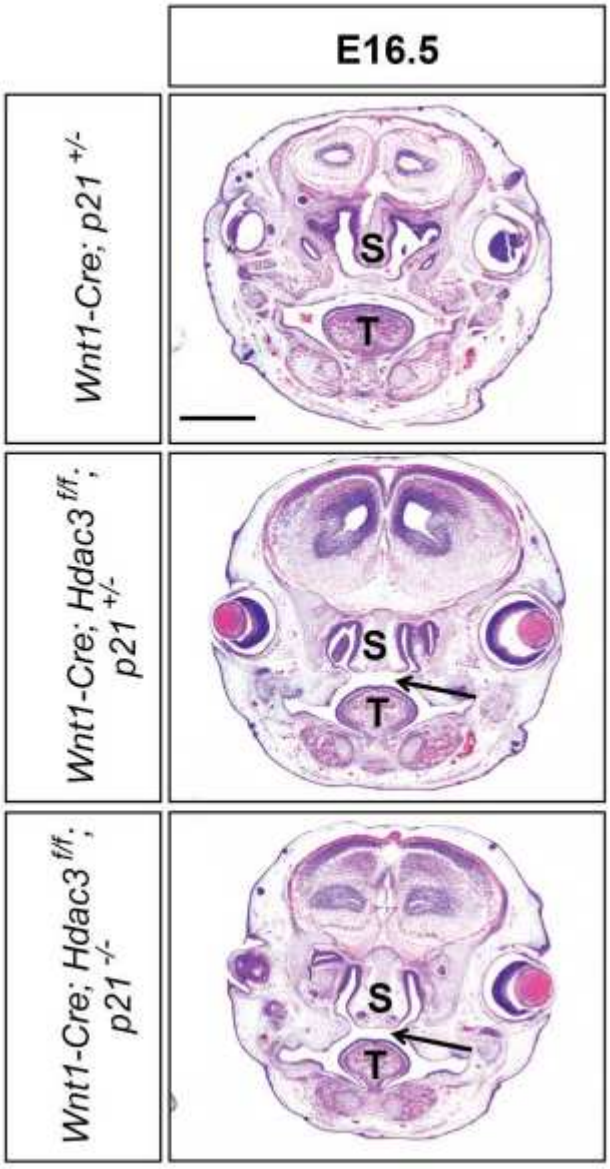

Figure 2.10: Loss of *p21* does not rescue craniofacial abnormalities in *Hdac3*^{Wnt1NCKO} mutants

H&E stained frontal sections of E16.5 heads. Neural crest deletion of Hdac3 on a p21+/- or p21-/- background results in cleft palate (arrow). Scale bar: 400μm.

Figure 2.11: Core regulators of palatogenesis are not significantly dysregulated in *Hdac3*^{Wnt1NCKO} embryos

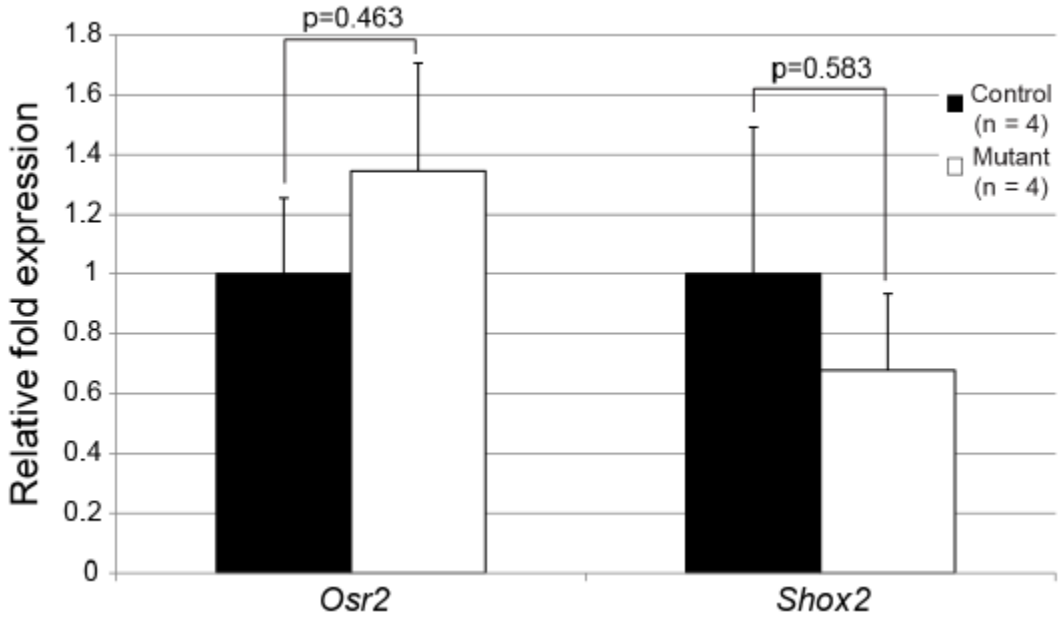

Figure 2.11: Core regulators of palatogenesis are not significantly dysregulated in *Hdac3*^{Wnt1NCKO} embryos

Quantitative RT-PCR of microdissected E12.5 cranial mesenchyme. Mutant embryos express similar levels of *Osr2* and *Shox2* - known regulators of palate development - as littermate controls.

Figure 2.12: Knockdown of *Msx1* or *Msx2* partially rescues proliferation defects of *Hdac3*^{Wnt1NCKO} explants

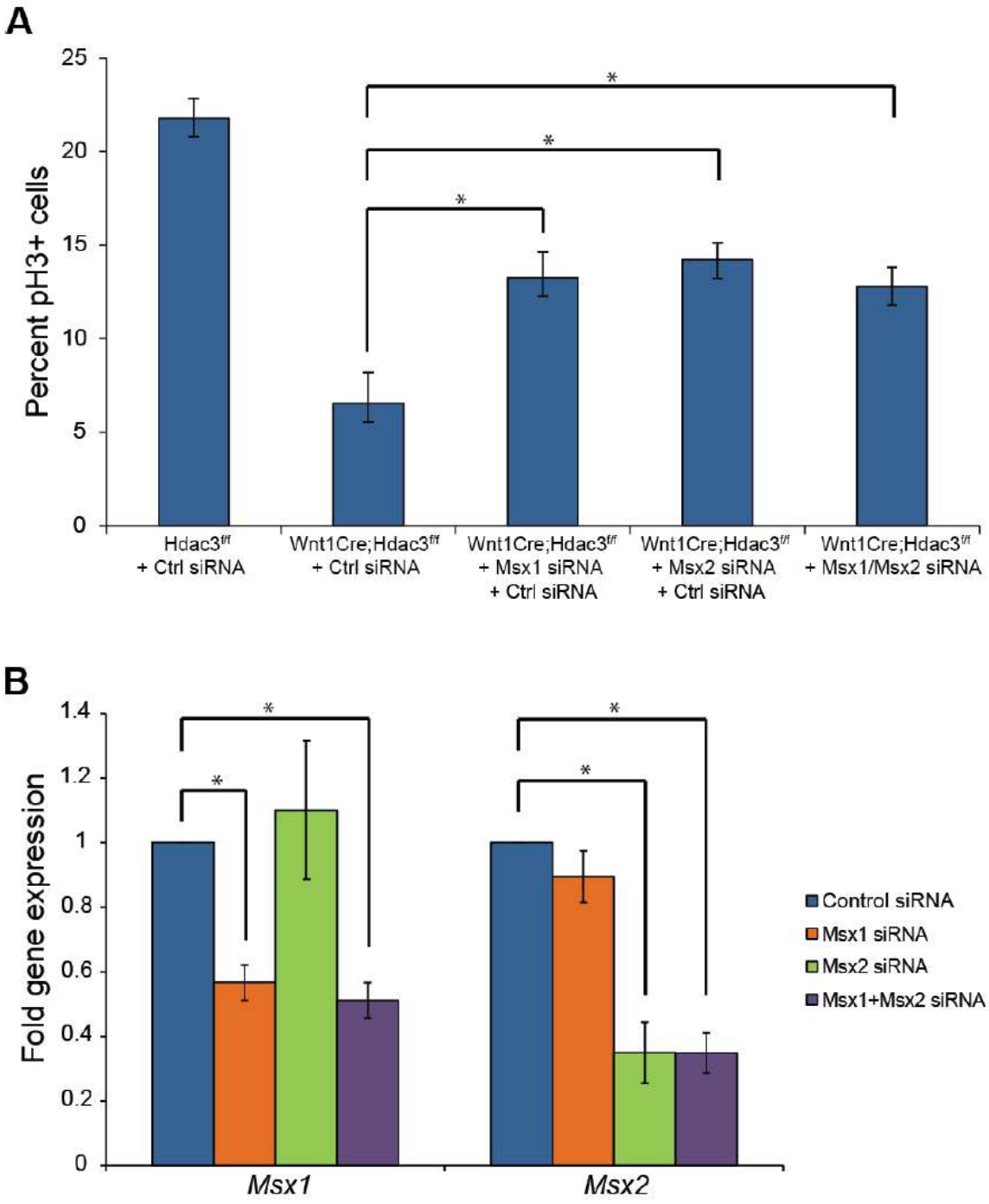

Figure 2.12: Knockdown of *Msx1* or *Msx2* partially rescues proliferation defects of *Hdac3*^{Wnt1NCKO} explants

(A) siRNA-mediated knockdown of *Msx1* and/or *Msx2* in microdissected E12.5 cranial mesenchyme partially restores proliferation of mutant cells to wild-type levels as measured by phospho-histone H3 immunohistochemistry. (B) Validation of siRNA-mediated *Msx* knockdown. Transfection of cranial mesenchyme with 50nM siRNA produces partial but significant loss of *Msx* transcripts as measured by quantitative RT-PCR. (*) denotes $p < 0.05$.

Chapter 3. Genome-Nuclear Lamina interactions regulate cardiac progenitor cell behavior

Summary

In Chapter 1, I introduced the cardiac progenitor cell populations that give rise to the cell types found in the heart including cardiomyocytes, smooth muscle and endothelial cells. Appropriate expansion and differentiation of these progenitor pools is critical for patterning of the developed heart. Progenitor cells require coordinated expression of lineage-specific genes to differentiate into one of several daughter cell lineages. Epigenetic regulators are ideally positioned to synchronize transcriptional activity of disparate genomic loci through several mechanisms including histone modifications, nucleosome repositioning and altered higher-order chromatin structure. Mapping of chromatin dynamics within the nucleus in several systems has revealed that gene positioning often correlates with changed expression patterns, however the direct effect of these changes upon cell fate remains unclear. In this chapter, I demonstrate that Hdac3 functions in a deacetylase-independent manner as a repressor of the cardiomyocyte lineage. Loss of *Hdac3* promotes differentiation into cardiomyocytes by de-repressing a myocyte gene program. Furthermore, I propose that Hdac3 serves as a tether between lineage-specific genes and the nuclear lamina, a transcriptionally silenced subnuclear region. Artificial tethering of Hdac3-bound genes to the nuclear lamina restores baseline myocyte differentiation, supporting this hypothesis.

Introduction

As I introduced in Chapter 1, cardiac development requires precise formation and differentiation of several progenitor populations. Classical lineage tracing studies in chick and mouse models first identified a region known as the cardiac crescent that contributes to the primitive heart tube and working myocardium (Cohen-Gould and Mikawa, 1996; Srivastava, 2006). Progenitors emerging from the cardiac crescent, or the first heart field, are followed by a second wave of cells that arise posterior to the cardiac crescent and eventually populate the right ventricle, atria and outflow tract. The progenitors of this second heart field (SHF) are thought to be multipotent, differentiating into cardiomyocytes, smooth muscle cells and endothelium (Kattman et al., 2006, 2011; Moretti et al., 2006; Wu et al., 2006). Specification of these precursor cells to various cardiovascular cell types requires coordinated regulation of numerous, lineage-specific genes. Precise control of progenitor cell commitment is essential for appropriate patterning of the developing embryo, and perturbations of the gene regulatory networks can lead to congenital defects (Bruneau, 2013; Davidson, 2010; Santen et al., 2012; Zaidi et al., 2013).

Epigenetic modifiers such as histone deacetylases (HDACs) localize to hundreds of genomic loci to regulate transcriptional activity, offering a convenient mechanism for synchronizing expression of broad gene programs. HDACs typically act by removing acetyl modifications from lysine residues of histone tails to promote a heterochromatic state and repression of gene transcription (Haberland et al., 2009b). Furthermore,

several HDACs are known to regulate cardiac morphogenesis and stress responses by altering expression of diverse sets of genes (Lewandowski et al., 2014; Montgomery et al., 2007; Sun et al., 2011; Trivedi et al., 2007, 2008, 2010). Hdac3 is unique among the canonical (class I and II) HDACs for its interaction with co-repressors NCoR and SMRT and its absolute requirement during early embryogenesis (Bhaskara et al., 2008; Guenther et al., 2001). While Hdac3 is essential for repression of broad genetic programs in neural crest, hematopoietic stem cells and hepatocytes, little is known of its function in cardiac progenitors (Singh et al., 2011b, 2013; Summers et al., 2013; Sun et al., 2012) although regulation of Tbx5 has been implicated (Lewandowski et al., 2014).

In addition to forming complexes with co-repressors such as NCoR, SMRT and NuRD, HDACs interact with proteins bound to the inner nuclear membrane including emerin, Lamin B receptor and Lamina-associated polypeptide 2 (LAP2) (Demmerle et al., 2013; Guarda et al., 2009; Somech et al., 2005). Accumulation of HDACs and other transcriptional repressors at the nuclear lamina creates a “silencing environment” responsible for low expression levels of genomic loci positioned at the nuclear periphery, whether by natural movement or artificial tethering (Burke and Stewart, 2013; Milon et al., 2012; Reddy and Singh, 2008; Reddy et al., 2008; Zullo et al., 2012). These lamina-associated domains (LADs) are most commonly heterochromatic and marked by repressive histone modifications (Towbin et al., 2012). Furthermore, Hdac3 is responsible for maintaining certain LADs at the nuclear periphery and repressing genes contained within these regions (Milon et al., 2012; Zullo et al., 2012). Genome-nuclear lamina interactions are also remarkably dynamic, changing significantly during progenitor cell differentiation as lineage-specific genes are being selectively silenced or

expressed (Kohwi et al., 2013; Peric-Hupkes et al., 2010). However, whether alterations in LADs can modulate developmental processes, or whether genome interactions with the nuclear lamina occur only in response to developmental events has been unclear. I sought to determine if cardiac progenitor commitment may be controlled by "selective locking" of cell type-specific genetic loci at the nuclear periphery, preventing ectopic gene expression and inappropriate differentiation.

In this chapter, I examine the role of nuclear organization in early progenitors during cardiovascular lineage commitment by modulating the epigenetic modifier Hdac3. Deletion of *Hdac3* in cardiac progenitor cells causes excessive differentiation into cardiomyocytes in both a cell-based model of cardiac development and in mouse embryos. Surprisingly, Hdac3 deacetylase activity is not required for repression of myocyte differentiation, suggesting a non-enzymatic role for Hdac3 in gene silencing. We discovered that loss of *Hdac3* releases several myocyte genes from association with the nuclear lamina concurrent with increased expression. Artificial tethering of Hdac3 to the nuclear periphery is sufficient to repress cardiomyogenesis. This work demonstrates that Hdac3 mediates genome-nuclear lamina interactions and subnuclear gene positioning and that genome tethering to the nuclear lamina is a mechanism for regulation of progenitor cell commitment.

Results

Hdac3 represses ES differentiation to cardiomyocytes

Hdac3 functions as a repressor of broad, genetic programs, attenuating expression of dozens of genes to modulate large-scale effects such as hepatic lipogenesis (Feng et al., 2011), cardiac response to metabolic stress (Sun et al., 2011), and neural crest specification (Singh et al., 2011b, 2013). We sought to determine whether Hdac3 regulates cardiac progenitor cell fate decisions during embryogenesis. We modeled cardiac development *in vitro* by differentiating mouse embryonic stem cells (ESCs) into multipotent Flk1+PDGFRα+ progenitors that can give rise to cardiomyocyte, endothelial cell and smooth muscle lineages (Kattman et al., 2006, 2011). Upon generating a mouse ESC line that enables tamoxifen-induced, Cre-mediated *Hdac3* deletion (Figure 3.1A), we induced these transgenic cells to differentiate into cardiac cell types and added tamoxifen to delete *Hdac3* when we observed peak expression of Flk1+PDGFRα+ progenitors at day 5. Next, we allowed the cells to differentiate until we observed significant numbers of beating cells at day 8. Analysis by flow cytometry revealed that progenitor populations in which *Hdac3* was deleted yielded significantly more cardiac Troponin T-positive (cTnT+) cardiomyocytes without increasing smooth muscle or endothelial cell counts (Figure 3.1B). Notably, this increase in cTnT+ cells was not due to a change in proliferation as measured by phospho-histone H3-positive cells (Figure 3.2), suggesting that loss of *Hdac3* in cardiac progenitors specifically affects progenitor fate decisions rather than regulating proliferation. We also observed higher

expression of cardiomyocyte-specific genes, while no significant change in gene expression of smooth muscle or endothelial cell markers was observed (Figure 3.1C). The addition of tamoxifen just 48 hours later when Flk1+PDGFRα cells were no longer detected, did not yield any significant increases in cardiomyocyte, smooth muscle or endothelial cell numbers as compared to controls (Figure 3.1D-E). These data suggest that Hdac3 acts to regulate differentiation during a narrow temporal window at the time when multipotent cardiac progenitors are present. Additionally, lentiviral overexpression of *Hdac3* during this same time window of differentiation further represses cardiomyocyte numbers relative to baseline (Figure 3.1F-H). These experiments in embryonic stem cells suggest that Hdac3 functions to repress progenitor cell differentiation towards the myocyte lineage.

Hdac3 represses differentiation of FHF and SHF cardiac progenitors

We hypothesized that Hdac3 plays a similar repressive role in cardiac progenitor cells present in the developing embryo. Using a floxed Hdac3 allele (*Hdac3f*), we deleted Hdac3 *in vivo* in SHF progenitors marked by LIM-homeobox transcription factor Isl1 expression (Mullican et al., 2011; Srinivas et al., 2001). We observed that loss of *Hdac3* in SHF cardiac progenitors resulted in embryonic lethality and ventricular hypoplasia (Figure 3.3A). Furthermore, *Hdac3*-null hearts were comprised of greater numbers of myocytes than littermate controls (Figure 3.3B), mirroring the enhanced myocyte differentiation phenotype observed in the mouse ESC culture system. Next, we

expanded the cell populations of *Hdac3* deletion using a more broadly-expressed Cre to include both first heart field (FHF) and SHF progenitors (Moses et al., 2001). Loss of *Hdac3* in cells expressing the cardiac homeobox gene *Nkx2.5* also yielded hypoplastic morphology and increased differentiation into cardiomyocytes (Figure 3.3C,D). By contrast, deleting *Hdac3* in committed cardiomyocytes as opposed to undifferentiated cardiac progenitor cells did not result in embryonic lethality or morphologic changes during embryogenesis (Figure 3.4) (Montgomery et al., 2008). These results complement our *in vitro* studies, establishing that Hdac3 acts during a narrow temporal window in FHF and SHF progenitors to repress differentiation to the myocyte lineage.

Hdac3 represses a myocyte gene program

Given the canonical function of Hdac3 as a transcriptional repressor, we hypothesized that Hdac3 suppresses cardiac progenitor specification to the cardiomyocyte lineage through silencing of a myocyte gene program. *Hdac3* deletion in differentiating mouse ESCs de-represses cardiomyocyte genes such as *Myh6*, *Tnnt2*, *Actc1*, but not smooth muscle or endothelial cell-specific genes (Figure 3.1C). *In vivo*, microarray analysis of *Hdac3*-null hearts deleted by *Nkx2.5*^{Cre} revealed an upregulation of myocyte-specific genes. Classification of upregulated genes by DAVID analysis revealed that the top category is regulators of muscle contraction. Finally, we validated several of these myocyte gene changes by qPCR and confirmed increased expression in *Hdac3*-null hearts (Figure 3.3E). These results are consistent with Hdac3 functioning

as a repressor of a myocyte gene program, with loss of *Hdac3* de-repressing these genes and driving precocious differentiation into cardiomyocytes.

Hdac3 represses cardiac differentiation independent of catalytic function

Recent studies suggest that Hdac3 maintains its function as a transcriptional repressor even without deacetylase activity (Sun et al., 2013; You et al., 2013). To establish whether Hdac3 catalytic activity is required for regulation of cardiac progenitor differentiation, we returned to the mouse ESC system (Figure 3.5A). Consistent with our earlier experiments, deleting *Hdac3* with addition of tamoxifen substantially enhanced differentiation into cardiomyocytes. As expected, exogenous expression of wild-type Hdac3 partially restored wild-type levels of differentiation (Figure 3.5B). To our surprise, exogenous expression of an Hdac3 mutant harboring a single Y298H substitution in the catalytic pocket that abolishes deacetylase activity of the enzyme while maintaining interactions with known binding partners (Lahm et al., 2007; Sun et al., 2013) rescued differentiation equally as well as wild-type Hdac3 (Figure 3.5B). This unexpected observation suggests that Hdac3 represses cardiomyocyte differentiation independent of its histone deacetylase activity.

We sought to determine whether Hdac3 catalytic activity is required for normal cardiac development *in vivo.* Mice harboring mutations in the Deacetylase Activating Domains of both NCoR and SMRT (*NS-mDAD*) lack detectable Hdac3 enzymatic activity

in vivo (You et al., 2013). Further analysis of these mice revealed that despite no detectable Hdac3 deacetylase activity, they are able to maintain normal cardiac development and morphology through birth (Figure 3.5C) in contrast to embryos lacking Hdac3 protein in cardiac progenitors (Figure 3.3). *NS-mDAD* mice survive to term and do not exhibit ventricular hypoplasia. Furthermore, expression analysis revealed that these mice express critical myocyte genes at levels similar to wild-type controls (Figure 3.5D). Taken together, our *in vitro* and *in vivo* studies suggest that Hdac3 exhibits a deacetylase-independent function to regulate cardiac development and progenitor differentiation.

Hdac3 functions with Lamina Associated Domains to repress myocyte genes

Hdac3 has been proposed to function as a component of a protein complex responsible for the structural maintenance of nuclear Lamina Associated Domains (LADs). Previous studies suggest that Hdac3 interacts with a zinc finger transcription factor cKrox (ThPOK) and nuclear membrane protein Lap2β to mediate tethering of condensed (repressed) regions of chromatin to the inner nuclear membrane (Melnick et al., 2002; Somech et al., 2005; Zullo et al., 2012). We hypothesized that Hdac3 acts in this complex to prevent excess cardiac progenitor differentiation by repressing critical myocyte genes via tethering to the nuclear membrane. Consistent with this model, knockdown of *cKrox*, a DNA-binding member of this LAD complex, phenocopies the significant increase in ESC to cardiomyocyte differentiation that we observe with *Hdac3* depletion (Figure 3.6A,B).

Furthermore, expression analysis and chromatin immunoprecipitation reveals that several myocyte-specific genes which are repressed by Hdac3 are bound by Lamin B1. Lamin B1 is a core component of the nuclear lamina and DNA bound by Lamin B1 is by definition within a LAD. Deletion of *Hdac3* in differentiating mouse ESCs releases myocyte genes including those encoding structural components (*Ttn*, *Trdn*) and ion channels (*Kcnh7*, *Kcnc2*, *Kcnq1*) from the nuclear periphery, as determined by loss of binding to Lamin B1 (Figure 3.6C). This loss of LaminB1 occupancy is accompanied by higher expression of these same genes (Figure 3.6D). These results lead us to propose that Hdac3 acts in cardiac progenitor cells to silence a lineage-specific gene program by retaining key genomic loci at the nuclear periphery.

Landscape of LADs during cardiac development

Previous studies of three-dimensional chromatin organization within the nucleus have focused on *in vitro* model systems, and little is known about the dynamics of lamina-chromatin interactions during normal embryonic development (Peric-Hupkes et al., 2010; Sadaie et al., 2013; Shah et al., 2013). To provide a global view of nuclear architecture during cardiac development, we mapped DNA-lamina interactions genome-wide at multiple embryonic timepoints by Lamin B1 chromatin immunoprecipitation followed by sequencing (ChIP-seq). We identified about 1500 lamina-bound regions in e9.5 and e12.5 hearts (Figure 3.7), comparable with numbers of LADs seen in other systems (Peric-Hupkes et al., 2010; Shah et al., 2013).

Forcible tethering of Hdac3-bound genes to the nuclear periphery represses differentiation

To specifically test whether Hdac3 represses progenitor differentiation by tethering myocyte genes to the nuclear lamina, we designed a system in which Hdac3 is obligated to function as a LAD tether. We generated a construct fusing Flag-tagged Hdac3 to nuclear membrane protein Lap2β (Hdac3-Lap2β). Lap2β exclusively localizes to the inner nuclear membrane, and immunocytochemistry confirms the Hdac3-Lap2β fusion also localizes to the nuclear membrane (Figure 3.8A,B). Returning to our mESC system, we deleted endogenous *Hdac3* with addition of tamoxifen and exogenously expressed the Hdac3-Lap2β fusion, enabling us to restrict Hdac3 to the nuclear periphery to interrogate function at this specific subnuclear compartment. Transduction of the Hdac3-Lap2β fusion restores differentiation to equivalent levels as transducing wild-type Hdac3, a result not seen with an eGFP-Lap2β control (Figure 3.8C). Furthermore, expression of the deacetylase-deficient Y298H Hdac3 mutant fused to Lap2B also restors differentiation equivalent to wild-type Hdac3. These data suggest that tethering Hdac3-bound loci to the nuclear membrane does not require deacetylase activity and is sufficient to repress cardiac differentiation into cardiomyocytes.

Discussion

Progenitor cells require coordinated expression of complex gene patterns to promote differentiation to specific lineages while repressing alternative cell fates (Pongubala et al., 2008). Higher-order chromatin organization within the subcompartments of the nucleus significantly alters activity of large genomic domains, making it possible to regulate whole gene programs simultaneously. The region surrounding the nuclear lamina is enriched for transcriptionally silent genes decorated by repressive histone modifications. Recent work suggests that genome-nuclear lamina interactions are dynamic, rearranging during progenitor cell commitment and differentiation (Kohwi et al., 2013; Peric-Hupkes et al., 2010). However, to date the functional significance of these rearrangements has remained unclear.

The results presented in this chapter demonstrate that LAD positioning is maintained by the epigenetic modifier Hdac3, and altered nuclear localization of lineage-specific genes is accompanied by precocious cardiac progenitor differentiation. Loss of *Hdac3* promotes upregulation of a myocyte gene program and excessive formation of cardiomyocytes both *in vivo* and in an ES cell-based system. A number of these myocyte-specific genes alter their interaction with the nuclear lamina during normal development and are repositioned away from the nuclear periphery upon *Hdac3* deletion. Artificial tethering of Hdac3-bound genes to the nuclear membrane partially restores baseline myogenesis. This work represents, to our knowledge, the first analysis

of a cardiac defect influenced by disruption of nuclear lamina-mediated gene program silencing.

Human diseases involving defects in the nuclear lamina, collectively known as laminopathies, manifest with developmental defects including muscular dystrophies, cardiomyopathies and premature aging. Hutchinson-Gilford progeria syndrome (HGPS) results from mutations in Lamin A and leads to deregulation of chromatin structure and increased DNA damage (Van Bortle and Corces, 2013; Kubben et al., 2012). Mutations in Lamin A or its interacting protein Emerin also cause Emery-Dreifuss muscular dystrophy (EDMD), a degenerative muscular disease that is nearly always associated with cardiac abnormalities. A *C. elegans* model of EDMD exhibits abnormal positioning of heterochromatin and a muscle-specific transgene (Mattout et al., 2011). These conditions are caused by disruption of the nuclear lamina, however further study is required to determine whether rearrangement of genome-nuclear lamina interactions explains some or all of the observed phenotypes.

I propose a model by which a lineage-specific gene program is repressed in progenitor cells by localizing to the “silenced environment” of the inner nuclear lamina (Figure 3.9). As I discuss in Chapter 4, it is unlikely that progenitor cell behavior is exclusively regulated by genome-nuclear lamina interactions, however higher-order chromatin organization remains a powerful mechanism for coordinated gene expression. Nuclear localization studies by FISH reveal differential clustering of active versus repressed gene loci (Shopland et al., 2006). Several epigenetic regulator complexes

including NuRD and Brahma are found at the nuclear periphery, suggesting that several components are in place for repression of tethered gene loci (Euskirchen et al., 2011; Milon et al., 2012). Furthermore, another component of the subnuclear structure, the nuclear matrix, plays an important role in transcriptional activation of developmentally required homeodomain protein targets (Skowronska-Krawczyk et al., 2014). Collectively with the work presented in this chapter, there is growing evidence that the distribution of the three dimensional chromatin organization within the nucleus can have powerful effects on gene expression networks and developmental dynamics.

Materials and methods

Mice

Isl1^{Cre}, *Nkx2.5*^{Cre}, *aMHC-Cre,* *Hdac3*^{flox}, and CMV-creERT mice were maintained on mixed CD1/B6/129 genetic backgrounds separated by 4-8 generations of interbreeding from pure parental strains (Agah et al., 1997; Hayashi et al., 2002; Moses et al., 2001; Mullican et al., 2011; Srinivas et al., 2001). NS-mDAD mice were maintained on a C57BL/6 background (You et al., 2013). Mice were genotyped using previously described Cre-specific PCR primers (5'-TGC CAC GAC CAA GTG ACA GC-3', 5'-CCA GGT TAC GGA TAT AGT TCA TG-3') (Heidt and Black, 2005), and primers designed to distinguish between the control and floxed *Hdac3* allele (5'-GCA GTG GTG GTG AAT GGC TT-3', 5'-CCT GTG TAA CGG GAG CAG AAC TC-3'). Littermate embryos were analyzed in all experiments unless otherwise noted. The University of Pennsylvania Institutional Animal Care and Use Committee approved all animal protocols.

ES cell derivation and differentiation

Embryonic stem cells were derived from *CMV-creERT; Hdac3*$^{f/f}$ mice as previously described (Nagy et al., 2002). Briefly, blastocysts were collected at e3.5 and

cultured on STO feeder cells in standard ESC media +LIF + 50µM MEK1 inhibitor (Cell Signaling #9900) for 7 days until blastocyst hatches and forms colony. Individual colonies were subcultured for about 1 week when MEK inhibitor is removed and cells passaged as a normal ESC line.

Cardiac differentiation was adapted from published protocols (Christoforou et al., 2008; Kattman et al., 2011). Briefly, ESCs were cultured and maintained on a feeder layer of mitotically inactivated MEFs in DMEM with 15% FBS (Fisher Scientific # SH3007003) and ESGRO leukemia inhibitory factor. Differentiation through hanging droplets method was initiated following ESC dissociation and suspension at 5 x 10^4 cells/ml in DMEM with 10% FBS (Atlanta Biologicals #S11550) without LIF in 20µl drops. Two days after droplets formation, embryoid bodies (EBs) were transferred in suspension on poly-HEMA coated dishes. After another two days, EBs were plated on gelatin coated dishes in cardiac differentiation media (StemPro-34 SF medium [Invitrogen #10639-011] supplemented with 5ng/ml VEGF [R&D systems], 10ng/ml bFGF [R&D systems], 12.5ng/ml FGF10 [R&D systems], 2.5µM XAV939 [Cayman Chemical #13596], 1mM Ascorbic Acid [Sigma] and 2mM Glutamax [Invitrogen]). Beating cells were visible within 48 hours.

4-Hydroxytamoxifen (Sigma #T176) was dissolved in ethanol and added at 1µg/ml final concentration to delete *Hdac3*.

Flow cytometry

ES-derived cells and embryonic hearts were fixed, permeabilized and stained for flow cytometry according to standard protocols. Briefly, cells were dissociated in 1mg/ml collagenase solution, fixed in Fixation buffer (eBioscience #00-8222-49), permeabilized in 1x Permeabilization buffer (eBioscience #00-8333-56) and stored in 1% BSA. Embryonic hearts were dissociated in 5mg/ml collagenase at 37^{o}C for 10 minutes with occasional trituration before fixation and permeabilization steps. Cells were stained with primary and secondary antibodies for 1 hour each in Permeabilization buffer, resuspended in Flow Cytometry buffer (eBioscience #00-4222-26) and analyzed on BD FACSAria II cytometer. Antibodies used were cardiac Troponin T (1:100, Thermo #MS-295-P), Smooth Muscle Actin (1:100, abcam #ab5694), CD31 (1:100, abcam #ab28364), Phospho-Histone H3 (1:50, Cell Signaling #9701), anti-mouse AlexaFluor 488 (1:200, Invitrogen #A21200) and anti-rabbit AlexaFluor 647 (1:200, Invitrogen #A21244)

RNA isolation, complementary DNA synthesis, quantitative RT-PCR and Microarray

ES-derived cells or microdissected embryonic hearts were isolated in Trizol (Invitrogen # 15596-026) and RNA was obtained using the Qiagen RNeasy spin column, with on-column DNAse I digestion. Complementary DNA (cDNA) was synthesized according to kit instructions with the Superscript III system (Invitrogen). Quantitative RT-

PCR was performed in triplicate using Sybr Green (Applied Biosystems). *Gapdh* was used as a reference control gene. Quantitative RT-PCR primers (Table 3.2) were designed using IDT software. Microarray analysis was performed by the University of Pennsylvania Next Generation Sequencing Core using 2-color hybridization technique with a whole genome mouse Agilent array. Four pools each of mutant *Nkx2.5^{Cre}; Hdac3$^{f/f}$* and littermate control RNA were hybridized to the array. Each pool contained three hearts microdissected from e9.5 embryos.

Western blot analysis

Lysates were run on 4-12% Bis-Tris protein gels (Invitrogen #NP0335) and blots were probed with anti-Hdac3 (1µg/ml, abcam #ab7030) or anti-β-actin (1:1000, Cell Signaling #4967) according to the instructions of the manufacturer and as previously described (Aghajanian et al., 2014). Visualization was achieved using ECLPrime (GE Life Sciences #RPN2232).

Histology

Histological analysis was performed on paraformaldehyde-fixed, paraffin embedded slides as previously described (High et al., 2008). Embryos were dissected in cold PBS, fixed overnight in 2% paraformaldehyde, dehydrated into 100% ethanol,

embedded in paraffin and sectioned. H&E staining was performed using standard procedures. All control and mutant histological images shown for comparison were taken at the same exposure and contrast settings, using NIS Elements software.

Plasmids, transfection and transduction

Expression plasmids for Flag-Hdac3 and Flag-Hdac3 Y298H were generously provided by P. Gallinari (Lahm et al., 2007). Wild-type and mutant Hdac3 were cloned into AgeI-BsrGI sites of lentivirus FUGW (Addgene plasmid 14883, deposited by David Baltimore, (Lois et al., 2002)) for transduction of ESC-derived cells. Lap2β was PCR amplified from pEGFP-Lap2β (generously provided by J. Ellenberg (Beaudouin et al., 2002)) and cloned into BsrGI site of FU-Hdac3 or FU-Hdac3 Y298H, creating a fusion protein with Hdac3 or Hdac3 Y298H. cKrox shRNA was generously provided by K. Reddy (Sigma clone TRCN0000194510). Lentiviruses were generated in Lenti-X 293T cells (Clontech # 632180) according to manufacturer instructions. Plasmid transfections were performed with Fugene 6 (Promega #E2691) according to manufacturer instructions.

Lamin B1 ChIP-qPCR and ChIP-seq

Lamin B1 ChIP was performed from ES-derived cells or microdissected embryonic hearts as previously described (Shah et al., 2013). hiSeq-50SR sequencing

was performed by the University of Pennsylvania Funcitonal Genomics Core. qPCR primers to validate ChIP targets in ES-derived cells were designed using IDT software. Primers used are listed in Table 3.3.

For assigning lamina-associated domains from sequencing data, the following method was used: We partitioned the genome into windows of length 1000 bp. Each window $\boldsymbol{w}$ has $\boldsymbol{a_w}$ input reads and $\boldsymbol{b_w}$ ChIP reads. We collected reads from several ChIP and input sets, and we processed only windows that have at least one read mapped in one of the sets. Other windows are ignored, we call them “null windows”. As a result, we do consider windows with $\boldsymbol{a_w} = \boldsymbol{b_w} = 0$ if they have reads in some other data sets. The “significance” of an interval of windows is related to the p-value that we observe for a particular number of signal reads in that interval, but we normalize that number in each window. In the null model the windows are permuted, so the content of each window is an independent event, and the probability of seeing some combination of independent events is the product but we add scores, not multiply. Therefore we use the score that is related to the LOGARITHM of the probability, thus the sum of scores for a block of windows is related to the logarithm of the product, so it is related to the probability for the block.

We consider the windows with a particular number of input reads:

$\boldsymbol{n_i}$ is the number of all windows with $\boldsymbol{a_w} = \boldsymbol{i}$ (***i*** input reads)

$\boldsymbol{s_{ik}}$ is the number of all windows with $\boldsymbol{a_w} = \boldsymbol{i}$ ***and*** $\boldsymbol{b_w} = \boldsymbol{k}$

m_i is the median for i, a number m such that

$s_{i0} + \ldots + s_{i(m-1)}$ and $s_{i(m+1)} + \ldots + s_{i\text{maximum}}$ are both smaller than $n_i / 2$

Score(i,m_i) = 0, zero significance for the median

For $k < m_i$ we define $t_{ik} = s_{i0} + \ldots + s_{ik}$ and Score(i,k) = log ($2t_{ik} / n_i$)

For $k > m_i$ we define $u_{ik} = s_{ik} + \ldots + s_{i\text{maximum}}$ and Score(i,k) = -log ($2u_{ik} / n_i$)

With this formula, if the count of signal reads is the median (among windows with the same number of reads), then it gets score 0, below, negative, above, positive.

The idea of the scoring is that we prefer to select windows with positive scores and avoid selecting windows with negative scores. However, with the described method of assigning scores, about half of the windows have positive score and about half, negative, while the target region occupy less than half of the genome. Therefore we use ***Score***(w) = Score(a_w, b_w) – α where α is the score adjustment, the same for all non-null windows. The larger score adjustment we use, the fewer windows belong to the selected regions. The score adjustment is one of the two parameters supplied by the user.

We create blocks of consecutive windows, so either all windows in a block belong to one of the selected regions, or none of them does. We start with maximum

blocks such that all windows in a block are negative (scores below zero) or all are positives (scores at least 0). In this way, blocks of windows from a particular chromosome form a list, sorted by the position, and positive and negative blocks alternate.

In the case of the mouse genome, we start with roughly 2.5E+06 windows and 1E+06 initial blocks. Then we performed the steps described below until there are exactly N positive blocks, and we return the positive blocks as the selected regions. N is the second parameter supplied by the user.

To perform a step of the algorithm, we consider a block with the minimum ABSOLUTE value of the sum of scores of its windows. If it is the first or the last block in a chromosome list, we remove it, otherwise we merge it with the two neighbor blocks.

Immunocytochemistry

Transfected 293T cells grown on glass coverslips, fixed in 4% paraformaldehyde for 10 minutes, permeabilized in 0.25% TritonX-100 +3% BSA for 15 minutes, blocked in 3% BSA and incubated in primary and secondary antibodies for 1 hour each. After washes, slides were mounted in DAPI-containing mounting solution (Invitrogen #P-36931) and imaged. All images shown for comparison were taken at the same exposure

and contrast settings, using NIS Elements software. Antibodies used were anti-GFP (1:100, Cell Signaling #2956), anti-Flag (1:1000, Sigma #F1804), anti-mouse AlexaFluor 488 (1:400, Invitrogen #A21200) and anti-rabbit AlexaFluor 568 (1:400, Invitrogen #A11011).

Table 3.1: SHF-specific *Hdac3* deletion results in embryonic lethality

Isl1^{Cre}; Hdac3$^{f/+}$ x *Hdac3$^{f/+}$*				
P0	No. Observed	Observed	No. Expected	Expected
Hdac3$^{+/+}$	12	0.12	12.3	0.13
Hdac3$^{f/+}$	31	0.32	24.5	0.25
Hdac3$^{f/f}$	17	0.17	12.3	0.13
Isl1^{Cre}; Hdac3$^{+/+}$	16	0.16	12.3	0.13
Isl1^{Cre}; Hdac3$^{f/+}$	22	0.22	24.5	0.25
Isl1^{Cre}; Hdac3$^{f/f}$	0	0	12.3	0.13
Total	98			
χ^2	0.004			

Table 3.2: qRT-PCR Primers for expression analysis

Gene name	Protein name	Sequence (5' – 3')
Gapdh	Gapdh	CGTCCCGTAGACAAAATGGT
		GAATTTGCCGTGAGTGGAGT
Hdac3	Hdac3	CCATTCTGAGGACTACATCGAC
		TGTGTAACGGGAGCAGAAC
Tnnt2	cTroponinT	ATCGAGGCTCACTTCGAGAAC
		GTCTTTGAGGGAAATCAGCTCC
Myh6	alpha-MHC	ACGGTGACCATAAAGGAGGA
		TGTCCTCGATCTTGTCGAAC
Actc1	Cardiac Actinin	GACCTCACTGACTACCTCATG
		TCTCGTTCTCAAAATCCAGGG
Ttn	Titin	GACACCACAAGGTGCAAAGTC
		CCCACTGTTCTTGACCGTATCT
Nkx2.5	Nkx2.5	GACAGGTACCGCTGTTGCTT
		AGCCTACGGTGACCCTGAC
Cnn1	Calponin	CTTCTGCACATTTTAACCGAGG
		AATGATCCCGTCTTTGAGGC

Pecam1	PECAM1	ACATTCACAGATAAGCCCACC
		TCTTTCACAGAGCACCGAAG
Calca	Calcitonin	CTCCAGGCAGTGCCTTTGAG
		GGCGAACTTCTTCTTCACTGAGA
Kcnq1	Kcnq1	ACCGTCTTCCTCATTGTTCTGG
		GACAATCTCCATCCAGAAGAGG
Kcnc2	Kcnc2	TCCAGTACGAAATCGAAACGG
		GGGTGAGAAAACAATTCGGACTA
Kcnh7	Kcnh7	CCAGGAAACTGGACCGATACT
		CCAATCGCATACCAGATGCAA

Table 3.3: qPCR primers for ChIP analysis

Gene name	Protein name	Sequence (5' – 3')
Actc1	Cardiac Actinin	GCTCAGTCTCATCCTCTACT
		TCAGTCTCACCTCCTGATAC
Ttn	Titin	CTCTATCTGGTGTTTCCTTTC
		AAAGGCAGAAGGGTCTAA
Calca	Calcitonin	CATGTGTAAGGAGCAGAGTAAG
		AGTTCCATGCCCACTATCT
Kcnq1	Kcnq1	CATCTAAGGTCCCTCACTTTG
		CAGGCATCCTCAGGAAATAG
Kcnc2	Kcnc2	CTGGCTCAGACCCATAAA
		AATGGAGGACACCAGAAG
Kcnh7	Kcnh7	TCTGTTCCTCTCTGTCATT
		GTCTGGGATTGGCTTATTT
Ctnnd	Catenin, Delta	GAGTAGAAAGGAGGGAGTAG
		TCTCTGACCTGTGATCTTT

Figure 3.1: Hdac3 represses ES differentiation to cardiomyocytes

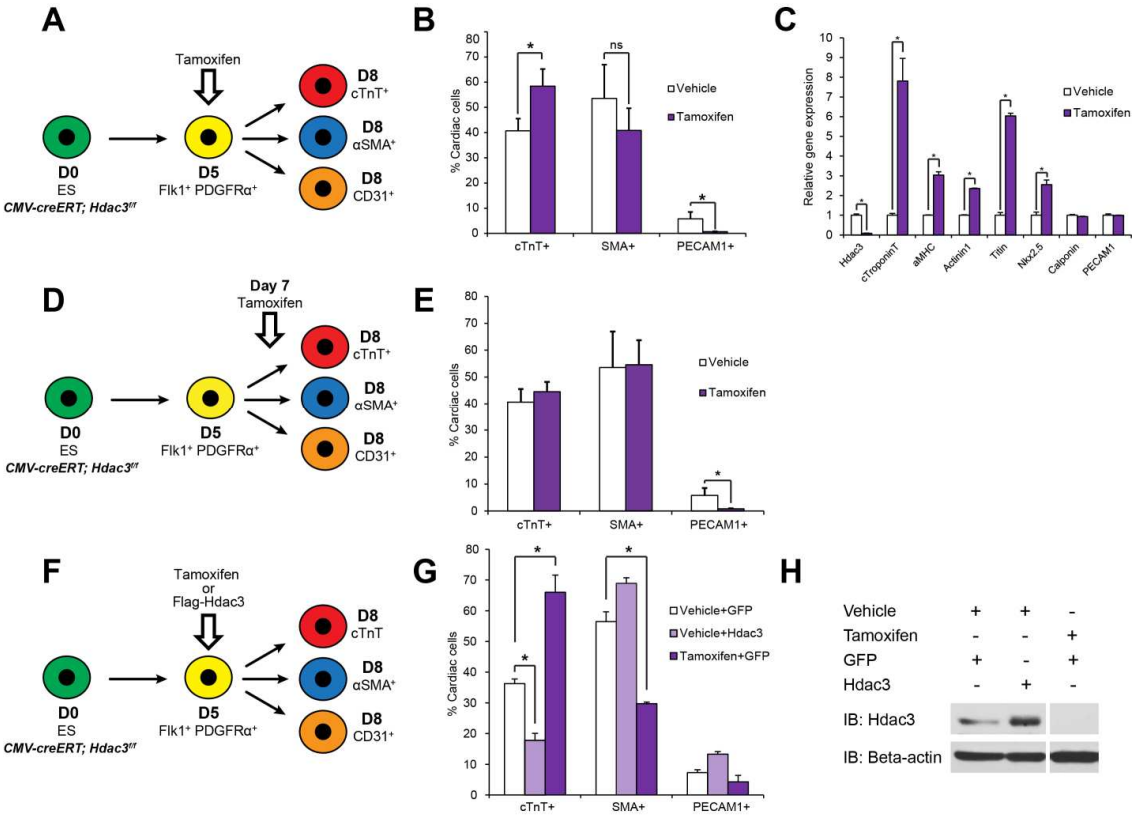

Figure 3.1: Hdac3 represses ES differentiation to cardiomyocytes

(A)Schematic of *Hdac3* deletion in differentiating mouse ESCs of genotype *CMV-creERT; Hdac3*$^{f/f}$. Deletion is induced with tamoxifen at day 5 when cardiac progenitors are present. (B) Analysis by flow cytometry of cardiac TroponinT (cTnT)$^{+}$, Smooth Muscle Actin(SMA)$^{+}$, and PECAM1^{+} cells on day 8 of differentiation. Y-axis of % cardiac cells represents percent of total cTnT^{+}, SMA^{+} and PECAM1^{+} cells. (C) Gene expression analysis by qRT-PCR on day 8 of differentiation after tamoxifen addition at day 5. (D) Schematic of*Hdac3* deletion with tamoxifen addition at day 7 of differentiation, two days after peak expression of Flk1^{+},PDGFRα^{+} progenitors. (E) Flow cytometry of cTnT^{+}, SMA^{+} and PECAM1^{+} cells after *Hdac3* deletion at day 7 of differentiation. (F) Schematic of *Hdac3* deletion and overexpression at day 5 of differentiation. (G) Flow cytometry analysis demonstrates fewer cTnT+ cells after *Hdac3* overexpression and more cTnT+ cells after *Hdac3* deletion. (H) Western blot analysis to confirm *Hdac3* overexpression and deletion. * denotes $p<0.05$. ns denotes $p>0.05$.

Figure 3.2: No change in proliferation upon *Hdac3* deletion

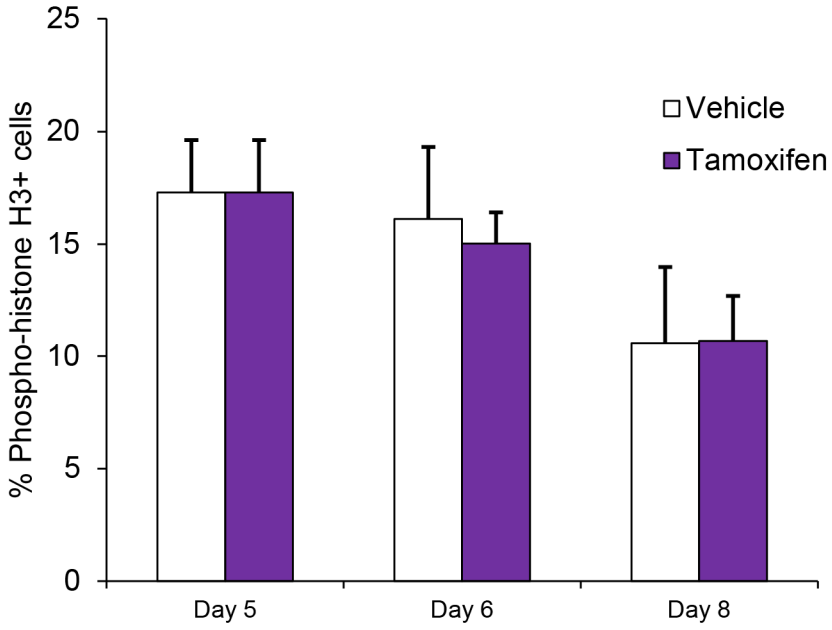

Figure 3.2: No change in proliferation upon *Hdac3* deletion

Flow cytometry analysis of phospho-histone H3+ cells in differentiating ESCs at days 5, 6 and 8 of differentiation after vehicle or tamoxifen addition at day 5.

Figure 3.3: Hdac3 inhibits differentiation of FHF and SHF cardiac progenitors *in vivo* by repressing a myocyte gene program

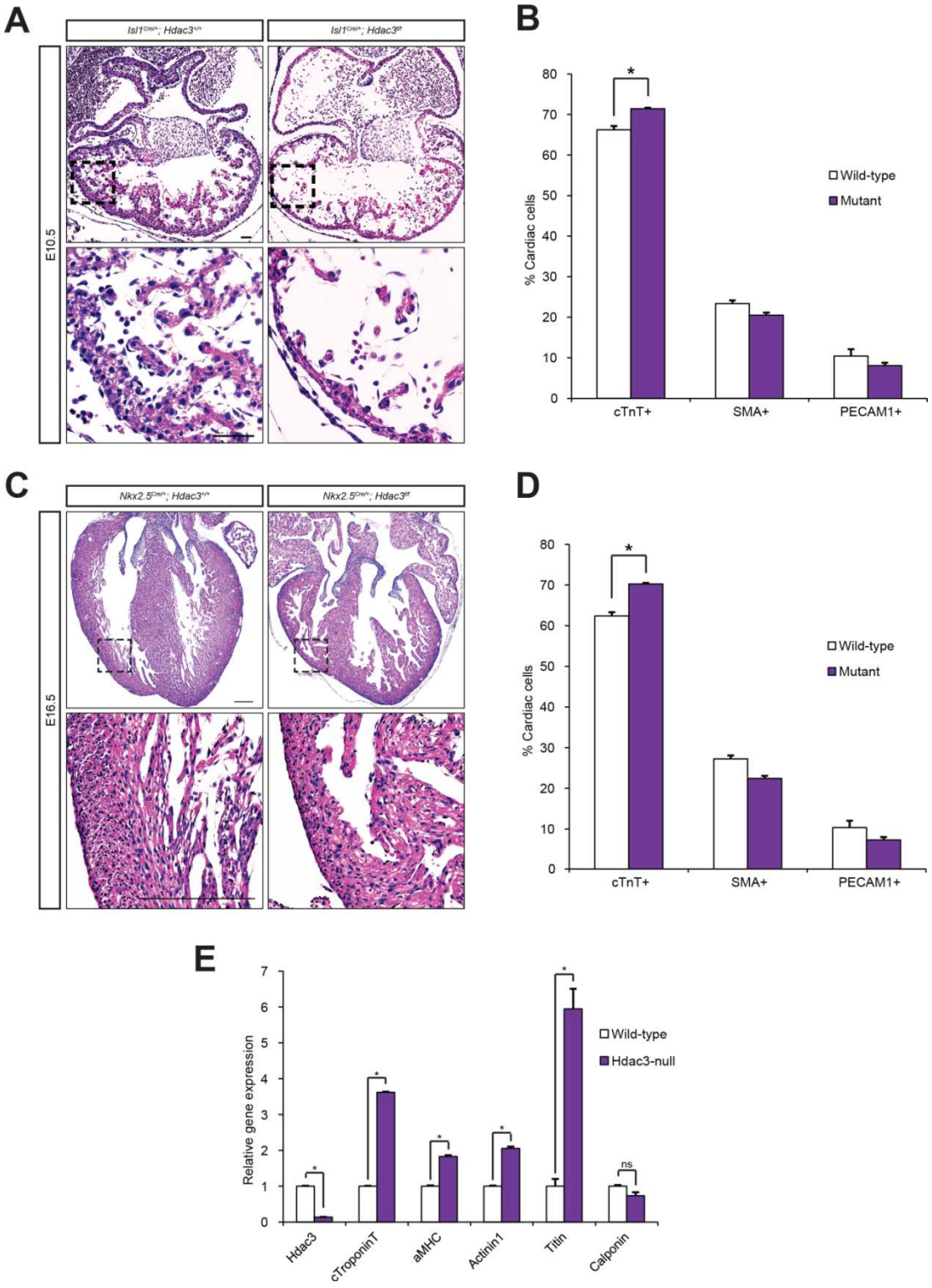

Figure 3.3: Hdac3 inhibits differentiation of FHF and SHF cardiac progenitors *in vivo* by repressing a myocyte gene program

(A)Deletion of *Hdac3* in *Isl1*-expressing SHF progenitors results in ventricular hypoplasia, thin myocardium and embryonic lethality. H&E staining at e10.5 reveals morphology and boxed area highlights thinned right ventricle wall in mutants relative to controls. Scale bars 50µm. (B) Flow cytometry analysis of cTnT+, SMA+ and PECAM1+ cells from dissociated e10.5 $Isl1^{Cre}$ control and *Hdac3*-null hearts. (C) Deletion of *Hdac3* in *Nkx2.5*-expressing FHF and SHF progenitors at e16.5. Box highlights area of right ventricle with thin myocardium. Scale bars 200µm. (D) Flow cytometry analysis of dissociated e16.5 $Nkx2.5^{Cre}$ control and *Hdac3*-null hearts. (E) Gene expression analysis by qRT-PCR of e9.5 $Nkx2.5^{Cre}$ control and *Hdac3*-null hearts. * denotes $p<0.05$. ns denotes $p>0.05$.

Figure 3.4: *Hdac3* deletion in cardiomyocytes does not disrupt cardiac morphology

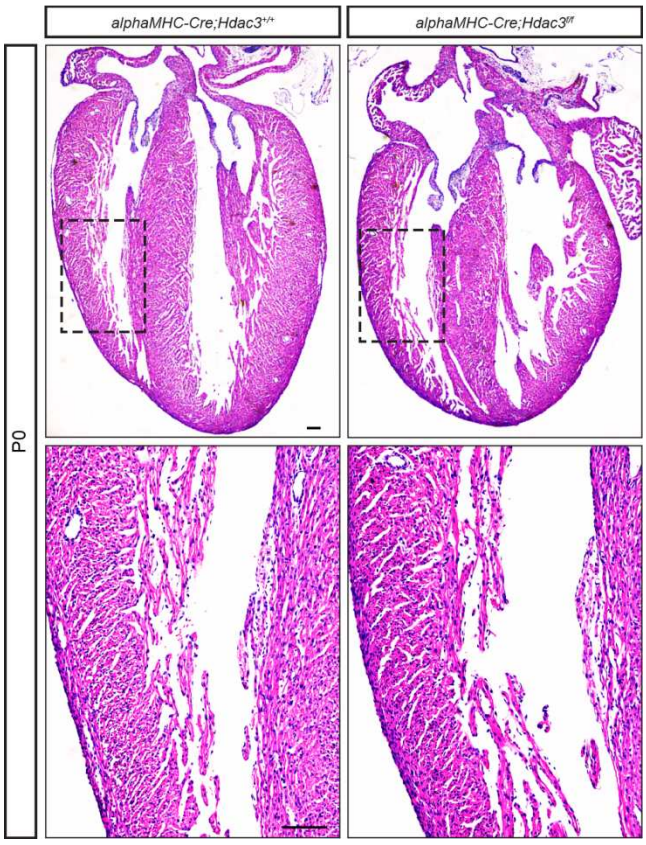

Figure 3.4: *Hdac3* deletion in cardiomyocytes does not disrupt cardiac morphology

Histological analysis of cardiomyocyte-specific deletion of *Hdac3* at P0 by H&E staining. Box highlights normal right ventricle myocardium in both control and *Hdac3*-null hearts. Scale bars 100µm.

Figure 3.5: Hdac3 represses cardiac differentiation independent of catalytic function

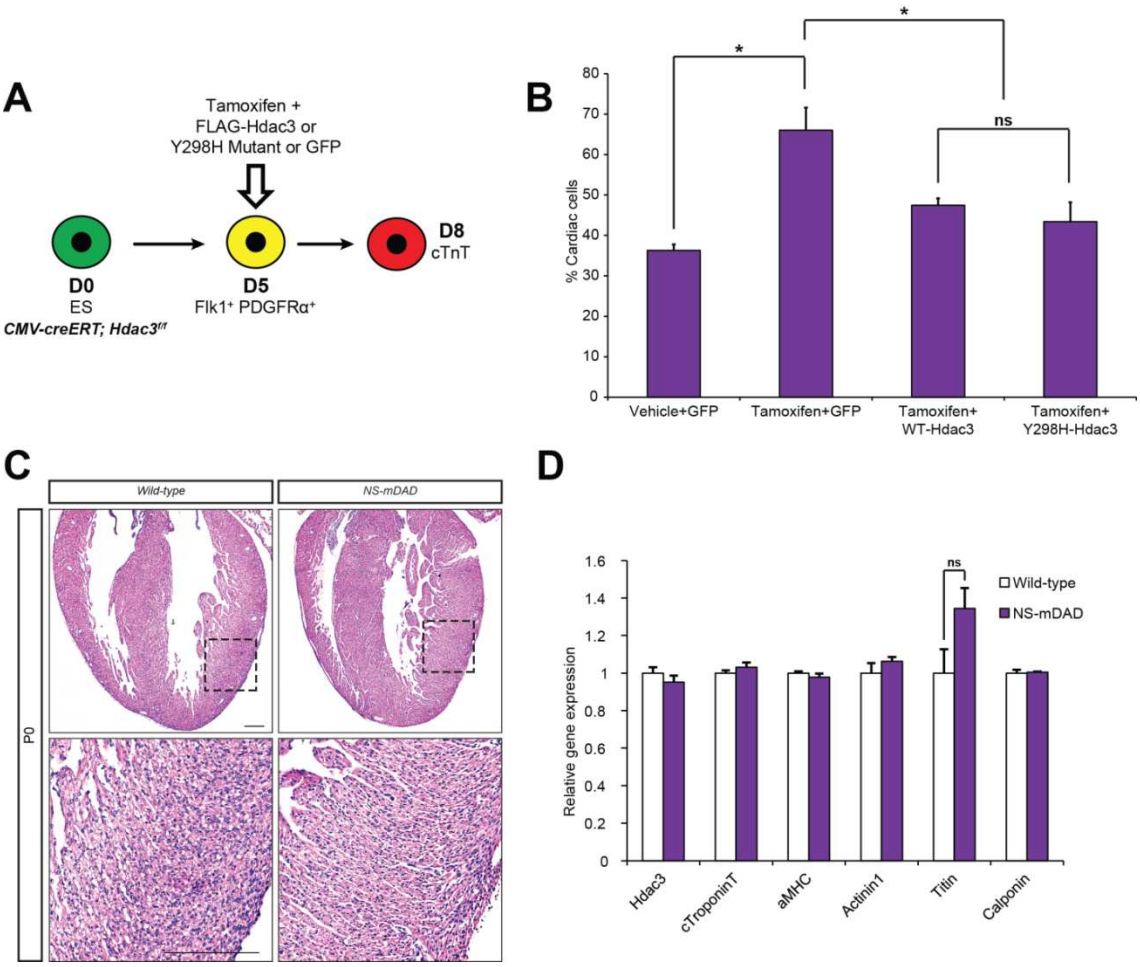

Figure 3.5: Hdac3 represses cardiac differentiation independent of catalytic function

(A)Schematic of *Hdac3* deletion and transduction of wild-type or Y298H mutant Hdac3 in differentiating ESCs. (B) Analysis of cTnT+ cells by flow cytometry of ESCs on day 8 of differentiation after addition of vehicle or tamoxifen at day 5 with simultaneous transduction of GFP control or wild-type Hdac3 or Y298H mutant Hdac3. (C) H&E staining of *NS-mDAD* mice at P0. Scale bars 200μm. (D) Gene expression analysis of myocyte genes by qRT-PCR from P0 NS-mDAD hearts. * denotes $p<0.05$. ns denotes $p>0.05$.

Figure 3.6: Hdac3 functions with Lamina Associated Domains to repress myocyte genes

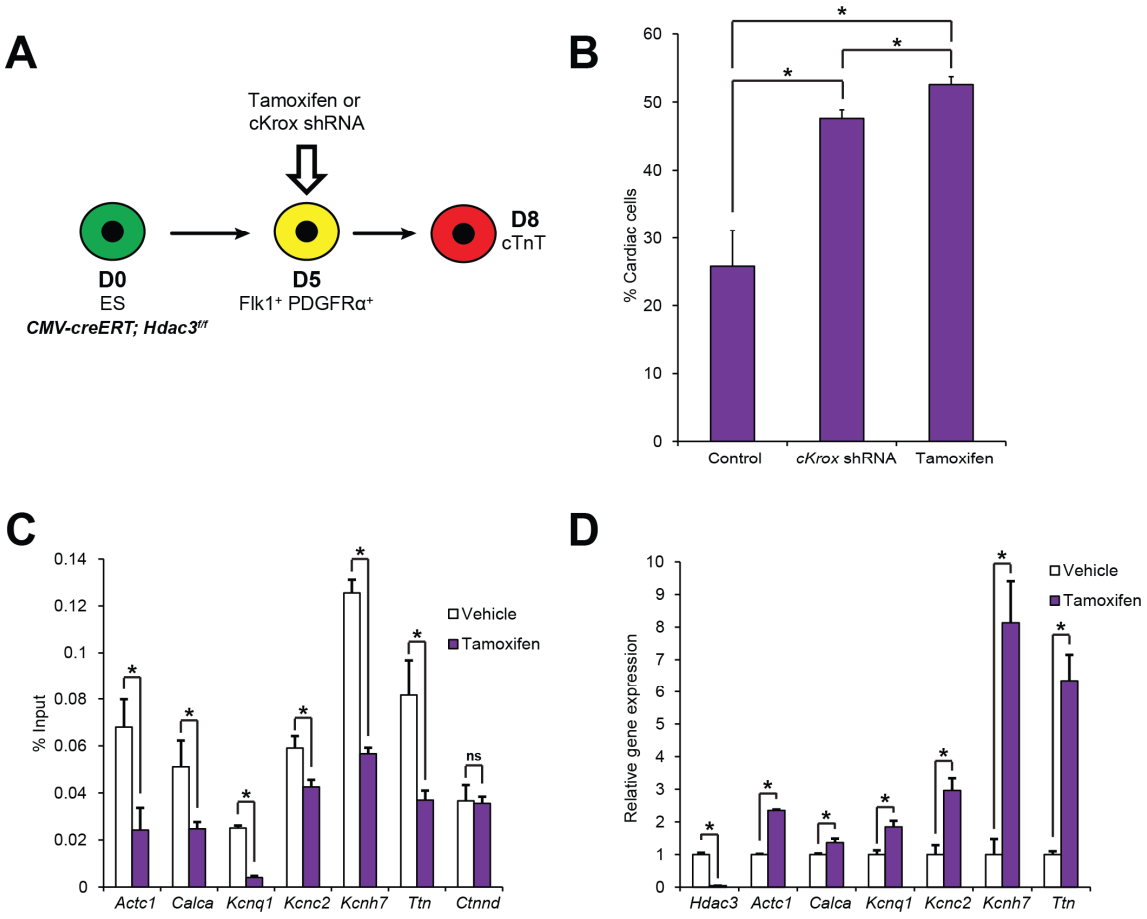

Figure 3.6: Hdac3 functions with Lamina Associated Domains to repress myocyte genes

(A)Schematic of *Hdac3* deletion or *cKrox* knockdown at day 5 of ESC differentiation. (B) Analysis by flow cytometry of cTnT+ cells with control shRNA or *cKrox* shRNA or tamoxifen addition. (C) LaminB1 ChIP-qPCR at myocyte genes was performed with ESCs at day 8 of differentiation after addition of vehicle or tamoxifen at day 5. (D) Gene expression analysis of myocyte genes in differentiation day 8 ESCs indicates myocyte genes in LADs are upregulated upon *Hdac3* deletion. * denotes $p<0.05$. ns denotes $p>0.05$.

Figure 3.7: Dynamic landscape of LADs during cardiac development

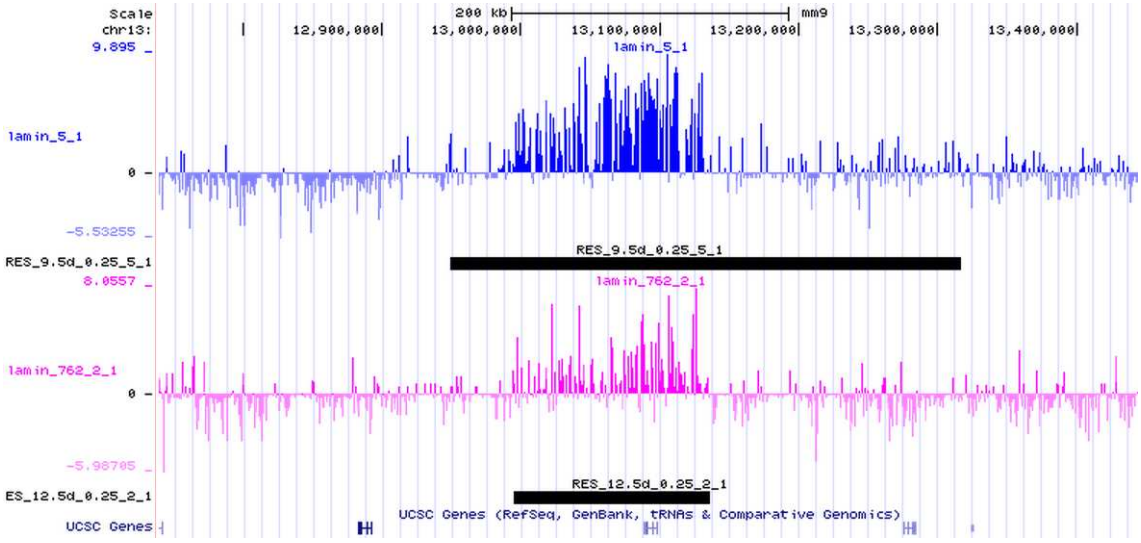

Figure 3.7: Landscape of LADs during cardiac development

LaminB1 ChIP-seq track from wild-type e9.5 and e12.5 hearts maps LADs genome-wide during cardiac development. Blue represents Lamin B1 occupancy at e9.5, pink represents occupancy at e12.5. Black bar annotates individual LADs. Scale bar: 200,000 bp

Figure 3.8: Forcible tethering of Hdac3-bound genes to the nuclear periphery represses differentiation

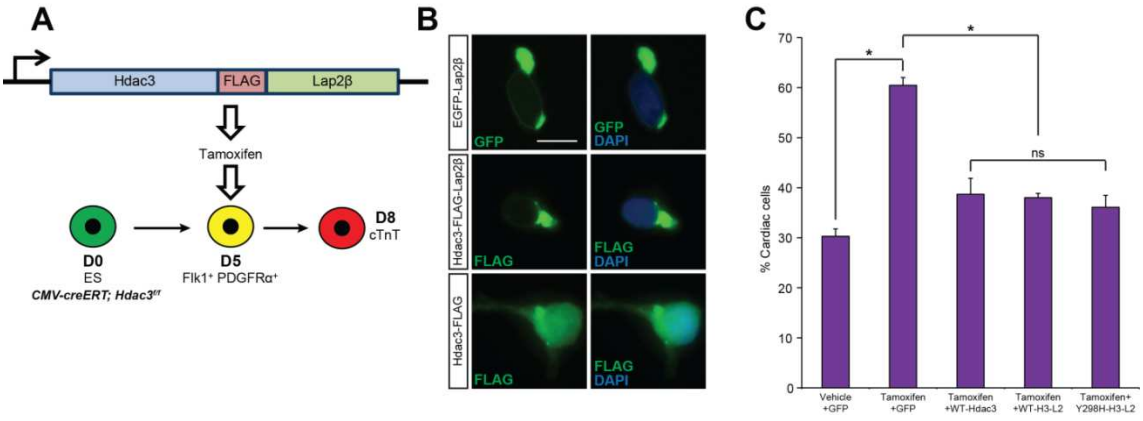

Figure 3.8: Forcible tethering of Hdac3-bound genes to the nuclear periphery represses differentiation

(A)Schematic of Hdac3-Lap2β fusion expressed in differentiating ESCs at day 5. (B) Immunofluorescence of 293T cells transfected with EGFP-Lap2β, Hdac3-Lap2β or wild-type Hdac3 and stained for FLAG or GFP with DAPI as a nuclear stain. Scale bars 10μm. (C) Analysis by flow cytometry of cTnT+ cells at day 8 of differentiation after vehicle or tamoxifen treatment and transduction with GFP, wild-type Hdac3 (WT-Hdac3), wild-type Hdac3-Lap2β fusion (WT-H3-L2) or Y298H Hdac3 mutant-Lap2β fusion (Y298H-H3-L2). * denotes $p<0.05$. ns denotes $p>0.05$.

Figure 3.9: Model of LAD-mediated repression of myocyte gene program in cardiac progenitor cells

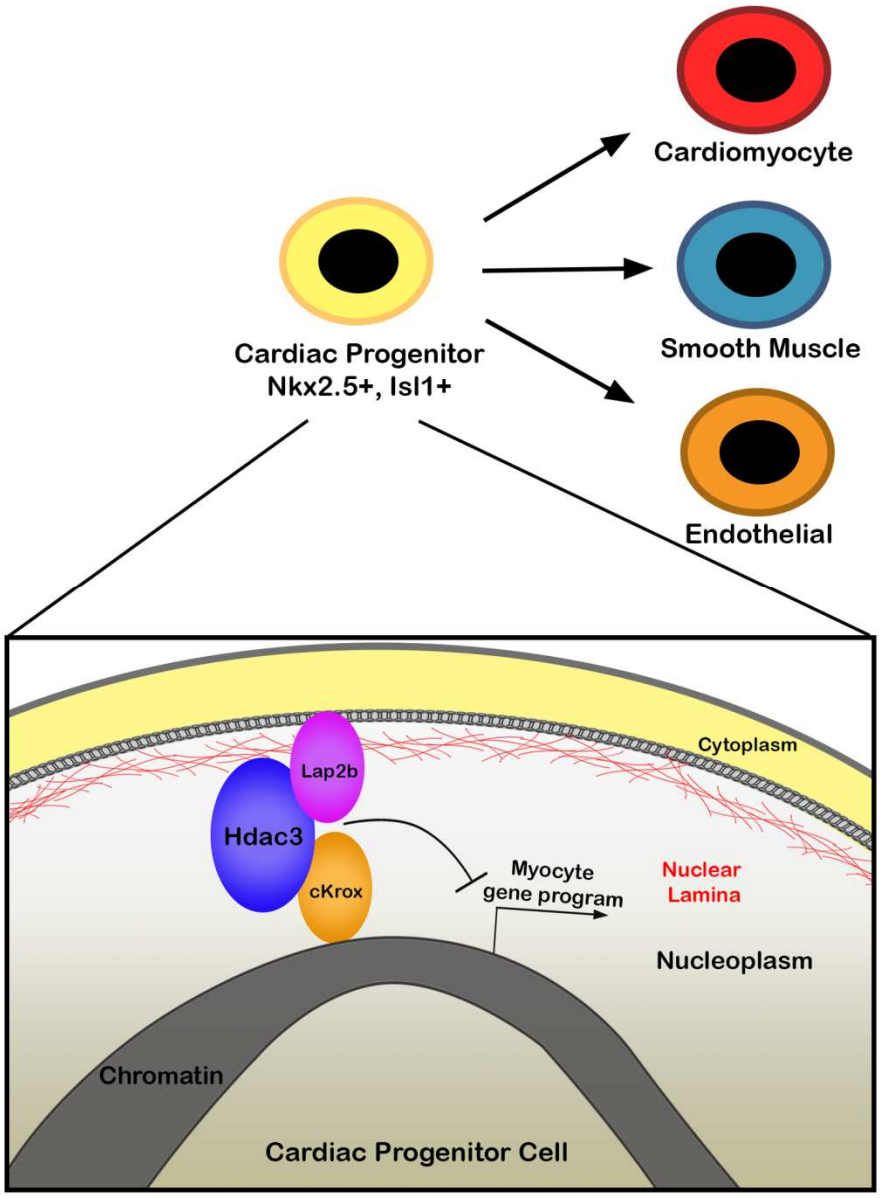

Figure 3.9: Model of LAD-mediated repression of myocyte gene program in cardiac progenitor cells

Schematic of cardiac progenitor differentiation into cardiomyocyte, smooth muscle and endothelial cell lineages. Within cardiac progenitor cells (marked by Nkx2.5 and Isl1 expression), Hdac3 interacts with Lap2β and cKrox to tether a myocyte gene program to the nuclear lamina, repressing transcriptional activity and myocyte commitment.

Chapter 4. Conclusions and Future Directions

Summary

Progenitor cells are developmental precursors with the capacity to differentiate into multiple cell types but with a limited ability to self-renew. Appropriate differentiation of progenitor cells requires coordinated expression of lineage-specific gene programs. Epigenetics is the study of heritable changes in gene expression not caused by differences in the DNA sequence. These changes can be widespread across large genomic regions, offering a convenient mechanism for synchronizing expression of numerous genes in a progenitor cell. In this dissertation, I studied the role of histone deacetylase 3, an epigenetic regulator, in the context of neural crest and cardiac progenitor cell expansion and commitment. Previous studies had identified the importance of Hdac3 in the development of these and other tissues, however the precise mechanism by which Hdac3 regulates progenitor cell behavior remained uncertain.

In Chapter 2, I demonstrate that Hdac3 functions in the neural crest as a repressor of cell proliferation and survival by regulating expression of a core network of factors required during craniofacial development. These well-studied pathways include the Bmp-Msx axis, with increased expression of *Msx1* and *Msx2* sufficient to reduce proliferation in *Hdac3* mutants. These changes in proliferation and survival of neural crest-derived

mesenchyme cause cleft palate, microcephaly, tooth hypoplasia and other craniofacial defects.

In Chapter 3, I examine the role of Hdac3 in cardiac progenitor cells of the first and second heart fields. These cells differentiate into cardiomyocyte, smooth muscle and endothelial cell lineages and go on to populate the heart. Similar to previous work, Hdac3 functions as a repressor to inhibit expression of a lineage-specific gene program. Silencing of cardiomyocyte genes prevents precocious differentiation of cardiac progenitor cells. Surprisingly, Hdac3 represses the myocyte fate independent of its deacetylase activity. Instead, Hdac3 functions at the nuclear membrane to tether myocyte genes to the nuclear lamina, preventing expression of this gene program and repressing differentiation down the cardiomyocyte lineage. Loss of *Hdac3* allows these cardiac progenitor cells to precociously differentiate into cardiomyocytes, resulting in ventricular hypoplasia and embryonic lethality.

These results implicate a role for subnuclear organization of chromatin as a regulator of progenitor cell behavior and lineage commitment during development. This is a novel direction for the nuclear architecture field and one that offers insight into how cells may coordinate the factors necessary to drive broad, dramatic changes like adopting new fates.

Future directions

How widespread is nuclear architecture regulation in development?

Previous work on nuclear architecture and lamina associated domains has primarily focused on *in vitro* model systems and transgenic cell lines. This includes mapping chromatin organization in cultured *Drosophila* cells and cell-based experiments artificially tethering reporter genes to the nuclear membrane (van Bemmel et al., 2013; Pickersgill et al., 2006; Reddy et al., 2008). The *in vitro* work with the closest developmental corollary is a pioneering study from the van Steensel group mapping genome-lamina interactions in mouse ESCs differentiating into neurons (Peric-Hupkes et al., 2010). At four stages of differentiation, the authors performed DamID to mark chromatin in contact with the nuclear lamina, profiling the dynamic changes in nuclear organization during differentiation. From this study, a few observations stand out. First, some LADs are remarkably dynamic, with the level of interaction with the lamina changing significantly at each time point. Second, during differentiation to the neuronal lineage, non-neuronal factors are being silenced and repressed at the nuclear periphery. Third, certain LADs did not change over the course of differentiation, but rather stayed constitutively bound at the periphery during neuronal specification. Together, these results suggest that a select portion of the genome dynamically alters subnuclear localization during progenitor cell commitment.

The primary study of nuclear architecture-mediated silencing *in vivo* focuses on localization of a single gene in *Drosophila* neural progenitor cells (Kohwi et al., 2013). The authors identified and visualized *hunchback*, a transcription factor responsible for promoting progenitor cell competence and inhibiting differentiation. *Fluorescent in situ hybridization* enabled tracking of this gene to the nuclear periphery as neuroblast progenitors begin to lose competence. Artificial loss of genome-lamina interaction permitted sustained expression of *hunchback* and prolonging of progenitor competence. This study in an invertebrate system suggests that nuclear organization and lamina-mediated gene regulation influences progenitor cell behavior.

In addition to the mapping study during ESC differentiation, additional work from the van Steensel group and others has profiled genome-lamina interactions in multiple cell types (van Bemmel et al., 2013; Filion et al., 2010; Kubben et al., 2012; Shah et al., 2013; Zullo et al., 2012). These LAD maps have consistently demonstrated that about 40% of the genome is found within 1500 lamina-bound domains of an average size of about 250 kilobases. This suggests that a number of genes are contained and silenced within these regions, however an even larger proportion of the genome is not actively bound to the nuclear lamina. Closer analysis of the makeup of these LADs finds that they tend to be gene-poor regions with little detectable transcriptional activity. While this is consistent with the model that lamina-bound, heterochromatic regions tend to be silenced, there are large portions of the genome that are not found in these domains but are still repressed. It is very unlikely that LADs and changes in nuclear architecture are the exclusive mechanisms for transcriptional regulation in progenitor cells. It is also

unlikely that the entirety of the phenotypes observed in *Hdac3*-deficient mice or in models lacking other lamina-related proteins is due to altered nuclear architecture.

Is neural crest regulation dependent on LADs?

To date, no study has linked nuclear architecture with regulation of the neural crest. The most closely related work has been by our lab and the Olson group, targeting epigenetic modifiers required for lamina-mediated silencing. Deletion of *Hdac3* in neural crest (see Chapter 2) results in cleft palate, microcephaly, tooth hypoplasia and outflow tract defects (Singh et al., 2011b, 2013). While these defects have not been directly attributed to altered chromatin organization, Hdac3 serves as a tether between the nuclear lamina and repressed loci. A straightforward first experiment is to map LADs in wild-type versus *Hdac3*-deficient neural crest derivatives. Loss of Lamin B1 occupancy at Bmp, Msx or Notch loci would be intriguing preliminary evidence of altered nuclear architecture affecting expression of gene regulatory networks.

Deletion of *Hdac1* in neural crest has been previously described (Haberland et al., 2009a). Unlike Hdac3, loss of *Hdac1* does not result in an overt phenotype or embryonic lethality. Given that Hdac1 functions as a mediator of deacetylation and repression of genes tethered at the nuclear lamina (Milon et al., 2012), I hypothesize that maintaining a locus at the nuclear periphery is more critical to gene function than deacetylation or other mechanisms of repression once the locus is at the lamina. The Olson group also described severe craniofacial defects with loss of *Hdac8*, another class

I Hdac (Haberland et al., 2009a). While no role for Hdac8 at the nuclear periphery has been described, it is possible that this enzyme functions in lamina-mediated silencing.

What comes first, tethering or repression?

The most convincing evidence that relocating chromatin to the nuclear lamina is sufficient for repression stems from artificial tethering experiments performed by Singh and Reddy (Reddy and Singh, 2008; Reddy et al., 2008). Through creative repurposing of the lac operon, the authors were able to inducibly tether a gene of interest to the nuclear lamina. First, the lac repressor (LacI) is fused to a structural element of the nuclear lamina (e.g. Emerin or Lamin B1). Then, the lac operator (*LacO*) sequence is cloned downstream of a reporter transgene and introduced into a cell stably expressing the LacI fusion protein. Upon removal of isopropyl-β-D-thio-galactoside (IPTG), the repressor fusion protein reversibly binds to the lac operator sequence, retaining the reporter gene at the nuclear periphery. LacI-*LacO* mediated tethering of a reporter gene significantly decreased its expression, providing direct evidence that the nuclear periphery is a “silenced environment” capable of repressing genomic loci brought in close proximity.

While these experiments elegantly demonstrate the capacity of the perinuclear region to repress transcriptional activity, they do not preclude the model that under native conditions a locus is first epigenetically silenced before being retained at the

nuclear periphery. To test this alternative hypothesis, a transgene could be artificially decorated with histone modifications and tracked to determine whether it migrates to the nuclear periphery. One potential system for modifying histone proteins at a specific gene is to generate a version of Cas9 fused to various epigenetic modifiers (e.g. Hdacs, histone methyltransferase, etc.) and target the gene of interest by transfecting small guide RNAs complementary to the transgene sequence. The epigenetic modifying enzymes would be directed to the transgene, presumably marking the chromatin for repression. This approach would determine whether epigenetic silencing of a gene is sufficient to induce translocation to the nuclear periphery.

Are there epigenetic factories at the lamina?

The subnuclear region near the lamina and inner nuclear membrane is often described as a “silenced environment.” Active tethering of transgenes to the nuclear periphery reduces expression at the RNA level (Reddy et al., 2008). Mapping studies *in vivo* and *in vitro* indicate that genomic regions bound at the nuclear lamina are typically silent, with relatively low transcriptional activity (Guelen et al., 2008; Kohwi et al., 2013; Peric-Hupkes et al., 2010; Zullo et al., 2012). Despite these correlative studies in several systems, the precise mechanism by which tethered genes are repressed remains unknown.

Circumstantial evidence from a several studies suggests that a host of epigenetic regulator enzymes and complexes reside at the nuclear periphery (Demmerle et al., 2012; Guarda et al., 2009; Hurd et al., 2010; Milon et al., 2012; Pegoraro et al., 2009; Shevelyov and Nurminsky, 2012). These proteins include epigenetic “writers” like HATs, “erasers” like Hdacs and “readers” like CHD7/8. These enzymes are also found within larger complexes at the nuclear membrane including NuRD and NCoR-SMRT. These data are partly accumulated from immunoprecipitation studies identifying interacting partners of structural proteins within the nuclear lamina and membrane. Much work needs to be done to determine whether these epigenetic complexes are enriched at the nuclear periphery or simply appear in immunoprecipitation studies based on stochastic abundance. Given our findings of Hdac3 residing at the nuclear periphery and acting as a LAD tether, there is reason to suspect that these epigenetic regulators may have unexpected repressive functions to maintain the “silenced environment” of the nuclear periphery.

LADs vs nuclear pore complex vs nuclear matrix

While gene positioning at the nuclear periphery typically results in binding to the nuclear lamina and transcriptional repression, this is not always the case. The nuclear membrane is also decorated with thousands of nuclear pore complexes (NPC). These large protein complexes of at least 30 different nucleoporin proteins are typically thought of as regulators of selective transport in and out of the nucleus. Nuclear pore proteins also interact with chromatin and several studies have linked chromatin-nuclear pore

complex interactions with gene activation (Arib and Akhtar, 2011; Van Bortle and Corces, 2013; Brown et al., 2008; Chambeyron and Bickmore, 2004; Meister et al., 2011). In cardiomyocytes, class IIa Hdac4 can physically interact with Nup155 to mediate chromatin-nucleoporin association and repress Hdac4 target genes (Kehat et al., 2011). Work in differentiating ESCs has demonstrated that as lineage-specific genes are expressed, some of the corresponding genomic loci move towards the nuclear membrane and interact with the nuclear pore complex (Chambeyron and Bickmore, 2004). One intriguing model for this phenomenon is that genes bound at the nuclear pore are optimally positioned for sensing and reacting to incoming signals from the cytoplasm. Tethering a gene to the nuclear pore complex may poise the locus for activation by cytoplasmic or extracellular signals. In support of this hypothesis, our lab has preliminary data that addition of retinoic acid, a potent activator of *Hox* genes, draws the *HoxA* locus to the nuclear periphery. While additional work must be done to distinguish interactions with the pore versus interactions with the nuclear lamina, the notion that gene repositioning serves as a mechanism for potentiating signaling cascades is very enticing.

As a counterpart to gene repression at the nuclear lamina, recent studies suggest that the nuclear matrix may play a role in gene activation (Li and Reinberg, 2011; Skowronska-Krawczyk et al., 2014). The nuclear matrix is a network of filaments within the nucleus without a well-established function. The matrix is thought to aid in cargo transport within the nucleus and positioning of the chromosomes during mitosis, however a novel function as a transcriptional co-activator has emerged. Work by Rosenfeld and colleagues demonstrated that Pit1, a homeodomain transcription factor,

requires interaction with both β-catenin and the nuclear matrix protein matrin-3 to activate downstream target genes. Through elegant loss-of-function and artificial tethering experiments, the authors establish that matrin-3 is required for recruitment of co-activators including p300 and ultimately gene transcription. As additional reports of lamina, nuclear pore complex and matrix-mediated transcriptional regulation emerge, the relevance of these mechanisms in a developmental context will have to be established.

How to visualize and manipulate nuclear architecture?

As our understanding of the relevance of nuclear architecture on development and progenitor cell biology deepens, the dynamics of chromatin organization remain undetermined. The current approaches for visualizing specific genomic loci rely primarily upon *in situ hybridization* of locus-specific probes in fixed, permeabilized cells. While this technique enables clear visualization of a genomic locus of interest, it limits analysis to a single timepoint, preventing studies of chromatin movement over time. It is possible to fix samples at several timepoints to track changes over the duration of the experiment, however without live imaging it is not possible to determine what changes have taken place in the same cell over time. Two novel approaches to live chromosome tracking have recently been described. The van Steensel group has published a method for live imaging based upon a modification of DamID. DNA adenine methyltransferase (Dam) is fused to the nuclear lamina and stably expressed in a cell, adding methyl-adenine bases to genomic loci that have come in contact with the nuclear lamina. By simultaneously expressing a fluorescently-tagged *DpnI* restriction enzyme, the methylated loci are

bound by DpnI-GFP and visualized (Kind et al., 2013). In parallel, the Huang group modified the CRISPR-Cas9 genome editing system to visualize specific genes by fluorescently-tagging the Cas9 enzyme (Chen et al., 2013). By introducing at least 30 guide RNAs to a gene of interest, the authors were able to tile Cas9-GFP molecules along the genomic locus and visualize it in real time. The advantage of the CRISPR-based approach to the Dpn-based approach is that addition of sequence-specific guide RNAs allows tracking of a specific gene. These methods may prove useful to determining the dynamics and timeframe of nuclear architecture changes in real time in differentiating cells or even *in vivo* in *C. elegans* or zebrafish.

To directly examine the significance of nuclear architecture changes on cell function or progenitor cell behavior, the field needs a system for manipulating gene position and analyzing the downstream effects. Much like the artificial tethering experiments using *LacO*-LacI, I have bound Hdac3 and any Hdac3-occupied genes to the nuclear periphery by fusing the protein to Lap2β, a factor embedded within the inner nuclear membrane (see Chapter 3). I was able to show that this lamina-bound form of Hdac3 is sufficient to repress cardiac progenitor differentiation into myocytes, similar to wild-type, unbound Hdac3. To extend these experiments further, it is essential to be able to directly affect positioning of an endogenous gene. One potential method is to modify the CRISPR-Cas9 system by fusing Cas9 to Lap2β, sequestering it at the nuclear periphery. Upon introduction of guide RNAs specific to a gene of interest, Cas9 will bind to the sequence complementary to the guide RNA and retain the gene at the nuclear membrane. This system could be leveraged to investigate the effect of repositioning any

gene to the nuclear periphery in any cell type, finally addressing the question of what effect gene location has on cell function and development.

Concluding Remarks

In this dissertation I have studied the role of Hdac3 in neural crest and cardiac progenitor cell commitment. This work describes the capacity of an epigenetic modifier to coordinate expression of broad gene programs controlling cell behaviors including proliferation, survival and differentiation. One of the most exciting findings is that Hdac3 functions in a deacetylase-independent manner to repress lineage-specific genes by tethering the relevant genomic loci at the nuclear lamina. This novel mechanism of regulation introduces chromatin dynamics within the nucleus as a system by which progenitor cells promote differentiation into a specific cell type. This work raises the possibility of tailor-made Hdac inhibitors used to regulate cell fate without affecting deacetylase activity or other enzymatic function. Potential clinical applications include expansion and differentiation of cardiac progenitor cells *ex vivo* or influence of progenitor cell commitment *in vivo*. It will be interesting to see the effect this work has on bridging the fields of developmental biology and nuclear architecture to influence future studies.

Bibliography

Achilleos, A., and Trainor, P. a (2012). Neural crest stem cells: discovery, properties and potential for therapy. Cell Res. *22*, 288–304.

Agah, R., Frenkel, P.A., French, B.A., Michael, L.H., Overbeek, P.A., and Schneider, M.D. (1997). Gene recombination in postmitotic cells. Targeted expression of Cre recombinase provokes cardiac-restricted, site-specific rearrangement in adult ventricular muscle in vivo. J. Clin. Invest. *100*, 169–179.

Aghajanian, H., Choi, C., Ho, V.C., Gupta, M., Singh, M.K., and Epstein, J. a (2014). Semaphorin 3d and semaphorin 3e direct endothelial motility through distinct molecular signaling pathways. J. Biol. Chem. *289*, 17971–17979.

Anand, P., Brown, J.D., Lin, C.Y., Qi, J., Zhang, R., Artero, P.C., Alaiti, M.A., Bullard, J., Alazem, K., Margulies, K.B., et al. (2013). BET bromodomains mediate transcriptional pause release in heart failure. Cell *154*, 569–582.

Arib, G., and Akhtar, A. (2011). Multiple facets of nuclear periphery in gene expression control. Curr. Opin. Cell Biol. *23*, 346–353.

Beaudouin, J., Gerlich, D., Daigle, N., Eils, R., and Ellenberg, J. (2002). Nuclear envelope breakdown proceeds by microtubule-induced tearing of the lamina. Cell *108*, 83–96.

Van Bemmel, J.G., Filion, G.J., Rosado, A., Talhout, W., de Haas, M., van Welsem, T., van Leeuwen, F., and van Steensel, B. (2013). A network model of the molecular organization of chromatin in Drosophila. Mol. Cell *49*, 759–771.

Berk, J.M., Simon, D.N., Jenkins-Houk, C.R., Westerbeck, J.W., Grønning-Wang, L.M., Carlson, C.R., and Wilson, K.L. (2014). Emerin intermolecular links to emerin and BAF. J. Cell Sci.

Bhaskara, S., Chyla, B.J., Amann, J.M., Knutson, S.K., Cortez, D., Sun, Z.-W., and Hiebert, S.W. (2008). Deletion of histone deacetylase 3 reveals critical roles in S phase progression and DNA damage control. Mol. Cell *30*, 61–72.

Bickmore, W. a, and van Steensel, B. (2013). Genome architecture: domain organization of interphase chromosomes. Cell *152*, 1270–1284.

Van Bortle, K., and Corces, V.G. (2013). Spinning the web of cell fate. Cell *152*, 1213–1217.

Bronner-Fraser, M., and Fraser, S. (1989). Developmental potential of avian trunk neural crest cells in situ. Neuron *3*, 755–766.

Bronner-Fraser, M., and Fraser, S.E. (1988). Cell lineage analysis reveals multipotency of some avian neural crest cells. Nature *335*, 161–164.

Bronner-Fraser, M., Sieber-Blum, M., and Cohen, a M. (1980). Clonal analysis of the avian neural crest: migration and maturation of mixed neural crest clones injected into host chicken embryos. J. Comp. Neurol. *193*, 423–434.

Brown, C.B., Feiner, L., Lu, M.M., Li, J., Ma, X., Webber, A.L., Jia, L., Raper, J.A., and Epstein, J.A. (2001). PlexinA2 and semaphorin signaling during cardiac neural crest development. Development *128*, 3071–3080.

Brown, C.R., Kennedy, C.J., Delmar, V.A., Forbes, D.J., and Silver, P.A. (2008). Global histone acetylation induces functional genomic reorganization at mammalian nuclear pore complexes. Genes Dev. *22*, 627–639.

Burke, B., and Stewart, C.L. (2013). The nuclear lamins: flexibility in function. Nat. Rev. Mol. Cell Biol. *14*, 13–24.

Cai, C.-L., Liang, X., Shi, Y., Chu, P.-H., Pfaff, S.L., Chen, J., and Evans, S. (2003). Isl1 identifies a cardiac progenitor population that proliferates prior to differentiation and contributes a majority of cells to the heart. Dev. Cell *5*, 877–889.

Chambeyron, S., and Bickmore, W. a (2004). Chromatin decondensation and nuclear reorganization of the HoxB locus upon induction of transcription. Genes Dev. *18*, 1119–1130.

Chang, C.-P., and Bruneau, B.G. (2012). Epigenetics and cardiovascular development. Annu. Rev. Physiol. *74*, 41–68.

Chen, B., Gilbert, L. a, Cimini, B. a, Schnitzbauer, J., Zhang, W., Li, G.-W., Park, J., Blackburn, E.H., Weissman, J.S., Qi, L.S., et al. (2013). Dynamic Imaging of Genomic Loci in Living Human Cells by an Optimized CRISPR/Cas System. Cell *155*, 1479–1491.

Christoforou, N., Miller, R.A., Hill, C.M., Jie, C.C., McCallion, A.S., and Gearhart, J.D. (2008). Mouse ES cell-derived cardiac precursor cells are multipotent and facilitate identification of novel cardiac genes. J. Clin. Invest. *118*, 894–903.

Codina, A., Love, J.D., Li, Y., Lazar, M. a, Neuhaus, D., and Schwabe, J.W.R. (2005). Structural insights into the interaction and activation of histone deacetylase 3 by nuclear receptor corepressors. Proc. Natl. Acad. Sci. U. S. A. *102*, 6009–6014.

Cohen-Gould, L., and Mikawa, T. (1996). The fate diversity of mesodermal cells within the heart field during chicken early embryogenesis. Dev. Biol. *177*, 265–273.

Crane, J.F., and Trainor, P. a (2006). Neural crest stem and progenitor cells. Annu. Rev. Cell Dev. Biol. *22*, 267–286.

Creazzo, T.L., Godt, R.E., Leatherbury, L., Conway, S.J., and Kirby, M.L. (1998). Role of cardiac neural crest cells in cardiovascular development. Annu. Rev. Physiol. *60*, 267–286.

Demmerle, J., Koch, A.J., and Holaska, J.M. (2012). The nuclear envelope protein emerin binds directly to histone deacetylase 3 (HDAC3) and activates HDAC3 activity. J. Biol. Chem. *287*, 22080–22088.

Demmerle, J., Koch, A.J., and Holaska, J.M. (2013). Emerin and histone deacetylase 3 (HDAC3) cooperatively regulate expression and nuclear positions of MyoD, Myf5, and Pax7 genes during myogenesis. Chromosome Res. *21*, 765–779.

Le Douarin, N.M., Renaud, D., Teillet, M.A., and Le Douarin, G.H. (1975). Cholinergic differentiation of presumptive adrenergic neuroblasts in interspecific chimeras after heterotopic transplantations. Proc. Natl. Acad. Sci. U. S. A. *72*, 728–732.

Dupin, E., and Sommer, L. (2012). Neural crest progenitors and stem cells: from early development to adulthood. Dev. Biol. *366*, 83–95.

Eisenberg, L.M., Kubalak, S.W., and Eisenberg, C.A. (2004). Stem cells and the formation of the myocardium in the vertebrate embryo. Anat. Rec. A. Discov. Mol. Cell. Evol. Biol. *276*, 2–12.

Euskirchen, G.M., Auerbach, R.K., Davidov, E., Gianoulis, T. a, Zhong, G., Rozowsky, J., Bhardwaj, N., Gerstein, M.B., and Snyder, M. (2011). Diverse roles and interactions of the SWI/SNF chromatin remodeling complex revealed using global approaches. PLoS Genet. *7*, e1002008.

Feng, D., Liu, T., Sun, Z., Bugge, A., Mullican, S.E., Alenghat, T., Liu, X.S., and Lazar, M.A. (2011). A circadian rhythm orchestrated by histone deacetylase 3 controls hepatic lipid metabolism. Science *331*, 1315–1319.

Filion, G.J., van Bemmel, J.G., Braunschweig, U., Talhout, W., Kind, J., Ward, L.D., Brugman, W., de Castro, I.J., Kerkhoven, R.M., Bussemaker, H.J., et al. (2010). Systematic protein location mapping reveals five principal chromatin types in Drosophila cells. Cell *143*, 212–224.

Guarda, A., Bolognese, F., Bonapace, I.M., and Badaracco, G. (2009). Interaction between the inner nuclear membrane lamin B receptor and the heterochromatic methyl binding protein, MeCP2. Exp. Cell Res. *315*, 1895–1903.

Guelen, L., Pagie, L., Brasset, E., Meuleman, W., Faza, M.B., Talhout, W., Eussen, B.H., de Klein, A., Wessels, L., de Laat, W., et al. (2008). Domain organization of human chromosomes revealed by mapping of nuclear lamina interactions. Nature *453*, 948–951.

Guenther, M.G., Barak, O., and Lazar, M.A. (2001). The SMRT and N-CoR corepressors are activating cofactors for histone deacetylase 3. Mol. Cell. Biol. *21*, 6091–6101.

Haberland, M., Mokalled, M.H., Montgomery, R.L., and Olson, E.N. (2009a). Epigenetic control of skull morphogenesis by histone deacetylase 8. Genes Dev. *23*, 1625–1630.

Haberland, M., Montgomery, R.L., and Olson, E.N. (2009b). The many roles of histone deacetylases in development and physiology: implications for disease and therapy. Nat. Rev. Genet. *10*, 32–42.

Hayashi, S., Lewis, P., Pevny, L., and McMahon, A.P. (2002). Efficient gene modulation in mouse epiblast using a Sox2Cre transgenic mouse strain. Mech. Dev. *119 Suppl* , S97–S101.

Ho, C.Y., Jaalouk, D.E., Vartiainen, M.K., and Lammerding, J. (2013). Lamin A/C and emerin regulate MKL1-SRF activity by modulating actin dynamics. Nature.

Hogan, B.L., Constantini, F., and Lacy, E. (1986). Manipulating the mouse embryo: A laboratory manual (Cold Spring Harbor Laboratory).

Hurd, E. a, Poucher, H.K., Cheng, K., Raphael, Y., and Martin, D.M. (2010). The ATP-dependent chromatin remodeling enzyme CHD7 regulates pro-neural gene expression and neurogenesis in the inner ear. Development *137*, 3139–3150.

Ishii, M., Merrill, A.E., Chan, Y.-S., Gitelman, I., Rice, D.P.C., Sucov, H.M., and Maxson, R.E. (2003). Msx2 and Twist cooperatively control the development of the neural crest-derived skeletogenic mesenchyme of the murine skull vault. Development *130*, 6131–6142.

Kattman, S.J., Huber, T.L., and Keller, G.M. (2006). Multipotent flk-1+ cardiovascular progenitor cells give rise to the cardiomyocyte, endothelial, and vascular smooth muscle lineages. Dev. Cell *11*, 723–732.

Kattman, S.J., Witty, A.D., Gagliardi, M., Dubois, N.C., Niapour, M., Hotta, A., Ellis, J., and Keller, G. (2011). Stage-Specific Optimization of Activin/Nodal and BMP Signaling Promotes Cardiac Differentiation of Mouse and Human Pluripotent Stem Cell Lines. Cell Stem Cell *8*, 228–240.

Kehat, I., Accornero, F., Aronow, B.J., and Molkentin, J.D. (2011). Modulation of chromatin position and gene expression by HDAC4 interaction with nucleoporins. J. Cell Biol. *193*, 21–29.

Kind, J., Pagie, L., Ortabozkoyun, H., Boyle, S., de Vries, S.S., Janssen, H., Amendola, M., Nolen, L.D., Bickmore, W.A., and van Steensel, B. (2013). Single-Cell Dynamics of Genome-Nuclear Lamina Interactions. Cell 1–15.

Kirby, M.L., Gale, T.F., and Stewart, D.E. (1983). Neural crest cells contribute to normal aorticopulmonary septation. Science *220*, 1059–1061.

Kohwi, M., Lupton, J.R., Lai, S.-L., Miller, M.R., and Doe, C.Q. (2013). Developmentally regulated subnuclear genome reorganization restricts neural progenitor competence in Drosophila. Cell *152*, 97–108.

Kubben, N., Adriaens, M., Meuleman, W., Voncken, J.W., van Steensel, B., and Misteli, T. (2012). Mapping of lamin A- and progerin-interacting genome regions. Chromosoma *121*, 447–464.

Lahm, A., Paolini, C., Pallaoro, M., Nardi, M.C., Jones, P., Neddermann, P., Sambucini, S., Bottomley, M.J., Lo Surdo, P., Carfí, A., et al. (2007). Unraveling the hidden catalytic activity of vertebrate class IIa histone deacetylases. Proc. Natl. Acad. Sci. U. S. A. *104*, 17335–17340.

Lee, T.I., and Young, R. a (2013). Transcriptional regulation and its misregulation in disease. Cell *152*, 1237–1251.

Lescroart, F., Chabab, S., Lin, X., Rulands, S., Paulissen, C., Rodolosse, A., Auer, H., Achouri, Y., Dubois, C., Bondue, A., et al. (2014). Early lineage restriction in temporally distinct populations of Mesp1 progenitors during mammalian heart development. Nat. Cell Biol.

Lewandowski, S.L., Janardhan, H.P., Smee, K.M., Bachman, M., Sun, Z., Lazar, M. a, and Trivedi, C.M. (2014). Histone deacetylase 3 modulates Tbx5 activity to regulate early cardiogenesis. Hum. Mol. Genet. 1–9.

Li, G., and Reinberg, D. (2011). Chromatin higher-order structures and gene regulation. Curr. Opin. Genet. Dev. *21*, 175–186.

Li, Q.Y., Newbury-Ecob, R.A., Terrett, J.A., Wilson, D.I., Curtis, A.R., Yi, C.H., Gebuhr, T., Bullen, P.J., Robson, S.C., Strachan, T., et al. (1997). Holt-Oram syndrome is caused by mutations in TBX5, a member of the Brachyury (T) gene family. Nat. Genet. *15*, 21–29.

Liang, X., Wang, G., Lin, L., Lowe, J., Zhang, Q., Bu, L., Chen, Y.-H., Chen, J., Sun, Y., and Evans, S.M. (2013). HCN4 Dynamically Marks the First Heart Field and Conduction System Precursors. Circ. Res.

Lois, C., Hong, E.J., Pease, S., Brown, E.J., and Baltimore, D. (2002). Germline transmission and tissue-specific expression of transgenes delivered by lentiviral vectors. Science *295*, 868–872.

Marchant, L., Linker, C., Ruiz, P., Guerrero, N., and Mayor, R. (1998). The inductive properties of mesoderm suggest that the neural crest cells are specified by a BMP gradient. Dev. Biol. *198*, 319–329.

Mattout, A., Pike, B.L., Towbin, B.D., Bank, E.M., Gonzalez-Sandoval, A., Stadler, M.B., Meister, P., Gruenbaum, Y., and Gasser, S.M. (2011). An EDMD mutation in C. elegans lamin blocks muscle-specific gene relocation and compromises muscle integrity. Curr. Biol. *21*, 1603–1614.

Meilhac, S.M., Esner, M., Kerszberg, M., Moss, J.E., and Buckingham, M.E. (2004a). Oriented clonal cell growth in the developing mouse myocardium underlies cardiac morphogenesis. J. Cell Biol. *164*, 97–109.

Meilhac, S.M., Esner, M., Kelly, R.G., Nicolas, J.-F., and Buckingham, M.E. (2004b). The clonal origin of myocardial cells in different regions of the embryonic mouse heart. Dev. Cell *6*, 685–698.

Meister, P., Mango, S.E., and Gasser, S.M. (2011). Locking the genome: nuclear organization and cell fate. Curr. Opin. Genet. Dev. *21*, 167–174.

Melnick, A., Carlile, G., Ahmad, K.F., Kiang, C., Corcoran, C., Bardwell, V., Prive, G.G., and Licht, J.D. (2002). Critical residues within the BTB domain of PLZF and Bcl-6 modulate interaction with corepressors. Mol. Cell. Biol. *22*, 1804–1818.

Milon, B.C., Cheng, H., Tselebrovsky, M. V, Lavrov, S. a, Nenasheva, V. V, Mikhaleva, E.A., Shevelyov, Y.Y., and Nurminsky, D.I. (2012). Role of histone deacetylases in gene regulation at nuclear lamina. PLoS One *7*, e49692.

Montgomery, R.L., Davis, C.A., Potthoff, M.J., Haberland, M., Fielitz, J., Qi, X., Hill, J.A., Richardson, J.A., and Olson, E.N. (2007). Histone deacetylases 1 and 2 redundantly regulate cardiac morphogenesis, growth, and contractility. Genes Dev. *21*, 1790–1802.

Montgomery, R.L., Potthoff, M.J., Haberland, M., Qi, X., Matsuzaki, S., Humphries, K.M., Richardson, J.A., Bassel-Duby, R., and Olson, E.N. (2008). Maintenance of cardiac energy metabolism by histone deacetylase 3 in mice. J. Clin. Invest. *118*, 3588–3597.

Moretti, A., Caron, L., Nakano, A., Lam, J.T., Bernshausen, A., Chen, Y., Qyang, Y., Bu, L., Sasaki, M., Martin-Puig, S., et al. (2006). Multipotent embryonic isl1+ progenitor cells lead to cardiac, smooth muscle, and endothelial cell diversification. Cell *127*, 1151–1165.

Moretti, A., Bellin, M., Jung, C.B., Thies, T.-M., Takashima, Y., Bernshausen, A., Schiemann, M., Fischer, S., Moosmang, S., Smith, A.G., et al. (2010). Mouse and human induced pluripotent stem cells as a source for multipotent Isl1+ cardiovascular progenitors. FASEB J. *24*, 700–711.

Morrison, S.J., Wandycz, a M., Hemmati, H.D., Wright, D.E., and Weissman, I.L. (1997). Identification of a lineage of multipotent hematopoietic progenitors. Development *124*, 1929–1939.

Moses, K.A., DeMayo, F., Braun, R.M., Reecy, J.L., and Schwartz, R.J. (2001). Embryonic expression of an Nkx2-5/Cre gene using ROSA26 reporter mice. Genesis *31*, 176–180.

Mullican, S.E., Gaddis, C.A., Alenghat, T., Nair, M.G., Giacomin, P.R., Everett, L.J., Feng, D., Steger, D.J., Schug, J., Artis, D., et al. (2011). Histone deacetylase 3 is an epigenomic brake in macrophage alternative activation. Genes Dev. *25*, 2480–2488.

Nagy, A., Gertsenstein, M., Vintersten, K., and Behringer, R.R. (2002). Manipulating the Mouse Embryo: A Laboratory Manual, Third Edition (Cold Spring Harbor: Cold Spring Harbor Laboratory).

Ohtani, K., and Dimmeler, S. (2011). Epigenetic regulation of cardiovascular differentiation. Cardiovasc. Res. *90*, 404–412.

Paige, S.L., Thomas, S., Stoick-Cooper, C.L., Wang, H., Maves, L., Sandstrom, R., Pabon, L., Reinecke, H., Pratt, G., Keller, G., et al. (2012). A temporal chromatin signature in human embryonic stem cells identifies regulators of cardiac development. Cell *151*, 221–232.

Pegoraro, G., Kubben, N., Wickert, U., Göhler, H., Hoffmann, K., and Misteli, T. (2009). Ageing-related chromatin defects through loss of the NURD complex. Nat. Cell Biol. *11*, 1261–1267.

Peng, T., Tian, Y., Boogerd, C.J., Lu, M.M., Kadzik, R.S., Stewart, K.M., Evans, S.M., and Morrisey, E.E. (2013). Coordination of heart and lung co-development by a multipotent cardiopulmonary progenitor. Nature *500*, 589–592.

Peric-Hupkes, D., Meuleman, W., Pagie, L., Bruggeman, S.W.M., Solovei, I., Brugman, W., Gräf, S., Flicek, P., Kerkhoven, R.M., van Lohuizen, M., et al. (2010). Molecular maps of the reorganization of genome-nuclear lamina interactions during differentiation. Mol. Cell *38*, 603–613.

Pickersgill, H., Kalverda, B., de Wit, E., Talhout, W., Fornerod, M., and van Steensel, B. (2006). Characterization of the Drosophila melanogaster genome at the nuclear lamina. Nat. Genet. *38*, 1005–1014.

Pongubala, J.M.R., Northrup, D.L., Lancki, D.W., Medina, K.L., Treiber, T., Bertolino, E., Thomas, M., Grosschedl, R., Allman, D., and Singh, H. (2008). Transcription factor EBF restricts alternative lineage options and promotes B cell fate commitment independently of Pax5. Nat. Immunol. *9*, 203–215.

Reddy, K.L., and Singh, H. (2008). Using molecular tethering to analyze the role of nuclear compartmentalization in the regulation of mammalian gene activity. Methods *45*, 242–251.

Reddy, K.L., Zullo, J.M., Bertolino, E., and Singh, H. (2008). Transcriptional repression mediated by repositioning of genes to the nuclear lamina. Nature *452*, 243–247.

Redkar, a, Montgomery, M., and Litvin, J. (2001). Fate map of early avian cardiac progenitor cells. Development *128*, 2269–2279.

Robb, L. (2007). Cytokine receptors and hematopoietic differentiation. Oncogene *26*, 6715–6723.

Sadaie, M., Salama, R., Carroll, T., Tomimatsu, K., Chandra, T., Young, A.R.J., Narita, M., Pérez-Mancera, P.A., Bennett, D.C., Chong, H., et al. (2013). Redistribution of the Lamin B1 genomic binding profile affects rearrangement of heterochromatic domains and SAHF formation during senescence. Genes Dev. *27*, 1800–1808.

Sauka-Spengler, T., and Bronner-Fraser, M. (2008). A gene regulatory network orchestrates neural crest formation. Nat. Rev. Mol. Cell Biol. *9*, 557–568.

Shah, P.P., Donahue, G., Otte, G.L., Capell, B.C., Nelson, D.M., Cao, K., Aggarwala, V., Cruickshanks, H.A., Rai, T.S., McBryan, T., et al. (2013). Lamin B1 depletion in senescent cells triggers large-scale changes in gene expression and the chromatin landscape. Genes Dev. *27*, 1787–1799.

Shevelyov, Y.Y., and Nurminsky, D.I. (2012). The nuclear lamina as a gene-silencing hub. Curr. Issues Mol. Biol. *14*, 27–38.

Shin, J.-Y., Méndez-López, I., Wang, Y., Hays, A.P., Tanji, K., Lefkowitch, J.H., Schulze, P.C., Worman, H.J., and Dauer, W.T. (2013). Lamina-associated polypeptide-1 interacts with the muscular dystrophy protein emerin and is essential for skeletal muscle maintenance. Dev. Cell *26*, 591–603.

Shopland, L.S., Lynch, C.R., Peterson, K. a, Thornton, K., Kepper, N., Hase, J. Von, Stein, S., Vincent, S., Molloy, K.R., Kreth, G., et al. (2006). Folding and organization of a contiguous chromosome region according to the gene distribution pattern in primary genomic sequence. J. Cell Biol. *174*, 27–38.

Singh, N., Trivedi, C.M., Lu, M., Mullican, S.E., Lazar, M. a, and Epstein, J.A. (2011a). Histone deacetylase 3 regulates smooth muscle differentiation in neural crest cells and development of the cardiac outflow tract. Circ. Res. *109*, 1240–1249.

Singh, N., Trivedi, C.M., Lu, M., Mullican, S.E., Lazar, M. a, and Epstein, J.A. (2011b). Histone deacetylase 3 regulates smooth muscle differentiation in neural crest cells and development of the cardiac outflow tract. Circ. Res. *109*, 1240–1249.

Singh, N., Gupta, M., Trivedi, C.M., Singh, M.K., Li, L., and Epstein, J.A. (2013). Murine craniofacial development requires Hdac3-mediated repression of Msx gene expression. Dev. Biol. *377*, 333–344.

Skowronska-Krawczyk, D., Ma, Q., Schwartz, M., Scully, K., Li, W., Liu, Z., Taylor, H., Tollkuhn, J., Ohgi, K. a., Notani, D., et al. (2014). Required enhancer-matrin-3 network interactions for a homeodomain transcription program. Nature.

Smith, Z.D., and Meissner, A. (2013). DNA methylation: roles in mammalian development. Nat. Rev. Genet. *14*, 204–220.

Somech, R., Shaklai, S., Geller, O., Amariglio, N., Simon, A.J., Rechavi, G., and Gal-Yam, E.N. (2005). The nuclear-envelope protein and transcriptional repressor LAP2beta interacts with HDAC3 at the nuclear periphery, and induces histone H4 deacetylation. J. Cell Sci. *118*, 4017–4025.

Später, D., Abramczuk, M.K., Buac, K., Zangi, L., Stachel, M.W., Clarke, J., Sahara, M., Ludwig, A., and Chien, K.R. (2013). A HCN4+ cardiomyogenic progenitor derived from the first heart field and human pluripotent stem cells. Nat. Cell Biol. *15*, 1098–1106.

Srinivas, S., Watanabe, T., Lin, C.S., William, C.M., Tanabe, Y., Jessell, T.M., and Costantini, F. (2001). Cre reporter strains produced by targeted insertion of EYFP and ECFP into the ROSA26 locus. BMC Dev. Biol. *1*, 4.

Srivastava, D. (2006). Making or breaking the heart: from lineage determination to morphogenesis. Cell *126*, 1037–1048.

Stalsberg, H., and DeHaan, R.L. (1969). The precardiac areas and formation of the tubular heart in the chick embryo. Dev. Biol. *19*, 128–159.

Summers, A.R., Fischer, M.A., Stengel, K.R., Zhao, Y., Kaiser, J.F., Wells, C.E., Hunt, A., Bhaskara, S., Luzwick, J.W., Sampathi, S., et al. (2013). HDAC3 is essential for DNA replication in hematopoietic progenitor cells. J. Clin. Invest.

Sun, Z., Singh, N., Mullican, S.E., Everett, L.J., Li, L., Yuan, L., Liu, X., Epstein, J.A., and Lazar, M.A. (2011). Diet-induced lethality due to deletion of the Hdac3 gene in heart and skeletal muscle. J. Biol. Chem. *286*, 33301–33309.

Sun, Z., Miller, R.A., Patel, R.T., Chen, J., Dhir, R., Wang, H., Zhang, D., Graham, M.J., Unterman, T.G., Shulman, G.I., et al. (2012). Hepatic Hdac3 promotes gluconeogenesis by repressing lipid synthesis and sequestration. Nat. Med. *18*, 934–942.

Sun, Z., Feng, D., Fang, B., Mullican, S.E., You, S.-H., Lim, H.-W., Everett, L.J., Nabel, C.S., Li, Y., Selvakumaran, V., et al. (2013). Deacetylase-Independent Function of HDAC3 in Transcription and Metabolism Requires Nuclear Receptor Corepressor. Mol. Cell *52*, 769–782.

Taneyhill, L. a, Coles, E.G., and Bronner-Fraser, M. (2007). Snail2 directly represses cadherin6B during epithelial-to-mesenchymal transitions of the neural crest. Development *134*, 1481–1490.

Thiagalingam, S., Cheng, K.-H., Lee, H.J., Mineva, N., Thiagalingam, A., and Ponte, J.F. (2003). Histone deacetylases: unique players in shaping the epigenetic histone code. Ann. N. Y. Acad. Sci. *983*, 84–100.

Till, J.E., and McCulloch, E.A. (2012). A direct measurement of the radiation sensitivity of normal mouse bone marrow cells. 1961. Radiat. Res. *178*, AV3–7.

Towbin, B.D., González-Aguilera, C., Sack, R., Gaidatzis, D., Kalck, V., Meister, P., Askjaer, P., and Gasser, S.M. (2012). Step-wise methylation of histone H3K9 positions heterochromatin at the nuclear periphery. Cell *150*, 934–947.

Trivedi, C.M., Luo, Y., Yin, Z., Zhang, M., Zhu, W., Wang, T., Floss, T., Goettlicher, M., Noppinger, P.R., Wurst, W., et al. (2007). Hdac2 regulates the cardiac hypertrophic response by modulating Gsk3 beta activity. Nat. Med. *13*, 324–331.

Trivedi, C.M., Lu, M.M., Wang, Q., and Epstein, J.A. (2008). Transgenic overexpression of Hdac3 in the heart produces increased postnatal cardiac myocyte proliferation but does not induce hypertrophy. J. Biol. Chem. *283*, 26484–26489.

Trivedi, C.M., Zhu, W., Wang, Q., Jia, C., Kee, H.J., Li, L., Hannenhalli, S., and Epstein, J.A. (2010). Hopx and Hdac2 interact to modulate Gata4 acetylation and embryonic cardiac myocyte proliferation. Dev. Cell *19*, 450–459.

Verzi, M.P., McCulley, D.J., De Val, S., Dodou, E., and Black, B.L. (2005). The right ventricle, outflow tract, and ventricular septum comprise a restricted expression domain within the secondary/anterior heart field. Dev. Biol. *287*, 134–145.

Wamstad, J. a, Alexander, J.M., Truty, R.M., Shrikumar, A., Li, F., Eilertson, K.E., Ding, H., Wylie, J.N., Pico, A.R., Capra, J. a, et al. (2012). Dynamic and coordinated epigenetic regulation of developmental transitions in the cardiac lineage. Cell *151*, 206–220.

Weissman, I.L., Anderson, D.J., and Gage, F. (2001). Stem and progenitor cells: origins, phenotypes, lineage commitments, and transdifferentiations. Annu. Rev. Cell Dev. Biol. *17*, 387–403.

Wu, S.M., Fujiwara, Y., Cibulsky, S.M., Clapham, D.E., Lien, C.-L., Schultheiss, T.M., and Orkin, S.H. (2006). Developmental origin of a bipotential myocardial and smooth muscle cell precursor in the mammalian heart. Cell *127*, 1137–1150.

Wu, S.M., Chien, K.R., and Mummery, C. (2008). Origins and fates of cardiovascular progenitor cells. Cell *132*, 537–543.

You, S.-H., Lim, H.-W., Sun, Z., Broache, M., Won, K.-J., and Lazar, M.A. (2013). Nuclear receptor co-repressors are required for the histone-deacetylase activity of HDAC3 in vivo. Nat. Struct. Mol. Biol. *3*, 1–7.

Zaidi, S., Choi, M., Wakimoto, H., Ma, L., Jiang, J., Overton, J.D., Romano-Adesman, A., Bjornson, R.D., Breitbart, R.E., Brown, K.K., et al. (2013). De novo mutations in histone-modifying genes in congenital heart disease. Nature *498*, 220–223.

Zeng, L., Xiao, Q., Margariti, A., Zhang, Z., Zampetaki, A., Patel, S., Capogrossi, M.C., Hu, Y., and Xu, Q. (2006). HDAC3 is crucial in shear- and VEGF-induced stem cell differentiation toward endothelial cells. J. Cell Biol. *174*, 1059–1069.

Zhou, Y., Kim, J., Yuan, X., and Braun, T. (2011). Epigenetic modifications of stem cells: a paradigm for the control of cardiac progenitor cells. Circ. Res. *109*, 1067–1081.

Zullo, J.M., Demarco, I. a, Piqué-Regi, R., Gaffney, D.J., Epstein, C.B., Spooner, C.J., Luperchio, T.R., Bernstein, B.E., Pritchard, J.K., Reddy, K.L., et al. (2012). DNA sequence-dependent compartmentalization and silencing of chromatin at the nuclear lamina. Cell *149*, 1474–1487.